

STABILITY OF RETAINED GOAF-SIDE GATEROAD UNDER DIFFERENT ROOF CONDITIONS BY LONGWALL MINING IN DEEP UNDERGROUND COAL MINE

張, 志義

<https://doi.org/10.15017/1866289>

出版情報：九州大学, 2017, 博士（工学）, 課程博士
バージョン：
権利関係：

**STABILITY OF RETAINED GOAF-SIDE GATEROAD UNDER
DIFFERENT ROOF CONDITIONS BY LONGWALL MINING
IN DEEP UNDERGROUND COAL MINE**

A DOCTORAL DISSERTATION
SUBMITTED TO GRADUATE SCHOOL OF ENGINEERING OF
KYUSHU UNIVERSITY
IN PARTIAL FULFILLMENT OF THE REQUIREMENTS FOR THE
DEGREE OF DOCTOR OF PHILOSOPHY IN EARTH RESOURCES
ENGINEERING

BY
ZHIYI ZHANG

SUPERVISED BY
PROFESSOR DR. **HEDEKI SHIMADA**

DEPARTMENT OF EARTH RESOURCES ENGINEERING
GRADUATE SCHOOL OF ENGINEERING
KYUSHU UNIVERSITY

MAY 2017

ABSTRACT

In China, coal production has been increasing quickly in recent decades with accelerating economic development and industrialization in China. Coal production makes up more than 55% of total energy consumption and produces 3.8 billion tons per year. The mining level of the underground coal mines in China is quickly becoming to be deep, which is the result of growing coal production and limited shallow coal resources, especially in East area. About 80% of the underground coal mines with a depth of more than 1,000 m are located in East China. As mining depth increases, however, it is very difficult to apply the conventional U type longwall mining system in deep mining environment, because the high in-situ stress and high gas emission environments always decrease coal recovery and cause the high risk of gas explosions at the coal face. Recently, Y type gateroad layout has been widely employed in deep underground longwall mining systems in order to increase the coal recovery rate and reduce the risk of gas outbursts through the improvement of ventilation systems and eliminating gateroad protection coal pillars. In this system, a previous gateroad, which is abandoned in the conventional U type settings after coal face passes by, is maintained by constructing artificial packfillings along the goaf side when the longwall face passes. The retained gateroad behind the longwall face is referred as Retained Goaf Side Gateroad (RGSG). The RGSG that plays a crucial role in the Y type longwall system, however, is difficult to control due to high in situ stress and soft rock mechanics which are prevalent in deep underground environments. Conventional roadway supporting technology cannot maintain the stability of the deep RGSG. Therefore, the purpose of this research is to develop effective RGSG supporting methods in deep mining environment under different roof conditions. The dissertation consists of six chapters and the main content in each chapter are listed as follows:

Chapter 1: This chapter introduces the background of this research, mining technology, geotechnical issues related to this research topic and an involved outline of the dissertation.

Chapter 2: This chapter describes the roof structures over the goaf and RGSG. After the coal seam is mined, overlying main roof follows O-X breakage style orderly and periodically when the coal face advances continually. As a result of this O-X style breakage over the goaf, a rock cantilever forms over the RGSG that is located at the side of goaf. The RGSG is seriously damaged due to the movements of the roof cantilever. The thicker the main roof is and the thinner the immediate roof is, the more serious the influence is. Therefore, the improvement of the roof structure over the RGSG when it is covered by thick main roof directly is proposed by shortening the length of roof cantilever. After the main roof is pre-split along the outer edge of the

packfillings, mechanical connection between the roof over the RGSG and other part over goaf is cut off, and the rotation and sink of the roof cantilever over the RGSG can be decreased considerably. Then, the damage to the RGSG due to the movement of the roof of the goaf can be reduced.

Chapter 3: This chapter discusses the alteration of stress and deformation of the rock mass around the RGSG due to an advance of the longwall face in different roof conditions by means of FLAC3D numerical software. Simulation results show that the bearing strength of the rock mass around RGSG reduces reasonably because the confining stress normal to the surface of roadway surrounding rock decreases considerably after roadway excavation. Consequently, the rock mass around RGSG breaks and deforms towards the inside of the roadway. During coal panel retreating, the influence of abutment stress induced by coal extraction can be divided into three stages: no influence farther than 40 m; severe influence from 40 m ahead of coal face to 60 m behind the coal face; slight influence from 60 m behind the coal face to 120 m behind the coal face. After experiencing these stress disturbances, the rock mass around the RGSG undergoes large deformations and the boltability of cable bolts and rock bolts in the surrounding rock of roadway becomes considerably lower because plastic zone in the rock mass around the RGSG is expanded gradually. As the thickness of the main roof increases and the thickness of the immediate roof decreases, the deformation of the rock mass around RGSG decreases during roadway excavation, however, the deformation increases considerably during coal panel retreating. The deformation of the rock mass around RGSG reaches the maximum value when the coal seam is directly beneath a hard main roof of 12 m thickness.

Chapter 4: This chapter proposes the four control measures of roadway stability including the staged supporting method, pre-split method for hard roof, grout bolting method and grouting reinforcement method. Basically, a staged supporting strategy is proposed to maintain the stability of the RGSG. In the first supporting stage, a pre-stressed bolting system aiming at providing high lateral confining stress is proposed to maintain the stability of the RGSG during roadway excavation. In the second supporting stage, a cable bolt system with a larger length is suggested within the influencing range of mining induced abutment pressure, considering the widening of the plastic zone in the surrounding rock of the roadway. In the third supporting stage, packfillings with gradually increasing strength and reinforcement to the roof over packfillings should be put into mind because of the continually increasing abutment stress behind the coal face. Pre-split technology is proposed to optimize the hard roof structure over the RGSG. The section shrinkage ratio of the RGSG under 12 m hard main roof is up to 82.5% when the first coal panel retreating finishes. Pre-split technology is applied to optimize the roof structure by

shortening the length of the roof cantilever. The deformations of the RGSG surrounding rock are reduced considerably as expected after roof is pre-split. According to the results of simulations, a floor heave of RGSG decreases most obviously by 57% with a 767 mm decrement, followed by a roof sag reduction of 55% with a 469 mm decrement. The deformations of the left and right sidewall are also reduced by 25% with a 235 mm decrement and by 24% with a 257 mm decrement, respectively. Improved grout bolting technology is proposed to control the large deformations of RGSG sidewalls. The final deformations of the RGSG sidewalls are still very large (more than 700 mm) although some improvements have been achieved by the application of roof pre-splitting. To control the large deformed sidewalls, a modified grout bolting technology is proposed. This modified technology not only can provide higher confining stress at the installation stage, but also controls the induced cracks more effectively and has larger bearing capacity during the followed grouting stage. These improvements play a crucial role in reducing the size of the plastic zone in the RGSG sidewalls. After the application of this technology to the RGSG sidewalls, the deformations of the left and right coal sidewalls can be reduced to 356 mm from 729 mm, and 456 mm from 792 mm, respectively. Grouting reinforcement is proposed to control the large heaved floor. After applications of roof pre-splitting and sidewall grout bolting technology, the deformation of RGSG floor that is not supported, plays the leading role in roadway section shrinkage again. Roadway floor heaving is in direct proportion to the ratio of horizontal stress to vertical stress in the floor strata. Grouting reinforcement is proposed to reduce the floor heaves by considering the weak rock mechanics of the mudstone, and only 1 m within the floor is grouted because the heaving within 1 m of the floor strata accounts for 72% of whole floor heaving. When the residual cohesion is increased to 30%, 50% and 70% of the original value and residual friction angle is increased to 24.5° , 25° and 25.5° , respectively by grouting, the amount of floor heaves are reduced considerably to 273 mm, 202 mm and 194 mm from 516 mm. After grouting, the plastic zone is effectively reduced.

Chapter 5: This chapter describes the applications of four control measures of roadway stability proposed in Chapter 4 in three typical deep underground coal mines. Firstly, the staged supporting method is applied in the Zhuji underground coal mine at a depth of 980 m. After the application of this measure, deformations of the RGSG are controlled effectively. However, the right sidewall convergence and floor heave are still large so that this RGSG has to be enlarged before the second coal panel retreating. Roadway section enlarging processes including floor dinting and sidewall widening are conducted. Secondly, in order to reduce the deformations of RGSG surrounding rock in deep mining environment during first coal panel mining and to avoid roadway section enlarging to the RGSG before the second coal panel mining, the grout bolting

method is applied in the Pan Yidong coal mine at a depth of 850 m. After installation of the grouting cable bolt, the integrity of the cracked surrounding rock is improved, and the separations in the roof strata are controlled effectively. The final profile is found to be large enough for the second longwall panel mining. Thirdly, the rock pre-split blasting method is applied in the Pingdingshan underground coalmine of 18 m hard main roof to reduce the influence of long roof cantilever movements on the surrounding rock of RGSG. When the first coal panel extraction is finished, the residual section area of the RGSG in the Pingdingshan coal mine is larger than 10 m², and it can be reused during retreating of the adjacent coal panel.

Chapter 6: This chapter concludes the results of this research.

Keywords: Deep underground coal mine; Retained goaf-side gateroad; Roadway supporting; Stress and Deformation evolution; Staged roadway supporting; Grout bolting technology; Hard roof pre-split; Floor heave

ACKNOWLEDGEMENTS

Deep appreciation and sincere gratitude are expressed to Professor Dr. Hideki Shimada, my supervisor, for his invaluable guidance, encouragement and support throughout the study. Fortunately, this dissertation is achieved with this strong supports and valuable comments. His expertise on mining and geological engineering has been invaluable and many inspiring discussions with him have been of great value to me. He has always been a lifelong learning role model for me to follow due to his noble charisma, profound academic attainments, rigorous scholarship and selfless work spirit.

Heartfelt appreciation and pure gratitude goes to Associate Professor Dr. Takashi Sasaoka, Assistant Professor Dr. Sugeng Wahyudi and Assistant Professor Dr. Akihrio Hamanaka for their invaluable discussions, guidance and modification to improve this study. Their encouragement is an important motivation for me to pursue the academic study.

Sincere gratitude also goes to two extremely important members of the doctoral examination committee, Professor Dr. Mitani Yasuhiro from Department of Civil and Structural Engineering and Associate Professor Dr. Inoue Masahiro from Department of Earth Resources Engineering, for their constructive comments and invaluable suggestions that greatly perfect this study.

Heartfelt appreciation is given to Professor Dr. Nong Zhang, my previous supervisor at the China University of Mining and Technology, for providing the crucial fieldwork and valuable data, which played a pivotal role in this study.

Special appreciation and gratitude are expressed to the powerful financial assistance for this study, sponsored by the State Scholarship Fund from China Scholarship Council. Especial appreciation should be given to Kyushu University for waiving entrance, examination and tuition fees during my study.

Many grateful thanks also go to the Laboratory of Rock Engineering and Mining Machinery of Kyushu University, China University of Mining and Technology, Huainan Mining Industry (Group) Co., Ltd. and China Pingmei Shenma Group for their strong support during the laboratory and field experiments.

I would like to express grateful appreciation to Ms. Oiwa and Ms. Michiko from International Student and Researcher Support Center, Ms. Nakayama, Ms. Tabuchi and

Ms. Mori from the office of the Department of Earth Resources Engineering for their long-term kind-hearted assistance during my study at Kyushu University.

I would like to thank Shuichi Fujita Sensei, Yasuhiro Yoshida Sensei, Dr. Mingwei Zhang, Dr. Deyu Qian, Dr. Kai Wen, Dr. Pongpanya Phanthoudeth, Dr. Naung Naung, Master Xiangyang Sun and all the members in the Lab of Rock Engineering and Mining Machinery for their enthusiastic and grateful help, cooperation and friendship during my study at Kyushu University and life in Fukuoka.

In the past ten years, three overwhelming strong passions have passed throughout my study life: the longing for a happy life, the seeking for scientific mining and unbearable pity for the suffering of underground mining worker due to mining disasters, which has reinforced my belief and faith to go on study mining engineering and earth resource engineering. Since 2011, my research areas are focused on roadway supporting of the underground coal mine, on which I have participated in more than 10 scientific research projects at home and overseas. Moreover, I have been to underground coal mines for field work and research more than 200 times. Through these practices, I have got much useful knowledge and first hand field data, which improved my good scholastic capacity and potential for further academic study and well enhanced the ability of my research and cooperation with others. This has been my life on mining engineering. I have found it worth studying and living, and will merrily continue it if the chance is still offered me. Therefore, I have always been self-motivated and try my best to catch the opportunities such as study in Japan and international conferences on mining and rock engineering to enrich my knowledge, broaden my horizon and communicate experience with other scholars and professors from all over the world.

Last but not the least, I would like to express my deepest heartfelt appreciation and gratitude to my parents, younger brother and sister, for their continuous encouragement, motivation, inspiration, patience, understanding and dedication with best wishes during my study. Feeling loved from my family provides invaluable emotional strength to cope successfully with almost any difficulty that arises in my study and life.

Zhiyi ZHANG

Kyushu University, Fukuoka, Japan

May 2017

TABLE OF CONTENTS

ABSTRACT	I
ACKNOWLEDGEMENTS.....	V
TABLE OF CONTENTS.....	VII
LIST OF FIGURES.....	X
LIST OF TABLES.....	XIII
ACRONYMS AND ABBREVIATION.....	XIV
NOMENCLATURE	XV
CHAPTER 1	1
INTRODUCTION.....	1
1.1 Research Background and Significance	1
1.2 Problems Statement.....	6
1.3 Research Content and Approach	8
References	11
CHAPTER 2	13
STRUCTURES OF THE ROOF STRATA OVER RGSG.....	13
2.1 O-X Breakage Style of the Roof Strata over a Longwall Goaf	13
2.1.1 Roof Strata over a Longwall Goaf in Strike Direction	15
2.1.2 Roof Strata over a Longwall Goaf in Inclination Direction	17
2.2 Structures of the Roof Strata over the RGSG.....	18
2.2.1 Roof Structures over the RGSG as the Thickness of Immediate Roof Varies	18
2.2.2 Improvement of the Hard Roof Structures over RGSG.....	22
2.3 Summary	23
Reference.....	25
CHAPTER 3	26
STRESS AND DEFORMATION DISTRIBUTION OF THE RGSG UNDER DIFFERENT ROOF CONDITIONS.....	26
3.1 Numerical Models	26
3.2 Basic Deformation and Stress Distribution	31
3.2.1 Basic Deformation and Stress Distribution during Roadway Excavation.....	31
3.2.2 Basic Deformation and Stress Distribution during Coal Panel Retreating	36
3.2.3 Basic Plastic Zones Distribution during Coal Panel Retreating	42
3.3 Stress and Deformation Distribution under Different Roof Conditions	44

3.3.1 Different Deformation and Stress Distribution during Roadway Excavation	44
3.3.2 Different Deformation and Stress Distribution during Coal Panel Mining	47
3.4 Summary	54
Reference.....	55
CHAPTER 4	57
STABILITY MAINTAINACE TECHNOLOGY OF THE DEEP RGSG	57
4.1 Basically Staged Supporting Strategy to the RGSG.....	57
4.1.1 Strategy during Gateroad Excavation.....	57
4.1.2 Strategy during Panel Extraction.....	57
4.2 Improvement of Hard Roof Structures over RGSG by Pre-Split Technology	58
4.2.1 Numerical Model.....	58
4.2.2 Deformation of the RGSG Surrounding rock after Improvement	59
4.2.3 Deformation Mechanism before and after Hard Roof Pre-Split.....	62
4.3 Improved Grout Bolting Technology to Control the RGSG Sidewalls.....	65
4.3.1 Improvements of the Grout Bolting Technology	66
4.3.2 Mechanism of the Grouting Technology in RGSG Sidewall.....	69
4.3.3 Effectiveness of the Grout Bolting Technology on RGSG Sidewalls.....	71
4.4 Grouting Reinforcement to Control the Large Heaved Floor.....	75
4.4.1 Mechanism of the Floor Heaves During Coal Panel Mining	76
4.4.2 Grouting Reinforcement of the Floor Heave	78
4.5 Summary	82
Reference.....	83
CHAPTER 5	85
FIELD APPLICATIONS.....	85
5.1 Application of Staged Supporting Method in RGSG with Depth of 900 m.....	85
5.1.1 Geological Condition.....	85
5.1.2 Simultaneous Extraction of Coal and Gas	86
5.1.3 Construction Process and Parameters.....	87
5.1.4 Field Measurements and Discussions.....	92
5.1.5 Roadway Maintenance for the adjacent Coal Panel Extraction.....	93
5.2 Application of Grout Bolting Method in RGSG with Depth of 850 m	96
5.2.1 Geological Condition.....	96

5.2.2 Construction Process and Parameters	97
5.2.3 Field Measurements.....	98
5.3 Application of Hard Roof Pre-Split in RGSG with Depth of 1100 m.....	101
5.3.1 Geological Condition.....	101
5.3.2 Construction Process and Parameters of Roof Pre-Split Blasting	102
5.3.3 Field Measurement	105
5.4 Summary	105
Reference.....	106
CHAPTER 6	108
CONCLUSIONS.....	108
6.1 Main Conclusions.....	108
6.2 Research Prospects	111

LIST OF FIGURES

Figure	Title	Page
Fig. 1-1	Chinese coal production and coal consumption ratio in recent decades	1
Fig. 1-2	Chinese coal resources distribution at different depth	2
Fig. 1-3	Chinese coal resources distribution and deep coal mines location	3
Fig. 1-4	3D structure of the U type gateroads layout	4
Fig. 1-5	3D structure of the Y type gateroads layout	4
Fig. 1-6	Ventilation system and coal pillar reservation in U and Y type longwall systems	5
Fig. 1-7	Failure cases of the deep RGSGs with conventional supporting method	8
Fig. 1-8	Fractures and stress distribution in the overlying strata of goaf	9
Fig. 1-9	Research outline of this dissertation	10
Fig. 2-1	Movement of the main roof and immediate roof over a goaf	14
Fig. 2-2	Plane view of the roof structure over a goaf	15
Fig. 2-3	Section view of the roof structure of goaf in strike direction	16
Fig. 2-4	Section view of the roof structure of goaf in inclination direction	17
Fig. 2-5	Roof structure of the RGSG under different roof condition	21
Fig. 2-6	Hard Roof structure of the RGSG after improvement	23
Fig. 3-1	3D dimensions of the FLAC numerical model	27
Fig. 3-2	Distribution and prestress of the roadway supporting during simulation	30
Fig. 3-3	Location of the measuring station and detecting points in measuring station	31
Fig. 3-4	Curves of deformations of RGSG surrounding rock during roadway excavation	31
Fig. 3-5	Curves of vertical stress in the RGSG surrounding rock after roadway excavation	33
Fig. 3-6	Curves of stress in the RGSG coal sidewall after roadway excavation	33
Fig. 3-7	Curves of horizontal stress in the RGSG after roadway excavation	35
Fig. 3-8	Curves of stress in the RGSG surrounding rock after roadway excavation	35
Fig. 3-9	Deformation of RGSG surrounding rock during coal panel retreating	38
Fig. 3-10	Distribution of vertical stress in right coal sidewall during coal panel retreating	39
Fig. 3-11	Distribution of vertical stress in left sidewall during coal panel retreating	41
Fig. 3-12	Evolution contour of vertical stress in RGSG during panel mining	42
Fig. 3-13	Plastic zone distribution of the RGSG during coal panel mining	43
Fig. 3-14	Curves of deformation of RGSG roof and floor after roadway excavation	44
Fig. 3-15	Curves of deformation of RGSG sidewalls after roadway excavation	45
Fig. 3-16	Stress in RGSG right coal sidewall and roof after roadway excavation	45
Fig. 3-17	Contour of horizontal stress in different RGSG roofs after roadway excavation	47

Fig. 3-18	Deformation curves of RGSG under different roofs during mining	50
Fig. 3-19	Deformation of RGSG surrounding rock under different roofs during coal mining	52
Fig. 3-20	Vertical Stress in RGSG right sidewall under different roofs during panel mining	53
Fig. 4-1	Numerical model of improvement of hard roof structure over the RGSG	59
Fig. 4-2	Curves of deformations of RGSG with and without roof pre-split	61
Fig. 4-3	Contour of deformation under different RGSG roofs before and after pre-split	64
Fig. 4-4	Deformation contour of the goaf overlying strata before and after roof pre-split	65
Fig. 4-5	Structures of the grouting cable bolt	66
Fig. 4-6	Mechanism of the cable bolt in cracked rock with and without grouting	68
Fig. 4-7	Result of pull out tests of conventional bolting and grout bolting in coal	69
Fig. 4-8	Structure model of the RGSG surrounding rock behind the coal face	70
Fig. 4-9	Conventional and modified supporting in RGSG sidewalls	71
Fig. 4-10	RGSG deformations after sidewalls are supported by grout bolting technology	73
Fig. 4-11	Plastic zones distribution of RGSG after grout bolting to sidewalls	74
Fig. 4-12	Deformation mechanism of the RGSG floor heaving before floor grouting	76
Fig. 4-13	Evolution of the stresses in RGSG floor during coal face moving	76
Fig. 4-14	Floor heave of the RGSG at different depth during coal face moving	77
Fig. 4-15	Stress-strain curves of mudstone sample after reinforced by grouting	79
Fig. 4-16	Deformations of the RGSG floor after reinforced by floor grouting	80
Fig. 4-17	Plastic zones distribution in RGSG surrounding rock after floor grouting	81
Fig. 5-1	Geological columnar section stratigraphy of Zhuji coal mine	85
Fig. 5-2	Simultaneous extraction system of coal and gas in Zhuji coal mine	86
Fig. 5-3	Staged supporting system designed for the RGSG in Zhuji coal mine	87
Fig. 5-4	First roadway supporting parameters during roadway excavation (mm)	88
Fig. 5-5	Second roadway supporting parameters before coal face (mm)	89
Fig. 5-6	Second supporting parameters to the gap before coal face (mm)	90
Fig. 5-7	Parameters of the reinforcing steel rebar in wall during third supporting stage	91
Fig. 5-8	Deformations curves of the RGSG during first coal panel mining	93
Fig. 5-9	Profiles of the roadway section in different mining stages	93
Fig. 5-10	Results of the drilling imaging in RGSG roof and right sidewall	94
Fig. 5-11	Vertical stress in shallow part of RGSG right rib	95
Fig. 5-12	Profiles of the RGSG in different processes of section enlarging	96
Fig. 5-13	Position and parameters of the grouting cable bolts in RGSG	98
Fig. 5-14	Integrity of the roof strata before and after hollow grouting cable application	99

Fig. 5-15	Curves of the cable force and roof separations	100
Fig. 5-16	Deformation curves of the roadway's surrounding rock	101
Fig. 5-17	Profiles of the RGSG 100 m behind the mining face	102
Fig. 5-18	Geological columnar section stratigraphy of Pingdingshan coal mine	102
Fig. 5-19	layout of the coal face and RGSG in Pingdingshan coal mine	103
Fig. 5-20	Distribution of the blasting holes in RGSG roof	104
Fig. 5-21	Parameters of the supplemental supporting system behind coal face	105
Fig. 5-22	Profile of the RGSG under hard roof before and after roof pre-split application	105

LIST OF TABLES

Table	Title	Page
Table1	Deformations of the RGSGs with different buried depths	7
Table2	Simulation schemes considering the different thickness of coal seam roof	28
Table3	Mechanics parameters of the rock strata used in simulation	29
Table4	Variations of the cohesion and friction angle of mudstone and coal	29
Table5	Parameters of the rock bolts and cable bolts in simulation	29
Table6	Parameters of the interface in the modified numerical model	59
Table7	Parameters of the pull out tests in mudstone	69
Table8	Residual cohesion and friction angle of coal sidewall after grouting	71
Table9	Residual cohesion and friction angle of floor strata after grouting	78
Table10	Parameters of the blasting settings	104

ACRONYMS AND ABBREVIATION

m/year	Meter per year
mm/d	Millimeter per day
RGSG	Retained goaf-side gateroad
MPa	Megapascal
kPa	Kilopascal
FLAC3D	Fast lagrangian analysis of continua in three dimensions
3D	Three dimension
MPa/m	Megapascal per meter
GPa	10^{11} pascal
SZZ	Vertical stress in z direction
SXX	Horizontal stress in x direction
kN	Kilonewton
m ³ /min	Cubic meters per minute
m ³ /min	Cubic meters per ton
UCS	Uniaxial compressive strength

NOMENCLATURE

k_1, k_2, k_3	Stress concentration factor
γ	Volume-weight of strata
h	Buried depth
h_1	Thickness of immediate roof
h_2	Thickness of main roof
m	Thickness of coal seam
c	Residual bulk factor the caved rock mass
Δh	Subsidence of main roof cantilever at outer edge
φ	Rotation angle of main roof cantilever
L	Length of main roof cantilever
S	Subsidence of this roof cantilever
x_0	Width of yield zone in coal sidewall
a	Width of RGSG
b	Width of packfillings
$\Delta \epsilon_1^{ps}$	Plastic shear increment in the directions of the maximum principal stress
$\Delta \epsilon_3^{ps}$	Plastic shear increment in the directions of the minimum principal stress
$\Delta \epsilon_m^{ps}$	Volumetric plastic shear increment
F	Preforce
σ_x	Stress in x direction
σ_y	Stress in y direction
τ_{xy}	Shear stress
ρ	Distance to point O
Δm	Enlargement of the space of a new crack in surrounding rock
K	Tension stiffness of the cable bolt
Δh_1	Effective extension of the cable bolt before grouting
F_1	Confining force imposed on surrounding rock
Δh_2	Effective extension of the cable bolt after grouting
λ	Lateral stress coefficient
k	Coefficient of vertical stress concentration

H	Thickness of overburdens
C_0	Cohesion of the coal
φ_0	Friction angle of coal
P_x	Confining force of the coal sidewall

CHAPTER 1

INTRODUCTION

1.1 Research Background and Significance

In China, coal production has been increasing quickly in recent decades. With the accelerating development of economy and industrialization in China, coal production increases accordingly, especially in recent years, because the fact that the energy generated by coal consumption accounts for the largest proportion of the total primary energy supply, comparing with that of other energy resource including oil and gas (Fu et al. 2013; Kong et al. 2014; Qian et al. 2015), as shown in Fig. 1-1. Coal production in 2000 is 1.1 billion tons and accounts for 70% of the total energy consumption in China. By 2005, 2010, 2013 and 2016, the production of coal increases sharply to 2.2, 3.3, 4.0 and 3.4 billion tons, taking up 72%, 69%, 67% and 63% of the total energy supply, respectively. Although the percentage of coal production in total energy consumption has decreased recently and will goes down continually in the future according to the Chinese government planning (Wang and Cheng 2012), the coal production still makes up more than 55% proportion of the total energy consumption and keeps 3.8 billion tons per year until 2030.

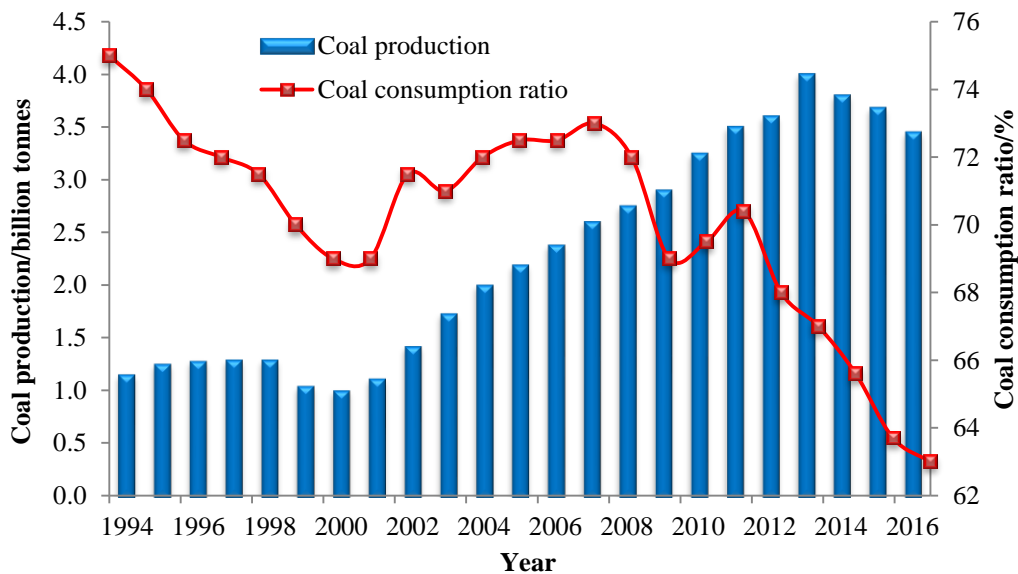


Fig. 1-1 Chinese coal production and coal consumption ratio in recent decades

In China, less than half of the coal resource is buried within 1,000 m under the ground, among which, there is 1,200 billion tons coal resource at a depth of less than 600 m, and 900 billion tons coal resource between 600 m and 1,000 m underground, as shown in Fig. 1-2. According to statistics (China National Coal Association 2013), about 80% of the coal resource within 600 m and 60 % of that from 600 m to 1,000 m underground has been mined out because of easy accessibility. At a deeper depth of more than 1,000 m, however, most of the coal resource is un-mined. By the way, coal distribution in China is characterized by rich in Northwest and poor in Southeast, which is contrary to the economy development, as shown in Fig. 1-3. Faster development of the economy in East area makes higher demand for the coal production there.

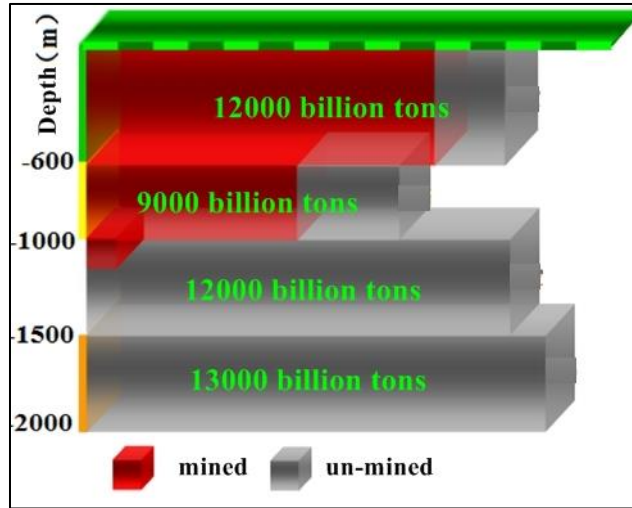


Fig. 1-2 Chinese coal resources distribution at different depth

Consequently, mining level of the underground coal mine in China is approaching to the deep quickly results from growing coal production and limited shallow coal resource, especially in East area. According to the research (He et al. 2005), mining depth of underground coal mine increases with an average speed of 8-12 m/year in China, and a higher speed of 10-25 m/year in East China where about 80% of the underground coal mines with depth of more than 1,000 m are located, as shown in Fig. 1-3.

As mining depth increases, however, the conventional U type longwall mining system (Fig. 1-4) cannot adjust to the new geotechnical conditions associated in the deep mining environment, like high in-situ stress and high gas emission.

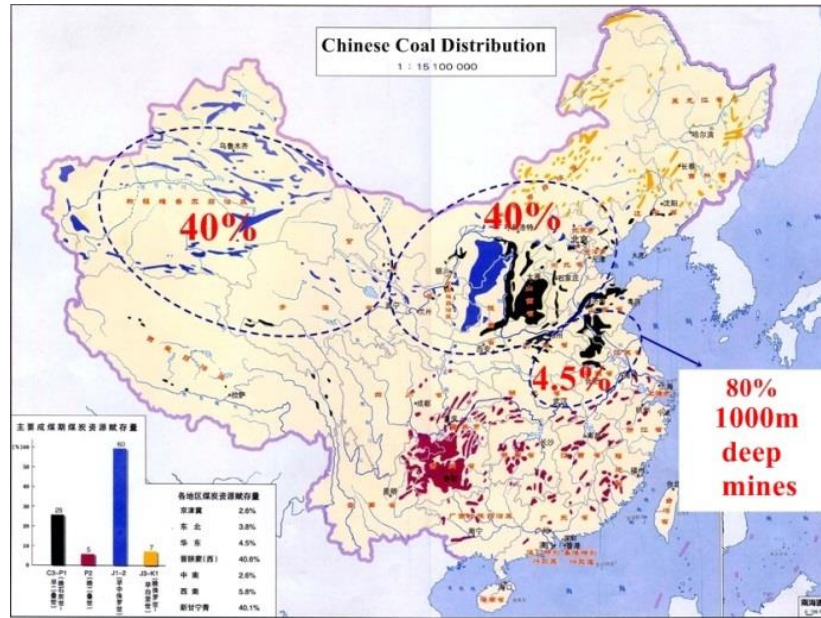


Fig. 1-3 Chinese coal resources distribution and deep coal mines location

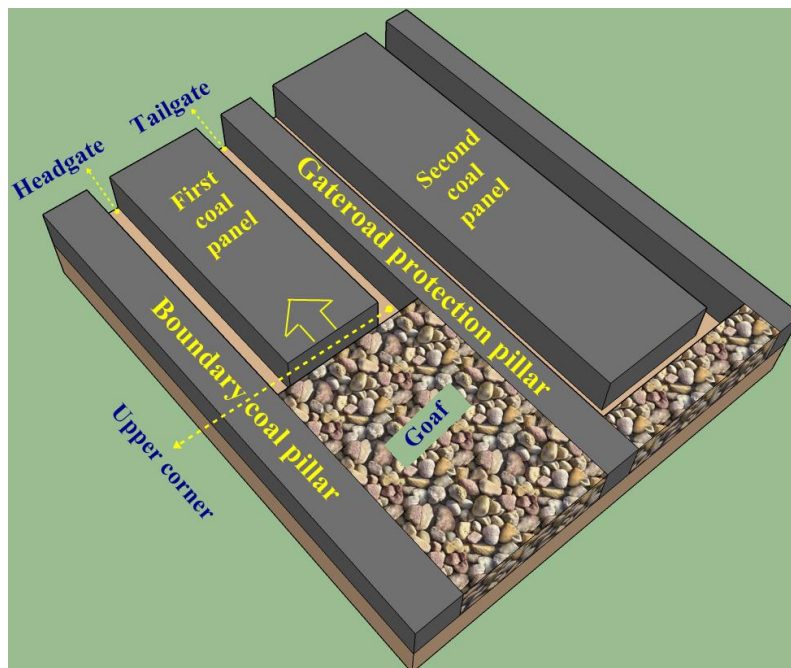


Fig. 1-4 3D structure of the U type gateroads layout

It is generally recognized that, roof strata will break and cave after beneath longwall panel extraction, and consequently, numerous cracks in overlying strata will form. The gas released from nearby strata will flow through these cracks into underlying empty space, especially into the goaf where is filled with caved rock. And then, the accumulated gas in goaf will further flow towards the upper corner of coal face, because

the air pressure there is lowest compared with other places of longwall face in the U type ventilation system. As a result, the upper corner becomes the dangerous place where the gas explosion takes place most frequently. In addition, coal pillars are always retained in underground coal mines to bear the heavy weight of overlying rock mass for the purposes of protecting gateroad space and preventing surface subsidence (Shabarov et al., 2000; Trubetskoy et al., 2011). As mining depth increases, however, this kind of roadway protection coal pillars inevitably becomes extremely large to resist the high stress in deep environment, which leads to serious coal resource loss and adverse stress concentration in neighbouring surrounding rock (Xu et al., 2006; Hudeček et al., 2011; Lu et al., 2012).

From the prospects of this, a modified gateroad layout referred to as the Y shaped one is being taken seriously again by researchers and practice engineers, as shown in Fig. 1-5.

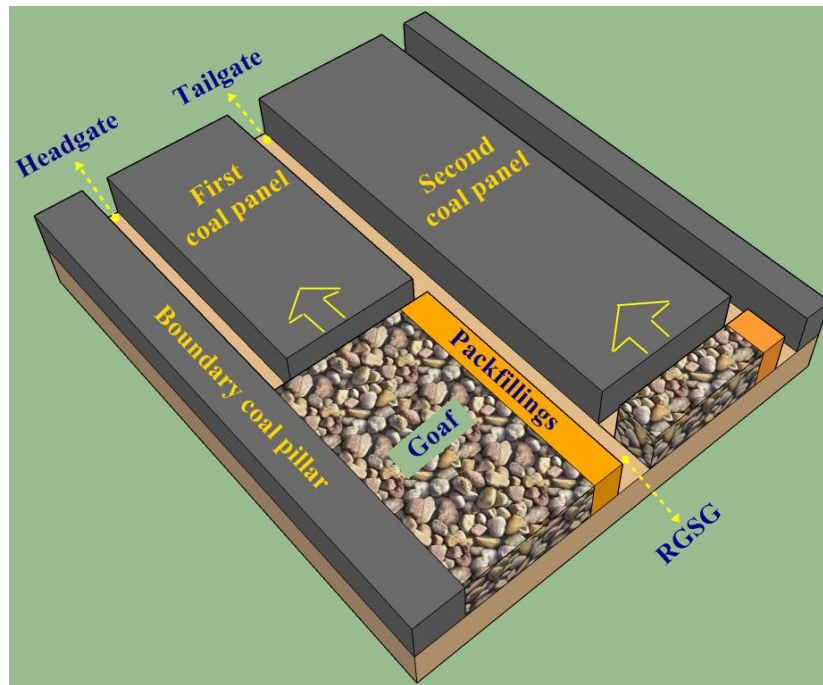


Fig. 1-5 3D structure of the Y type gateroads layout

In this system, a previous gateroad, which is abandoned in the conventional U type settings after coal face passes by, is maintained available by constructing an artificial packfillings (isolating goaf area and supporting roadway roof) along goaf side when coal face passes. This retained gateroad behind coal face is referred to as Retained Goaf Side

Gateroad (RGSG). Compared with conventional U type gateroad layout, this Y shaped one has following advantages:

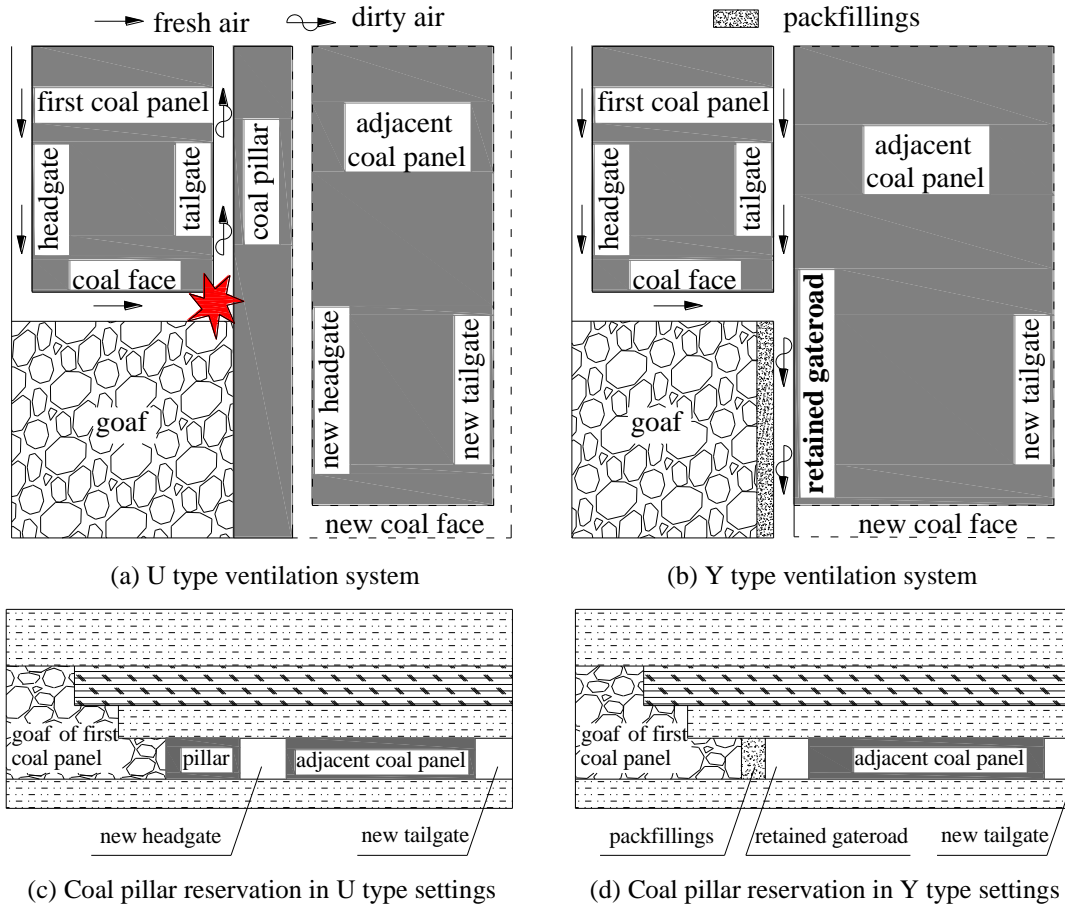


Fig. 1-6 Ventilation system and coal pillar reservation in U and Y type longwall mining systems

(1) Forming the Y type ventilation system to eliminate excessive gas emissions in the upper corner of coal face. The conventional U type ventilation system (Fig. 1-6(a)) has only one entrance and one exit for air circulation, which easily causes excessive gas emissions in the upper corner of coal face due to limited air quantity and air pressure there. In the Y type ventilation system (Fig. 1-6(b)), however, this RGSG can be used as the outlet of dirty air when the first coal panel mining. Consequently, there are two gateroads for fresh air flowing in, which produces more air with higher pressure through the upper corner, preventing gas emissions from goaf flowing into the upper corner of coal face, eliminating the gas accumulation there efficiently (Yuan, 2008; Yang et al., 2014).

(2) Removing large coal pillars. In Y type settings (Fig. 1-6(d)), the RGSG can be reused when the adjacent coal panel mining, as a result, the large coal pillars between two adjacent coal panels in the U shaped one (Fig. 1-6(c)) can be removed, by constructing a relatively small artificial packfillings. Consequently, coal recovery is increased, the stress concentration caused by the large coal pillars is weakened, and the cost for driving a new gateroad for adjacent panel mining is saved.

1.2 Problems Statement

Although the RGSG can resolve the problems that the U type longwall mining system accounts when it is used in the deep mining environment, high in-situ stress there inevitably make challenges to the stability control of the RGSG. Different from the ordinary gateroads in the U type longwall system, the RGSG experiences disturbance not only from roadway excavation and front abutment pressure induced by the first coal face mining, but is also impacted by the stress redistributions behind the first coal face and before the second coal face. Therefore, maintaining the stability of this type of roadways is more difficult. Many researches have been carried out concerning the stability control of the RGSG in recent decades. Qi et al. (1999) put forward the theoretical method to calculate the supporting resistance and deformation of the packfillings of the RGSG. Li (2000) divided the motion process of the RGSG roof into three stages and proposed corresponding design principles for retained roadside packfillings. After that, the RGSG was introduced in top-coal caving longwall face and high water wall-constructing material was tested (Hua 2004; Zhu et al. 2008). Zhu established the mechanical model and calculating formulas for the surrounding rock of the RGSG in a fully-mechanized sub-level caving face; Deng et al. (2010) used roadside cable bolt and single hydraulic prop to reinforce the concrete wall. Ma (2011) concluded a mechanical model for the roof of the RGSG in gangue backfilling mining system; Chen (2012) researched the floor heaving mechanism of the RGSG in different mining stages and proposed corresponding reinforcing method; Zhang (2013) and Deng (2014) analyzed supporting and deformation of the surrounding rock of the RGSG in inclined coal seam; Ning (2014) used a soft-strong roadside support in the RGSG to adjust the varying load imposed by overlying roof strata in different mining stages.

Most of the RGSGs in shallow area can be maintained effectively according to above valuable theory and techniques. As mining depth increases, however, some special geotechnical conditions create new challenges to the support of the deep-seated RGSG.

(1) High-stress environment in deep coal mines. The in-situ stresses in a mine are composed of the stresses generated by the weight of overlying strata and others induced by geological structures. The former contributes mainly to the vertical in-situ stress and the latter contributes primarily to the horizontal in-situ stress (Brown and Hoek 1978; Leont'ev et al. 2013). Hence, the vertical in-situ stress increases in proportion to the thickness of overburden at a rate of approximately 0.021 MPa/m with assumption that the average density of the overburden is typically 2,100 kg/m³. Consequently, the high in-situ stresses are largely the driving forces of the instability of deep underground excavations.

(2) Plastic mechanics in deep coal mines. As discussed above, rock will suffer high in-situ stresses in a deep mining environment. According to the existing literatures, rock records obvious plastic behavior under the high stress condition (Yang et al. 2014; Kurlenya et al. 2014), instead of the elastic one in the shallow buried. In addition, the roadway's surrounding rock in deep coal mines are usually weak (e.g., mudstone, shale and coal), which means that the surrounding rock is more sensitive to a stress disturbance and more prone to experience large deformations.

Table 1 Deformations of the RGSGs with different buried depths

Coal mine	Buried depth (m)	Wall-to-wall Convergence (mm)	Roof-to-floor convergence (mm)	Section shrinkage rate
Pan II	430	700	1,020	51.7%
Xieqiao	610	870	2,148	76.6%
Guqiao	780	1,510	2,139	79.4%
Dingji	850	1,800	2,360	81.3%

The high in-situ stress and plastic rock mechanics in deep coal mines require higher requirement for the roadway supporting techniques. Conventional support methods (e.g., a steel arch shed, rock bolt and cable bolt) cannot maintain the long-term stability of the deep-seated RGSG. According to the field investigations conducted in the Anhui province, China, deformations and failure cases of some deep-seated RGSGs supported by the conventional methods are shown in Table 1 and Fig. 1-7. Results show that the

section shrinkage of the deep-seated RGSG is up to 80% and this shrinkage performs rising tendency as the buried depth increases.



(a) Steel arch shed



(b) Conventional rock bolt



(c) Conventional cable bolt



(d) Single hydraulic props



(e) Floor heaving



(f) Packfillings collapse

Fig. 1-7 Failure cases of the deep RGSGs with conventional supporting method

1.3 Research Content and Approach

Concentrated stress in the surrounding rock of goaf induced by overlying strata movement is the driving force of the instability of nearby working space. It is well known that the overlying strata near coal seam will break and cave after the underlying coal panel is extracted and the overlying strata far from the coal seam will just break or sink to

some extent because of the supporting of the previous caved rock. Consequently, three zones over the extracted goaf will form, including caved zone, fractured zone and continuous deformation zone, respectively, from bottom to up, as shown in Fig. 1-8.

The movements of overlying strata will trigger the redistribution of the in-situ stress around the goaf, and the wider these zones are, the larger the redistributed abutment stresses in the surrounding rock are and the severer the corresponding disturbance to the working space in a longwall system is, especially to the RGSG that located along the side of the goaf.

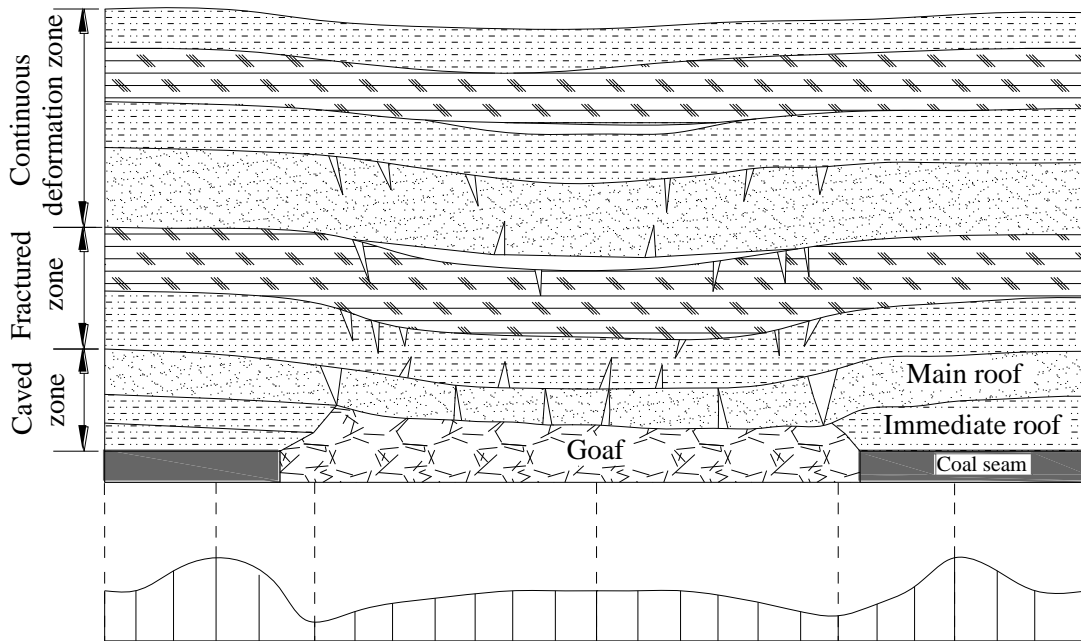


Fig. 1-8 Fractures and stress distribution in the overlying strata of goaf

Concentration factor of the mining induced stress is determined by the range of disturbed zones in the overlying strata which is controlled mainly by the occurrence of the rock strata near coal seam. When the roof strata near coal seam are weak and thick, the extracted space due to coal mining can be filled fully by the caved rock mass. Consequently, little free space is provided for the further sink of overlying strata, and the corresponding disturbance to the underlying working space is weak.

From the prospects of this, this paper focuses on the stability maintainance of the RGSG in deep underground coal mine. Because of the fact that the RGSG is located at the edge of extracted goaf, and the disturbing stress in the roadway surrounding rock is mainly induced by the structure adjustment of overlying strata of beside longwall goaf,

which is originally determined by the occurrence of the roof strata near the coal seam. This research is started from the analysis of the roof structure over the RGSG as the thickness of hard main roof and weak immediate roof varies. And then, distribution of stresses and deformations in the RGSG surrounding rock under different roof conditions are studied using numerical method, and corresponding characteristics of the roadway instability are revealed. After that, the methods of maintaining the roadway stability are proposed in terms of above concluded roadway instability characteristics to support the RGSG under different roofs and the effectiveness of these methods are verified by means of numerical analysis and field experiment. The research outline is illustrated in Fig. 1-9.

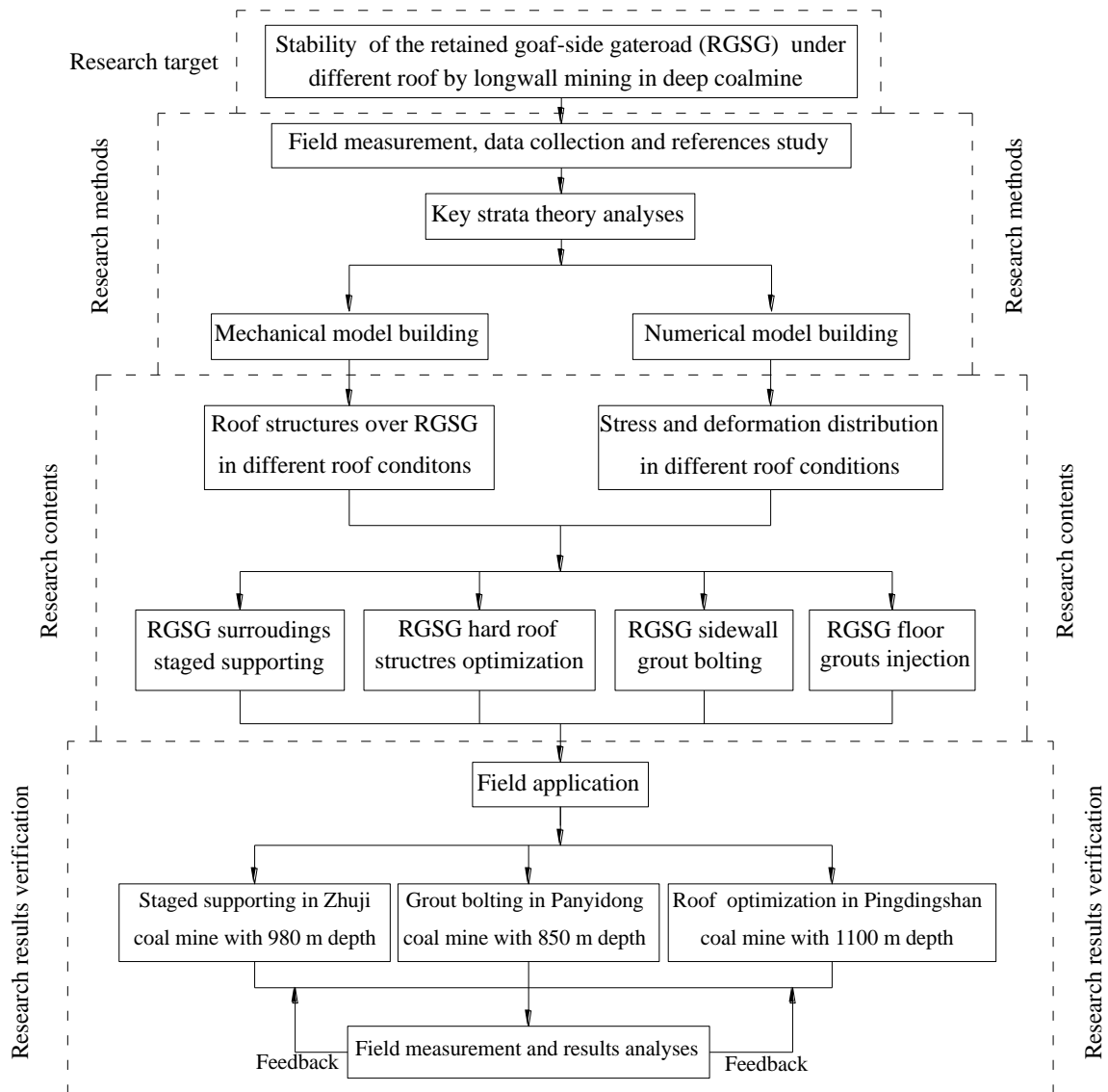


Fig. 1-8 Research outline of this dissertation

References

- Fu F, Liu H, Polenske KR, Li Z (2013) Measuring the energy consumption of Chinese domestic investment from 1992 to 2007. *Applied Energy* 102: 1267-74.
- Kong SL, Cheng YP, Ren T, Liu HY (2014) A sequential approach to control gas for the extraction of multi-gassy coal seams from traditional gas well drainage to mining-induce stress relief. *Applied Energy* 131: 67-78.
- Qian DY, Shimada H, Sasaoka T, Wahyudi S, Pongpanya (2015) Stability of roadway in upper seam of deep multiple rich gas coal seams through ascending stress-relief mining. *Memoirs of the Faculty of Engineering, Kyushu University* 75(2): 1-22.
- Wang L, Cheng Y (2012) Drainage and utilization of Chinese coal mine methane with a coal-methane Co-exploitation Model: Analysis and Projections. *Resources Policy* 37(3): 315-321.
- China National Coal Association (2013) Forum on mining technology of 1000 m-plus deep coal mines in China, Taian, China (In Chinese)
- He MC, Xie HP, Peng SP, Jiang YD (2005) Study on rock mechanics in deep mining engineering. *Chinese Journal of Rock Mechanics and Engineering* 24(16): 2803-13 (In Chinese)
- Shabarov AN, Selivonik VG, Sidorov DV (2000) Calculation of pillar unloading parameters during mining of ore deposits. *Journal of Mining Science* 36, 22-29.
- Trubetskoy KN, Ruban AD, Zaburdyaev VS (2011) Characteristics of methane release in highly productive coal mines. *Journal of Mining Science* 47, 467-475.
- Xu T, Tang CA et al. (2006) Numerical investigation of coal and gas outbursts in underground collieries. *Int J Rock Mech Min Sci* 43, 905-919.
- Hudeček V, Stoniš M (2011) Method of drilling of coal pillar. *Journal of Mining Science* 47, 367-375.
- Lu CP, Dou LM, Liu H (2012) Case study on microseismic effect of coal and gas outburst process. *Int J Rock Mech Min Sci* 53, 101-110.
- Yuan L (2008) Gas distribution of the mined-outside and extraction technology of first mined key seam relief-mining in gassy multi-seams of low permeability. *Journal of China Coal Society* 33, 1362-1367.
- Yang W, Lin BQ, Yan Q, Zhai C (2014) Stress redistribution of longwall mining stope and gas control of multi-layer coal seams. *Int J Rock Mech Min Sci* 72, 8-15.
- Qi TY, Guo YG, Hou CJ (1999) Study on the adaptability for the pack-fillings of the gob-side entry retaining. *Journal of China Coal Society* 03, 256-260.

- Li HM (2000) Control design of roof rocks for gob-side entry. *Chinese Journal of Rock Mechanics and Engineering* 19, 651-654.
- Hua XZ (2004) Study on gob-side entry retaining technique with roadside packing in longwall top-coal caving technology. *Journal of Coal Science and Engineering* 10, 9-12.
- Zhu CQ, Miao XX, Liu Z (2008) Mechanical analysis on deformation of surrounding rock with road-in packing of gob-side entry retaining in fully-mechanized sub-level caving face. *Journal of Coal Science and Engineering* 14, 24-28.
- Deng Y, Tang J, Zhu X., Fu Y, Dai Z (2010) Analysis and application in controlling surrounding rock of support reinforced roadway in gob-side entry with fully mechanized mining. *Mining Science and Technology* 20, 839-845.
- Ma Z, Gong P, Fan J, Geng M, Zhang G (2011) Coupling mechanism of roof and supporting wall in gob-side entry retaining in fully-mechanized mining with gangue backfilling. *Mining Science and Technology*. 21, 829-833.
- Chen Y, Bai J, Yan S, Xu Y, Wang X, Ma S (2012) Control mechanism and technique of floor heave with reinforcing solid coal side and floor corner in gob-side coal entry retaining. *International Journal of Mining Science and Technology* 22, 841-45.
- Zhang YQ, Sun LL, Zhang WZ, Cao LD (2013) The numerical simulation and supporting design of gob-side entry retaining in gradient medium thick coal seam. *Applied Mechanics and Materials* 368-370, 1812-1815.
- Deng Y, Wang S (2014) Feasibility analysis of gob-side entry retaining on a working face in a steep coal seam. *International Journal of Mining Science and Technology* 24, 499-503.
- Ning J, Wang J, Liu X, Qian K, Sun B (2014) Soft-strong supporting mechanism of gob-side entry retaining in deep coal seams threatened by rockburst. *International Journal of Mining Science and Technology* 24, 805-810.
- Brown ET, Hoek E (1978) Trends in relationships between measured in-situ stresses and depth. *Int J Rock Mech Min Sci* 15, 211-215.
- Leont'ev AV, Makarov AB, Tarasov AY (2013) In-situ stress state assessment in the Nurkazgan Mine. *Journal of Mining Science* 49, 550-556.
- Yang SQ, Xu P, Ranjith PG (2014) Evaluation of creep mechanical behavior of deep-buried marble under triaxial cyclic loading. *Arab J Geosci*, 8(9), 6567–6582.
- Kurlenya MV, Mirenkov VE, Shutov VA (2014) Rock deformation around stopes at deep levels. *Journal of Mining Science* 50, 1001-1006.

CHAPTER 2

STRUCTURES OF THE ROOF STRATA OVER RGSG

Structures dynamic adjustment of the overlying strata is the source of the abutment stress in the goaf surrounding rock. Overlying strata will move after coal seam is extracted, and meanwhile, the balance of in-situ stress is broken. Stress will redistribute along with the adjustment of roof structures, and the nearby engineering space will be disturbed by this redistributed stress until the roof strata structures get a new balance. Therefore, having a deep insight of the structures of the overlying strata is the basement of understanding of the stress distribution in goaf surrounding rock which is the driving force of nearby roadway instability.

2.1 O-X Breakage Style of the Roof Strata over a Longwall Goaf

The fact that the RGSG is located behind the coal face and at the edge of the extracted goaf determines that the roof structure of the RGSG is formed as a result of the movements of the strata over the longwall goaf. For this, analyzing the structure of the overlying strata of a longwall face firstly is essential, if we want to throw light on the characteristics of roof structure over the RGSG.

Several relative researches about the roof structures over a longwall face have been carried out in recent decades. Stoke firstly proposed the cantilever theory in 1916, in which he believed that the roof over an extracted goaf behaved like an hanging cantilever of which one end is fixed in coal and the other is free and this cantilever broken periodically when the hanging length extended to a certain value. Hack and Gillitzer proposed the pressure arch theory in 1928, in which they claimed that the roof blocks could get structure and stress balance shaped in arch of which one side is supported by the coal ahead of coal face and the other is supported by the caved rock in goaf, and the support in coal face just needed to bear the weight of the rock mass within this arch. Кузнецов of the Soviet Union put forward the articulation theory and divided randomly caving zone and regularly moving zone according to the movement of overlying strata after coal extraction. He hold the opinion that the rock blocks in the regularly moving zone can form stable structure by articulation each other and calculated the bearing

strength of the supports in coal face in the assumptions of “given deformation” and “given load”, respectively. Whittaker (1977) proposed the cantilever theory over a longwall face. Smart (1982) put forward the detached block theory based on static rock mechanics. Chines Qian (1982) established arch-articulated beam theory over goaf by combination of the previous articulation theory and numerous measurements of ground behaviors in longwall mining field. He claimed that the overlying strata always formed O-X style breakage after coal panel was extracted and then formed stable articulated structure over the goaf. This theory explains most of the ground behaviors in longwall mining system. And then, Miu and Qian (1999; 2000 and 2003) further proposed the Key Strata Theory to reveal the influences of longwall mining on the underground water, the gas distribution in near strata and the surface subsidence. Qian’s theory has become to the basement for the researchers and engineers to control the ground behavior in the longwall mining system.

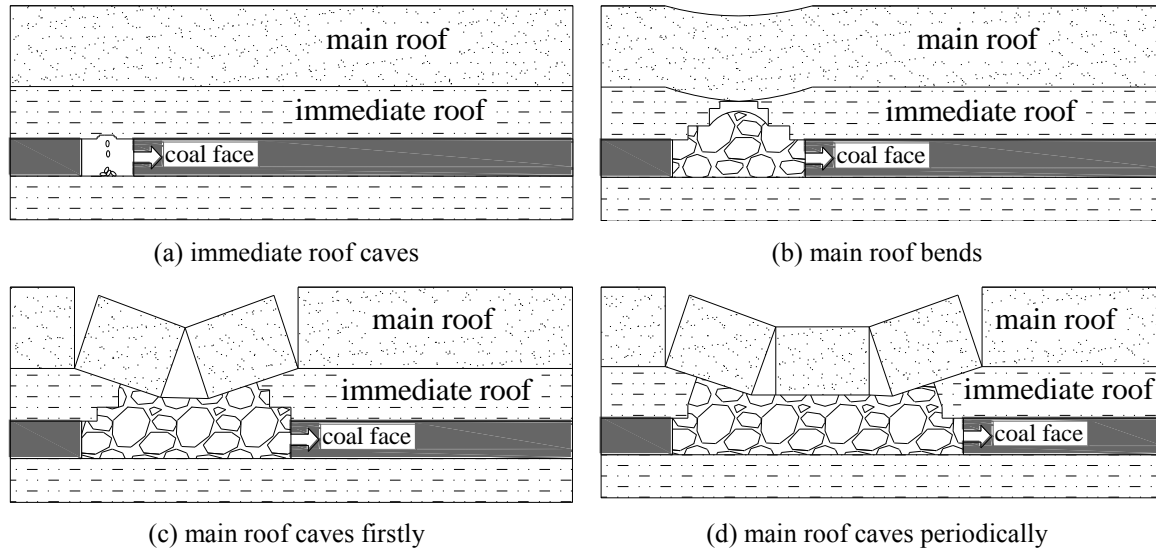


Fig. 2-1 Movement of the main roof and immediate roof over a goaf

According to the Key Strata Theory, movements of overlying strata of a longwall panel are controlled primarily by several key strata with large hardness and thickness. Once these key strata break, O-X style cracks will form, and all the weak strata over them will break and sink immediately, which causes significant influence on the working space under them. Usually, the immediate roof over coal seam is multilayer and is comprised of one or many kinds of weak rock mass with low mechanical properties, like mudstone, shale, etc. The main roof over the immediate roof is integral and is made up of hard roof

mass with high mechanical properties, like sandstone and siltstone, etc. The main roof always acts as one of the Key Strata whose movements impose serious impact on the underlying engineering space. As shown in Fig. 2-1, immediate roof will break and cave quickly because of gravity and low strength when coal face advances from opening cut position. Meanwhile, the main roof is exposed and the bending moment appears in it. As the coal face advances continually, the bending moment in the main roof increases accordingly results from the exposed area rising. When the bending moment in the main roof reaches its strength limit, cracks will appear, and followed by caving first time. After that, the main roof will experience periodical break as the coal face moves forward continually. Finally, the main roof forms O-X style breakage, as shown in Fig. 2-2.

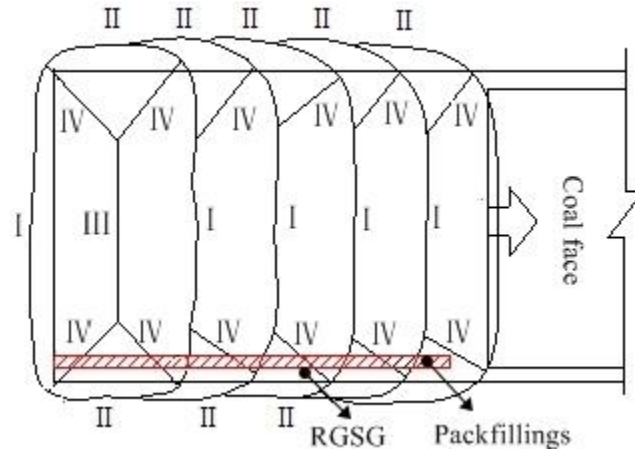


Fig. 2-2 Plane view of the roof structure over a goaf

Ideally, the four-edges clamped roof plate over extracted goaf breaks firstly along its long edges I because the fact that the bending moment there reaches the tensile strength limit firstly, and then undergoes cracks along the short edges II. O shaped cracks form, and the force condition of this roof plate changes to four-edges simply supporting. After that, the middle position III of this four-edge simply supported roof plate will break, and finally followed by the inclined cracks IV as this rock plate caves toward middle position from two mutually perpendicular directions. Finally, X shaped cracks inside preformed O shaped one form. As the coal face advances continually, cracks I, II and IV will occur periodically.

2.1.1 Roof Strata over a Longwall Goaf in Strike Direction

Roof structures adjustment over goaf in strike direction determines the influence time on the beneath RGSG. When the main roof breaks and caves periodically with the advancing of the coal face, the previous caved immediate roof is compacted gradually. At the same time, strata in higher position start to curve, break and cave due to the increase of exposed area. However, these strata cannot cave randomly because of limited free space. The more fully the extracted space is filled by the caved immediate roof, the less free space is provide for the movements of this part of strata. As a result, these broken rock blocks connect to each other and form stable articulated beam. In a much higher range, strata cannot break results from more limited free space which is needed for large bending moment formation in the strata. Consequently, these strata just curve and deform continuously. With the moving of coal face continually, the disturbed range over goaf becomes wider and wider until reach new stress and structure balance. Finally, three zones divided according to the cracks development form in vertical direction, including caved zone, fractured zone and continuous deformation zone, as shown in Fig. 2-3.

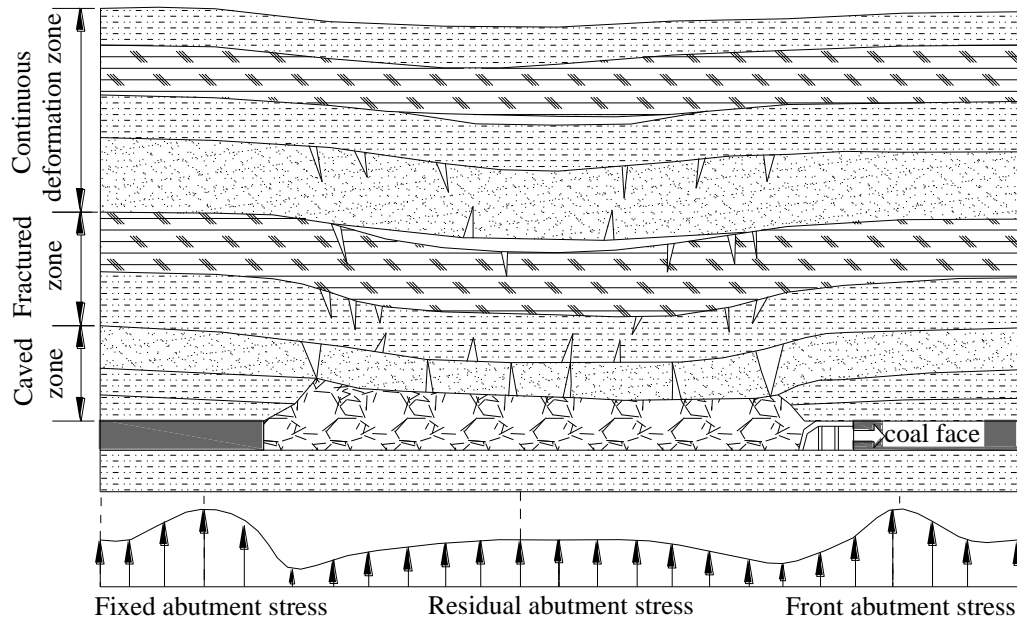


Fig. 2-3 Section view of the roof structure of goaf in strike direction

As described above, three zones in the overlying strata with different cracks distribution form when the coal seam is mined. During the structure adjustment of overlying strata, in site stress in these rock mass will redistribute and transfer towards the deep of surrounded solid rock. Consequently, concentrated abutment stress appears in the

solid coal before coal face and behind the opening cut. Because the caved rock is compacted gradually by the subsidence of overlying strata, its bearing strength increases and the stress in it also recover to some extent. The RGSG is located along the side of goaf, and hence, it will suffer all the period of stress re-distribution in the coal face moving direction. This stress re-distribution starts at the beginning of coal seam extraction and stops when the overlying strata reach new structural and force balance. The longer the structures adjustment of overlying strata is, the severer the influence on the RGSG stability is. According to the field observation, the weaker and the thicker the immediate roof strata are, the shorter the roof structure adjustment over goaf is.

2.1.2 Roof Strata over a Longwall Goaf in Inclination Direction

Roof structures adjustment over goaf in inclination direction determines the influence intensity on the beneath RGSG. Similar to the roof structures adjustment in strike direction, the overlying strata in inclination direction also curve, break and move to seek new balance after coal extraction, as shown in Fig. 2-4. These movements will impose adverse influence directly on the under RGSG.

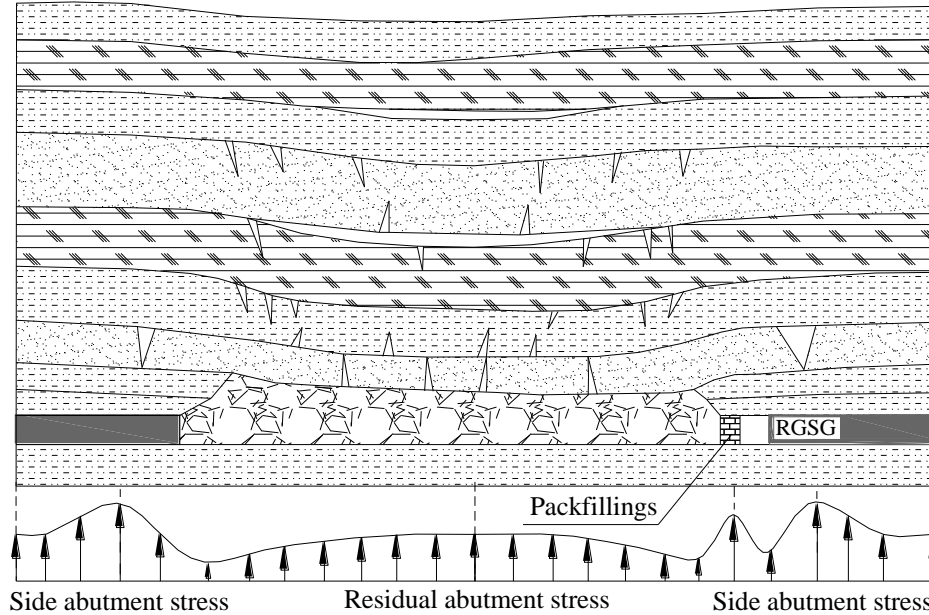


Fig. 2-4 Section view of the roof structure of goaf in inclination direction

During the adjustment of the overlying strata in inclination direction, concentrated side abutment stress appears in packfillings and coal sidewall. It is important to note that the side abutment pressure in packfillings and coal sidewall is different from the above

mentioned residual abutment stress which is located at the middle of goaf. The stress in packfillings, coal sidewall and rock mass in goaf is generated by the compression of overlying strata. It means that the packfillings, coal sidewall and caved rock mass in goaf bear the weight of overlying strata together, and the side abutment stress in packfillings and solid coal sidewall will decrease when the residual abutment stress in caved rock mass increases and vice versa. The former is responsible for the instability of the RGSG at the edge of goaf, and the latter is determined by increasing bearing strength due to compaction.

As a result of the O-X style breakage, main roof cantilever shaped in triangle along the goaf side will form, under which the RGSG located. The harder and the thicker the main roof strata are, the longer this roof cantilever is. Because of the fact that the heavy weight from cantilever itself and overlying strata is so large that the present roadside packfillings is not capable of bearing, this roof cantilever rotates pivot on the crack position until touches the already caved rock. This rotation movement generates additional vertical force and horizontal force which makes main factors of the instability of the RGSG packfillings.

2.2 Structures of the Roof Strata over the RGSG

As concluded above discussion, stability of the RGSG is difficult to control because the high abutment stress generated by the strata movement over goaf both in strike and in inclination direction and the additional stress induced by the roof movements over the goaf. The RGSG shows different instability characteristics under different roof conditions.

2.2.1 Roof Structures over the RGSG as the Thickness of Immediate Roof Varies

Usually, the immediate roof strata can cave timely and fill the excavation to some extent after coal is extracted, and the movements of the overlying strata can be weakened because of the supporting of caved immediate roof strata, and the corresponding influence on underlying working space is not so severer. When the immediate roof is weak and thick enough, the excavation will be filled fully after coal is mined. The main roof will not break and all the weight of overlying strata will be supported by the intact main roof, and the RGSG suffers minimum influence, especially on the RGSG packfillings, as shown in Fig. 2-5(a). In this situation, however, the deformations of other

parts of roadway (roof and floor) are still very large, resulting from the low mechanical parameters of the surrounding rock. Supporting point of this kind of large roadway should be focused on the improvement of weak rock mechanics.

As the thickness of the weak immediate roof decreases, caved rock mass cannot fills the excavation fully after compaction. As a result, the main roof will break due to insufficient supporting of the caved rock mass and heavy load from overlying strata, as shown in Fig. 2-5(b). Theoretically, this broken roof cantilever will rotate pivots on the crack position until touch the caved rock mass in goaf. The subsidence (Δh) of this roof cantilever at outer edge can be calculated according to Equation 1.

$$\Delta h = h_1 + m - ch_1 = m - (c - 1)h_1 \quad (1)$$

Where, h_1 is the thickness of immediate roof; m is the thickness of coal seam; c is the residual bulk factor the caved rock mass. And the rotation angle (φ) can be calculated using Equation 2.

$$\varphi = \sin^{-1}\left(\frac{\Delta h}{L}\right) \quad (2)$$

Where, L is the length of the main roof cantilever, which is determined by the mechanical characters of the roof strata. The harder and thicker the main roof is, the longer this cantilever is.

Therefore, the subsidence of this roof cantilever at any horizontal positions can be illustrated as Equation 3.

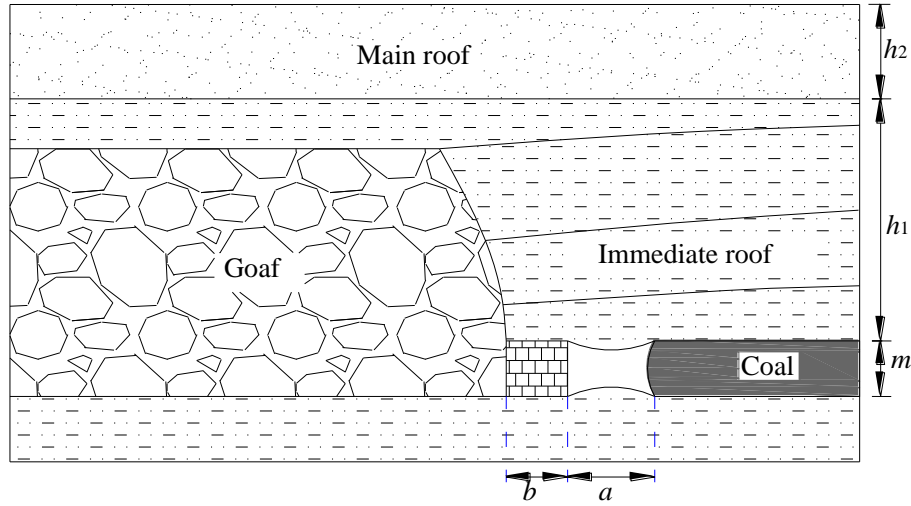
$$S = \tan \varphi \cdot x \quad (3)$$

Where, x is the horizontal distance from the calculated position to the inner end of roof cantilever. In Fig. 2-5(b), x_0 is the width of yield zone in coal sidewall; a is the width of RGSG; b is the width of packfillings.

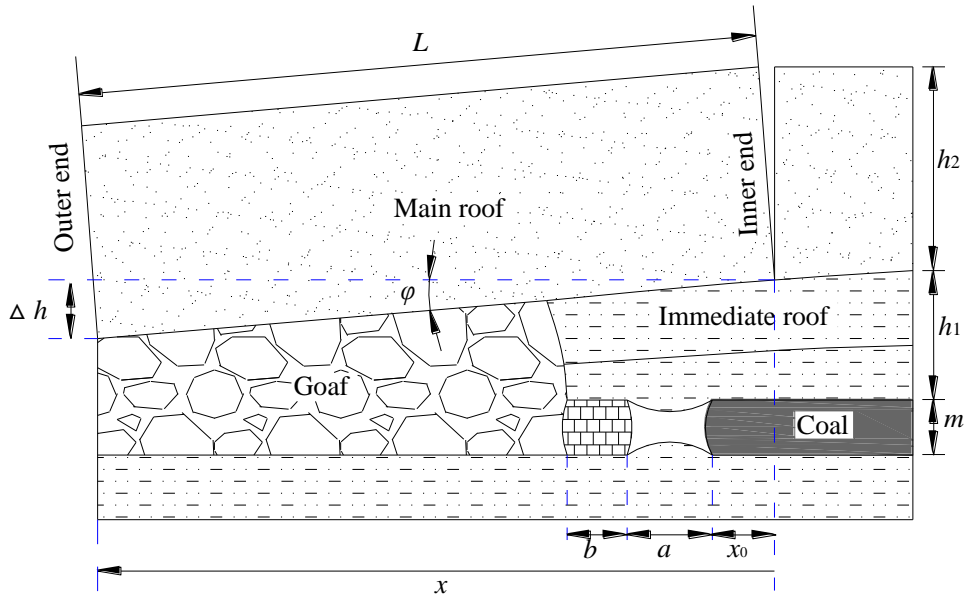
Subsidence of this roof cantilever will compress the underlying rock mass, including the RGSG surrounding rock. As for the caved rock mass in goaf, it's bearing strength increases because of compaction; for the roadway packfillings and coal sidewall, lateral dilatation and cracks appear; for the roadway roof and floor, squeeze into roadway space will happen. In this situation, the deformations of roadway surrounding rock are larger than that in the first situation, and the compressive strength on packfillings also becomes larger. Therefore, not only the roof and floor, but also coal sidewall and

packfillings should be put into consideration when making a design for the RGSG stability maintainance in this kind of situation.

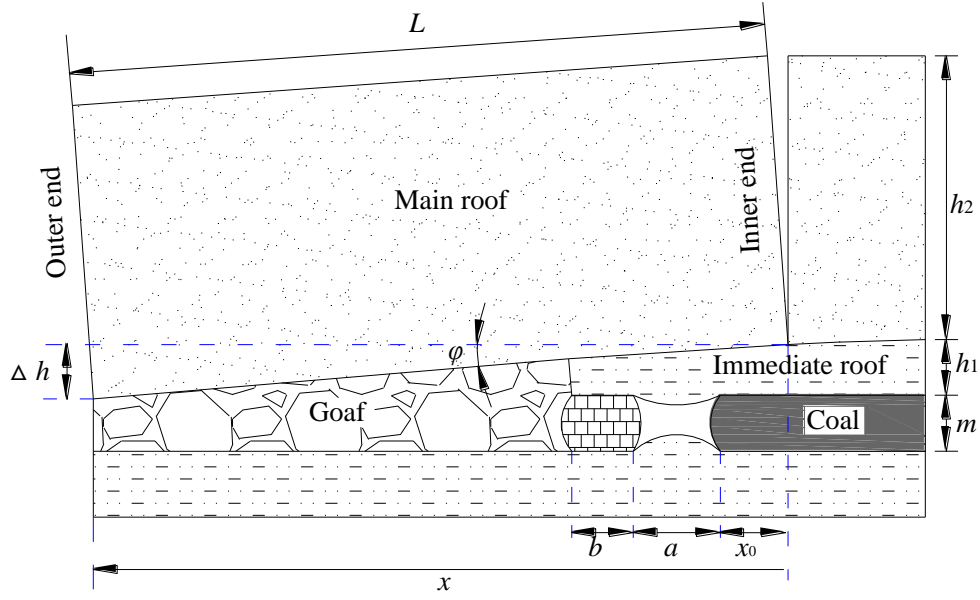
When the thickness of the immediate roof decreases continually (in Fig. 2-5(c)), the subsidence (Δh) and the rotation angle (φ) of the main roof cantilever increase accordingly. As a result, a longer roof cantilever with larger thickness will form over the RGSG. Increased roof subsidence and rotation caused by this longer main roof cantilever inevitably leads to more compression to the underlying rock mass, leading to severer deterioration to the RGSG surrounding rock.



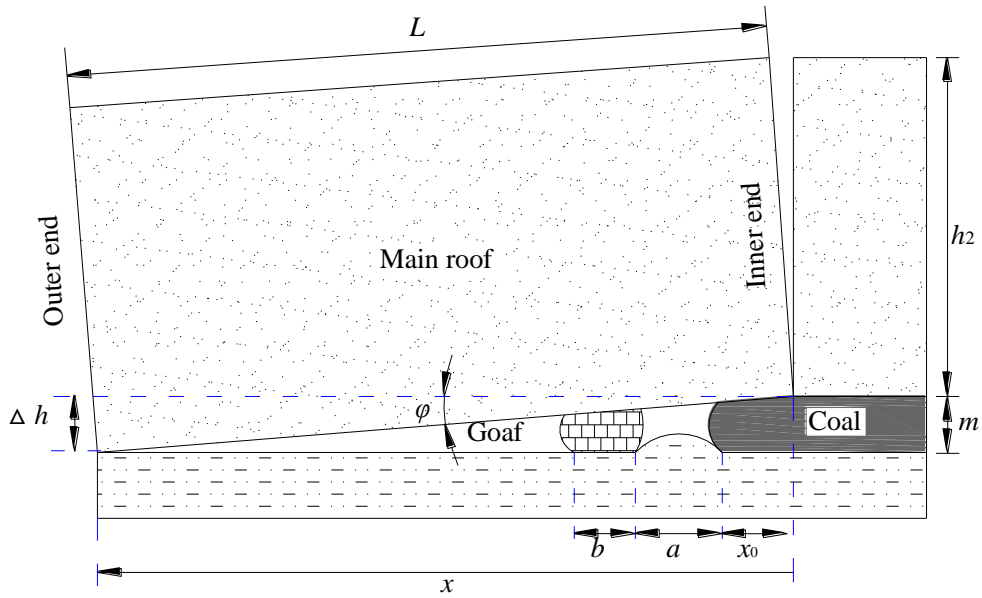
(a) Roof structure of the RGSG under thick immediate roof



(b) Roof structure of the RGSG under middle-thick immediate roof



(c) Roof structure of the RGSG under thin immediate roof



(d) Roof structure of the RGSG under main roof directly

Fig. 2-5 Roof structure of the RGSG under different roof condition

When the immediate roof disappears and the coal seam is covered by the hard main roof directly, the RGSG stability is most difficult to control. The hard roof will not break for a long time after coal extraction, resulting from high strength. A heavy load from the large area roof weighting will be imposed on the surrounding rock of the underlying working space, especially on the RGSG at edge of the goaf. When the hard roof breaks, a larger free space ($\Delta h=m$) is provided for a longer rock cantilever moves. Large

deformation energy generated by the main roof cantilever subsidence is absorbed by the roadway surrounding rock except for roof. As a result, RGSG floor, packfillings and coal sidewall are deteriorated significantly, especially the packfillings will collapse results from too much compression and likely topples due to the additional horizontal force generated by the roof cantilever rotation. Last but not the least, wind blast damage is also likely happens at the moment of hard roof cracking. In this situation, roadway supporting interest should be focused on the reduction of the influence of hard roof cantilever movement through roof structure improvement.

2.2.2 Improvement of the Hard Roof Structures over RGSG

According to above analysis, stability of RGSG is difficult to control, especially beneath hard main roof directly. According to the field measurement to a RGSG engineering under immediate sandstone of 18 m thick, in an underground coal mine of China, the average mining thickness is 2.0 m, average length of roof cantilever is 30 m, average width of yield zone is 4.0 m, width of roadway is 5.0 m, and width of packfillings is 3.0 m. Substituting these values of parameters into Equation 1, 2 and 3, the roof subsidence due to rotation, over middle of yield zone, roadway and packfillings are 134 mm, 436 mm and 704 mm, respectively. This subsidence deteriorated roadway surrounding rock seriously. For instance, cracks and fissures occurred in coal sidewall and packfillings, bedding separations formed in roof. As a consequence, several roadway instabilities including roof caving, coal sidewall and packfillings collapse and floor heaving were triggered.

Although some adaption were made on the RGSG packfillings to adjust this kind of situation (Tan et al. 2015), to resolve this problem radically, nature fracturing position of the hard roof strata over the RGSG has to be interfered artificially using some rock breaking technologies. In the past, the hard rock breaking technology was mainly used to reduce the risk of rock burst (Petr et al. 2013; Song et al. 2014) and to protect the mining equipment in coal face (Sun et al. 1990; Aler et al. 1996; Huang et al. 2013; Wang et al. 2013; Huang et al. 2015), through blasting or hydraulic fracturing. Application of this technology in the RGSG is few, and relative investigations are not enough.

As discussed in Section 2.1.1, the side abutment pressure generated by the movements of overlying strata in whole goaf area is difficult to change, once certain

geological and mining conditions are determined. The additional abutment pressure influencing roadway significantly and produced by the long roof cantilever movements, however, can be reduced by shortening the cantilever length through some special geotechnics. When roof is pre-split ahead of coal face along the outer edge of packfillings, this hard roof is expected to break along this crack after coal is extracted (Fig. 2-6).

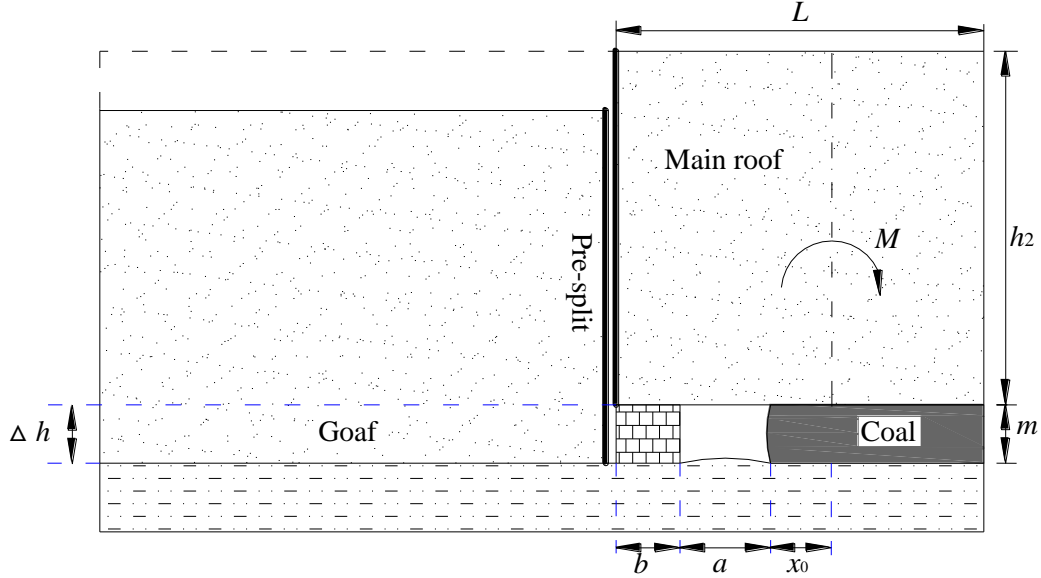


Fig. 2-6 Hard Roof structure of the RGSG after improvement

Compared with the situation in the Fig. 2-5(d), long roof cantilever over the RGSG is shortened considerably after improvement, as shown in Fig. 2-6. The mechanical connection between the roof over roadway and other part over goaf is cut off, and the part of roof over RGSG just needs to bear the weight of overlying strata within a small scope (x_0+a+b), being free from the severe roof caving in goaf area. Additionally, there will be no obvious cracks along the strike direction in the roadway overlying roof stratum, therefore, this intact rock mass can resist the rotation by itself with a large opposing torque M . Consequently, the rotation of the roof over the RGSG can be decreased considerably, and the roadway surrounding rock suffers little additional abutment pressure and corresponding deterioration.

2.3 Summary

RGSG is located behind the coal face and at the edge of the extracted goaf, and the roof structure of the RGSG is formed as a result of the movements of the strata over the

longwall goaf. Therefore, the roof structure over a longwall goaf is analyzed first in this chapter, and followed by the study of roof structure over RGSG. Finally the improvement of the roof structure over RGSG when it is beneath hard main roof directly is proposed. The detailed conclusions are as follows.

(1) O-X shaped cracks form in the main roof over goaf after coal seam is extracted. After coal seam is mined, overlying immediate roof cracks and caves timely and irregularly, and the main roof, however, follows O-X breakage style orderly when the coal face advances continually. O shaped cracks form firstly around the rectangular goaf and X shaped fractures form subsequently in previous formed O shaped one.

(2) RGSG is influenced significantly by the movements of the overlying strata of goaf. Because the fact that the RGSG is located at the edge of extracted goaf, it is disturbed by the abutment stress induced by the movements of goaf overlying strata. Roof structures adjustment over goaf in strike direction determines the influence time on the beneath RGSG. Roof structures adjustment over goaf in inclination direction determines the influence intensity on the beneath RGSG.

(3) Main roof cantilever forms over the RGSG and influences the stability of the RGSG by followed sinking and rotation. As a result of the O-X style breakage of the main roof over goaf, a triangular shaped rock cantilever forms over the RGSG. Because of insufficient supporting of the caved rock mass and heavy load from overlying strata, this rock cantilever over RGSG sinks and rotates. Consequently, surrounding rock of the RGSG are deteriorated results from compression of cantilever movements. The thicker the main roof is and the thinner the immediate roof is, the more serious the influence is.

(4) Roof structure over the RGSG is optimized by shortening the length of main roof cantilever through pre-split technology. The influence on RGSG from overlying strata movements in strike direction is difficult to change once a certain geological condition is determined, and another influence in inclination direction, however, can be reduced by shortening the length of main roof cantilever. After the main roof is pre-split, mechanical connection between the roof over roadway and other part over goaf is cut off, and the rotation of the roof over the RGSG can be decreased considerably, and the roadway surrounding rock suffer little additional abutment pressure and corresponding deterioration.

Reference

- Whittaker BN (1977) Design Loads for Gateside Packs and Support Systems. Mining Engineer.
- Smart BGD, Davies DO et al. (1982) Application of the Rock Strata Title Approach to Pack Design in an Arch—Sharped Roadway. Mining Engineer.
- Qian M (1982) A study of the behavior of overlying strata in long wall mining and its application to strata control, Strata Mechanics. Elsevier Scientific Publishing Company, 13-17.
- Miu XX, et al. (1999) The analysis of complex effect of key stratum in overlying strata within mining influence. Ground Pressure and Strata Control (3-4): 19-21.
- Miu XX, Qian MG (2000) New development of theoretical study on key strata of mining rock strata. Journal of China University of Mining 29(1): 25-28.
- Qian MG, et al. (2003) Key strata theory of rock strata control. Xuzhou: Coal Mining University Press.
- Tan YL, Yu FH, Ning JG, Zhao TB (2015) Design and construction of entry retaining wall along a gob side under hard roof stratum. Int J Rock Mech Min Sci;77:115–21.
- Konicek P, Soucek K, Stas L, Singh R (2013) Long-hole destress blasting for rockburst control during deep underground coal mining. Int J Rock Mech Min Sci;61:141–53.
- Song DZ, Wang EY, Liu ZT et al. (2014) Numerical simulation of rock-burst relief and prevention by water-jet cutting. Int J Rock Mech Min Sci;70:318-31.
- Sun GZ, Wang J, Zhang WB (1990) Theory and application of controllable hydrofracturing techniques to control hard roof collapse in Datong coal mine. International Journal of Rock Mechanics and Mining Sciences & Geomechanics Abstracts;27:A75.
- Aler J, Du Mouza J, Arnould M (1996) Measurement of the fragmentation efficiency of rock mass blasting and its mining applications. International Journal of Rock Mechanics and Mining Sciences & Geomechanics;33:A315.
- Huang BX, Yu B, Feng F, Li Z et al. (2013) Field investigation into directional hydraulic fracturing for hard roof in Tashan Coal Mine. Journal of Coal Science and Engineering;19:153–9.
- Wang FT, Tu SH, Yuan Y et al. (2013) Deep-hole pre-split blasting mechanism and its application for controlled roof caving in shallow depth seams. Int J Rock Mech Min Sci;64:112–21.
- Huanga BX, Wang YZ, Cao SG (2015) Cavability control by hydraulic fracturing for top coal caving in hard thick coal seams. Int J Rock Mech Min Sci;74:45–57.

CHAPTER 3

STRESS AND DEFORMATION DISTRIBUTION OF THE RGSG UNDER DIFFERENT ROOF CONDITIONS

As mentioned above, Qian's theory was introduced into the analyses of roof structure over the RGSG and several valuable models were founded, including curved triangular block model (1987), rock plate superposition model (1993), and given deformation model (2000). These valuable models facilitate the theoretical calculating of the required bearing strength of the RGSG surrounding rock and give scientific guidance to the engineering practice in the field. However, some essential parameters are always difficult to be quantified because the fact that measurement of caving activity in the field is dangerous and costly to some extent.

Numerical techniques have proven to be a powerful tool in the study of the rock mechanics problems in underground openings. Advances in computational science over the last fifty years have seen many numerical methods developed for solving rock engineering problems. These methods can be classified into continue, discontinue and hybrid methods. Continue methods are well suited to solve problems involving heterogeneous or non-linear material properties. Rock failure is identified when the stresses applied on an element exceed the predefined failure strength. Among the continue methods, the FLAC3D numerical software have been widely used to simulate underground coal mine excavations. In this paper, this software is used to analyze the stress and deformation distribution in the RGSG surrounding rock when coal panel retreating, to reveal the failure characteristics of the RGSG and to design corresponding methods to control the roadway stability.

3.1 Numerical Models

In order to analyze the accurate stress and deformation distribution in the surrounding rock of the RGSG with different roof conditions, a representative 3D numerical model is built using the FLAC3D software, according to the typical geological condition in Eastern of China where most of the deep underground coal mines with depth

of more than 1,000 m are located. Several considerations involved in this simulation are listed as follows.

(1) Considering the computing efficiency and accuracy, this model has 1170,000 zones with the 3D dimensions of 60 m along z -direction, 400 m along y -direction and 300 m along x -direction, as shown in Fig. 3-1. The displacement boundaries of the model are set as roller boundaries along the sides, and pinned boundary along the bottom. A vertical stress as much as 19.7 MPa is applied at the top of model to simulate the weight of overburden of 940 m thickness, assuming the average volume weight of the overlying strata is $2.1 \times 10^4 \text{ N/m}^3$, and the at-rest pressure coefficient is taking as 1.0 when setting the horizontal stress at other boundaries.

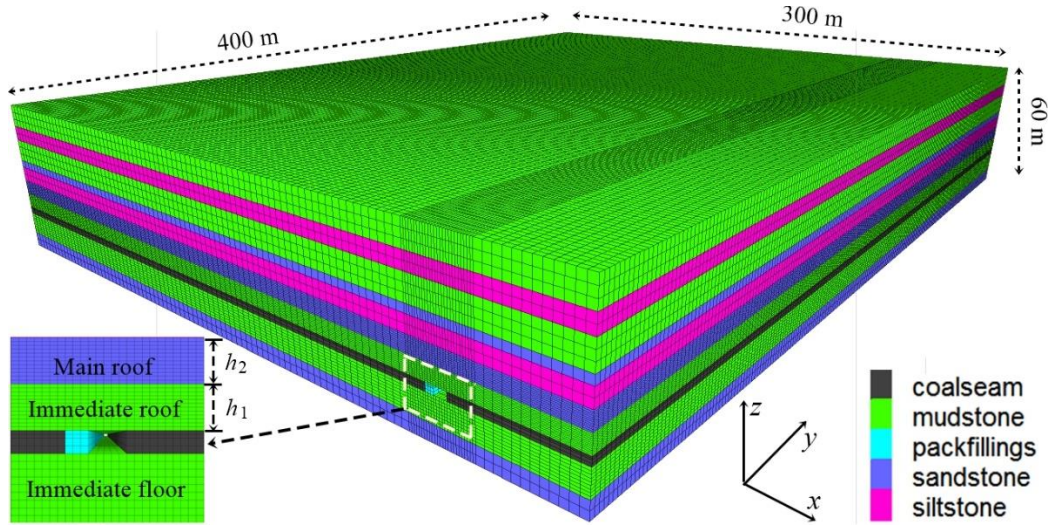


Fig. 3-1 3D dimensions of the FLAC numerical model

(2) In this model, coal seam is 3 m thick and gateroad is 5.0 m wide and 3.0 m high, and the packfillings is 3 m wide and 3 m high. The immediate roof is mudstone and the main roof is sandstone. In order to model the caving activity of the immediate roof and supporting function of the caved rock mass to the overlying strata, the immediate roof is also excavated together with coal seam, and the excavation is filled with soft elastic material (Yan et al., 2013). The whole thickness of the immediate roof and the main roof is setting to be a certain value of 12 m which is the thickness that the immediate roof needs to fully fill the excavation when 3 m thick coal seam is mined, and here the residual bulk factor of the immediate mudstone is taken as 1.25. Seven types of the combinations of immediate roof and main roof are considered in this simulation, as

shown in Table 2. The thickness of main sandstone increases as immediate mudstone becomes thin gradually, and the backfilling thickness is calculated in each situation according the corresponding thickness of the immediate roof.

Table 2 Simulation schemes considering the different thickness of coal seam roof

Schemes No.	Thickness of coal seam m/m	Thickness of immediate roof h_1/m	Thickness of main roof h_2/m	Thickness of excavation $m+h_1/m$	Thickness of backfilling $/m$
I	3	12	0	15	15.0
II	3	10	2	13	12.5
III	3	8	4	11	10.0
IV	3	6	6	9	7.5
V	3	4	8	7	5.0
VI	3	2	10	5	2.5
VII	3	0	12	3	0

(3) The coal seam, mudstone strata are set as strain softening constitutive materials to simulate the softening behavior of these weak rock mass in deep mining environment, whose strength decreases as the plastic shear strain increases, rather than keeps constant as the Mohr-Coulomb model (Mortazavi 2009). The specific relationships between the decrements of a particular mechanical parameter and the shear strain increment can be illustrated as following Equations 4 and 5 (Itasca Consulting Group Inc. 2012). The ultimate elastic bulk and shear modulus of the packfillings in goaf are set as 0.268 GPa and 0.156 GPa, respectively. Other rock strata including sandstone, siltstone and packfillings are set as Mohr constitutive material. The mechanical parameters of all rock mass used in this model is listed in Tables 3 and 4, which have been modified following the works of Mohammad (1997).

$$\Delta k^S = \frac{1}{\sqrt{2}} \sqrt{(\Delta \epsilon_1^{Ps} - \Delta \epsilon_m^{Ps})^2 + (\Delta \epsilon_m^{Ps})^2 + (\Delta \epsilon_3^{Ps} - \Delta \epsilon_m^{Ps})^2} \quad (4)$$

Where $\Delta \epsilon_1^{Ps}$ and $\Delta \epsilon_3^{Ps}$ are the plastic shear increment in the directions of the maximum principal stress and minimum principal stress, and the $\Delta \epsilon_m^{Ps}$ is the volumetric plastic shear increment and can be calculated as Equation 5 (Itasca Consulting Group Inc. 2012).

$$\Delta\epsilon_m^{Ps} = \frac{1}{3}(\Delta\epsilon_1^{Ps} + \Delta\epsilon_3^{Ps}) \quad (5)$$

Table 3 Mechanical parameters of the rock strata used in this simulation

Strata	Density (kg/m ³)	Bulk modulus (GPa)	Shear modulus (GPa)	Cohesion (MPa)	Friction angle (°)
Siltstone	2,600	3.03	1.84	1.5	28
Mudstone	2,400	2.68	1.56	Table 4	Table 4
Coal	1,450	1.19	0.37	Table 4	Table 4
Sandstone	2,700	5.40	4.00	2.2	33
Packfillings	2,500	4.50	3.00	2.0	30

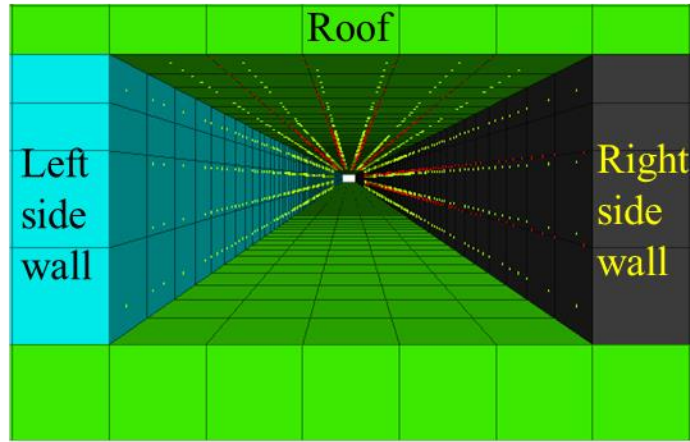
Table 4 Variations of the cohesion and friction angle of mudstone and coal

Mechanical parameters	Mudstone		Coal	
Plastic shear strain	0	0.1	0	0.1
Cohesion/ (MPa)	1.2	0.12	0.8	0.08
Friction angle/ (°)	27	24	23	20

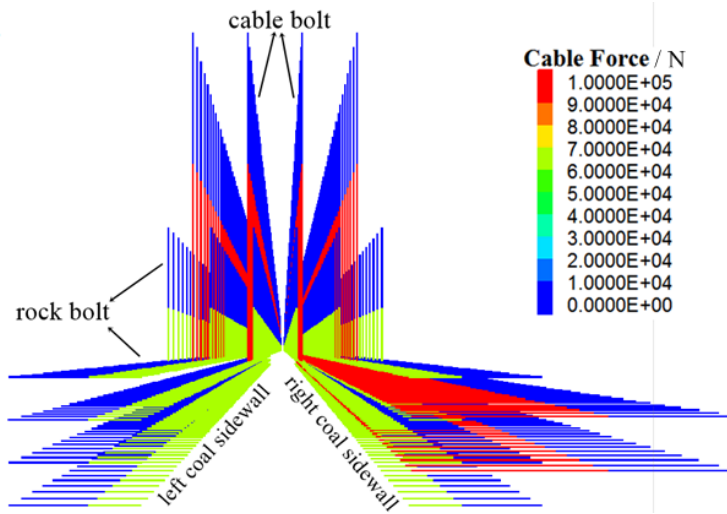
(4) Roadway supporting is also installed in these simulations according to the present criterion applied in the underground coal mines in Eastern China, as shown in Fig. 3-2. Detailedly, conventional rock bolts (end anchored) with a diameter of 22 mm and a length of 2500 mm in roof and coal sidewalls, with an inter-row space of 0.8 m×0.8 m; conventional cable bolts (end anchored) with a diameter of 22 mm and a length of 6000 mm only in roof strata and right coal sidewall, with an inter-row space of 1.0 m×0.8 m. In the left coal sidewall, cable bolt is not installed because the obstruction to the coal cutting. The parameters used in rock bolt and cable bolt setting are listed in Table 5.

Table 5 Parameters of the rock bolt and cable bolt in this simulation

Supporting type	E _{mod} (N/m ²)	Y _{tens} (N)	X _{care} (m ²)	Gr _{coh} (N/m)	Gr _k (N/m ²)	Gr _{per} (m)	Anchorage length (m)
Rock bolt	2×10^{10}	2.5×10^5	3.7×10^{-4}	9×10^5	2×10^7	9×10^{-2}	1.4
Cable bolt	8×10^{10}	5.8×10^5	3.7×10^{-4}	1×10^5	2×10^7	9×10^{-2}	2.4



(a) Distribution of the rock bolts and cable bolts in roadway surrounding rock



(b) Prestress of the rock bolts and cable bolts

Fig. 3-2 Distribution and prestress of the roadway supporting during simulation

(5) The simulation sequences are as follows: (i) generating initial stresses, (ii) excavating the gateroad and installing roadway supporting, (iii) retreating coal panel and constructing the packfillings along the goaf side. During roadway excavation and coal panel retreating, the stresses and deformations in roadway's surrounding rock are monitored, and the measuring station and point distribution are shown in Fig. 3-3. The measuring station is located 160 m away from the opening cut to monitor the stress and deformation distribution in roadway surrounding rock as the distance from coal face to measuring station changes.

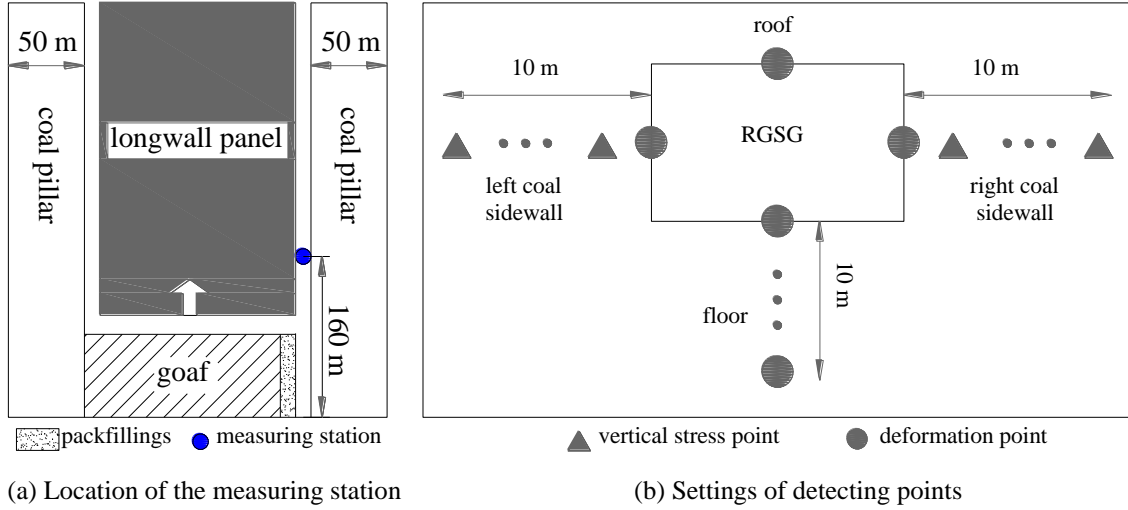


Fig. 3-3 Location of the measuring station and detecting points settings in measuring station

3.2 Basic Deformation and Stress Distribution

3.2.1 Basic Deformation and Stress Distribution during Roadway Excavation

3.2.1.1 Deformation distribution during roadway excavation

In order to understand the behavior of roadway surrounding rock under the disturbance of roadway excavation activity, deformations of the roadway surrounding rock are measured, and the results are shown in Fig. 3-4. The x coordinate is the computing steps after roadway excavation and the Global Mechanical Ratio Limit of this simulation is 1.0×10^{-5} .

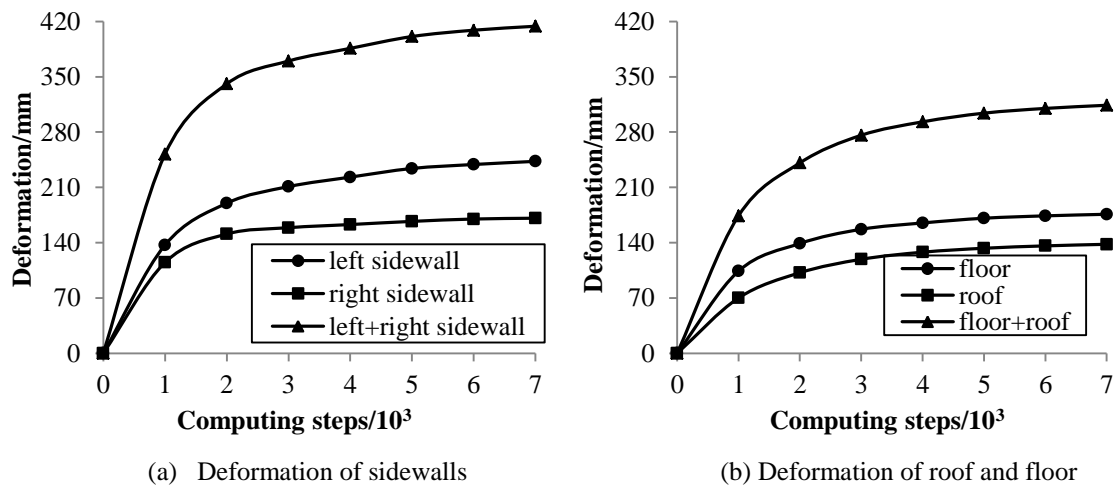


Fig. 3-4 Curves of deformations of RGSG surrounding rock during roadway excavation

From the Fig. 3-4(a), we can see that the deformations of coal sidewalls increase sharply after roadway excavation, and reach approximately 115 mm when the computing steps are 1.0×10^3 . After that, the increase speed of coal sidewalls slow down, and the deformation of left one continually rises to 243 mm when the computing steps are 7.0×10^3 and the deformation of right one rises slightly to 171 mm when the roadway surrounding rock reach balance again. Apparently, during the roadway excavation stage, the deformation of left coal sidewall plays main contribution to the roadway section shrinkage, according for about 51.4% of the whole decrement of roadway width.

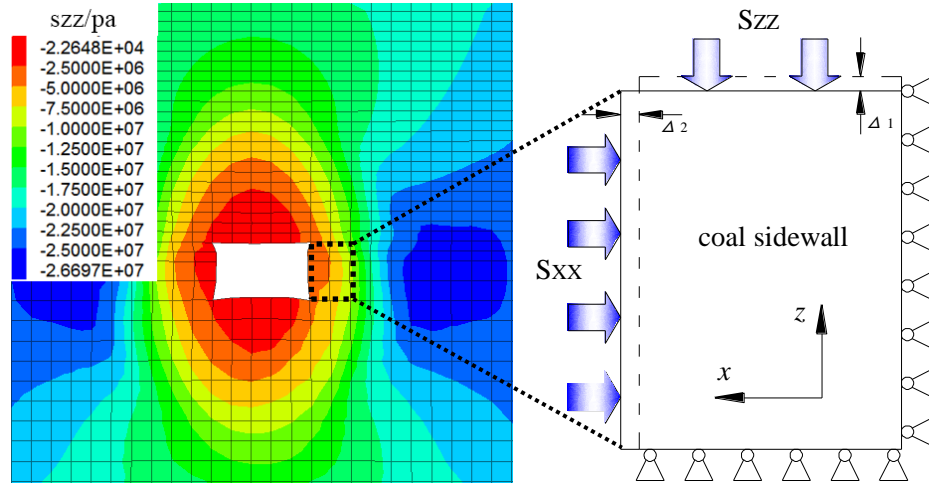
From the Fig. 3-4(b), we can find that the deformations of roof and floor experience similar variation to that of coal sidewalls. Roof sag and floor heave increase sharply after roadway excavation, and reach approximately 70 mm and 104 mm, respectively when the computing steps are 1.0×10^3 . And then, the deformation increasing speed slows down, and the deformation of roof gradually rises to 138 mm when the computing steps are 7.0×10^3 and the deformation of floor rises centrally to 176 mm when the roadway surrounding rock reach balance again. During this period, the deformation of floor is larger than that of roof, although the roof is supported by rock bolts and cable bolts, and the floor is not supported.

3.2.1.2 Stress distribution during roadway excavation

As known that, the in-situ stress in roadway surrounding rock redistributes after roadway excavation, and consequently, roadway surrounding rock perform corresponding deformations. To reveal the deformation mechanism of roadway surrounding rock during the stage of roadway excavation, stresses redistributions in roadway surrounding rock are measured.

(1) Stress distribution in roadway sidewall

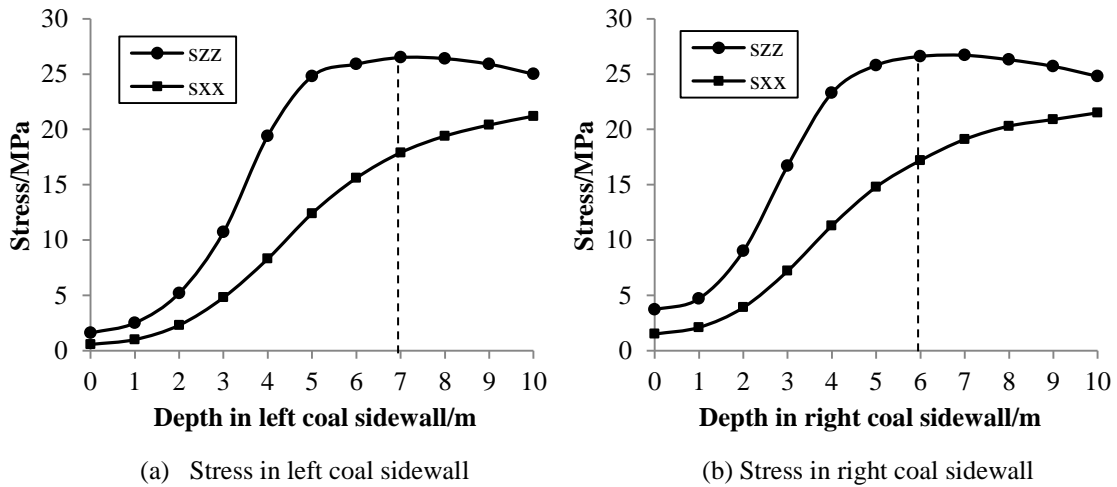
Figure 3-5(a) represents the vertical stress contour in roadway surrounding rock after roadway excavation. We can see that, vertical stress concentrates in coal sidewalls, and in roof and floor, however, the vertical stress releases significantly in a large range. Meanwhile, roadway coal sidewall performs deformation towards roadway space to some extent. In order to illustrate the deformation mechanism of the coal sidewall, a model is built as shown in Fig. 3-5(b).



(a) Vertical stress contour in roadway surrounding rock (b) Mechanical model of coal sidewall

Fig. 3-5 Curves of vertical stress in the RGSG surrounding rock after roadway excavation

Before roadway excavation, this part of rock in coal sidewall can bear high stress because it is under the three dimensional stresses environment (Brook 1997), in which the confining stress is as much as 21 MPa in x direction. After roadway excavation, the high confining stress in x direction disappears, and consequently, the bearing strength of this part of rock in coal sidewall reduces considerably, and the shallow part of coal sidewall cannot resist the high vertical stress. As a final result, shallow part of surrounding rock undergoes breakage, goes into plastic stage and experiences vertical compression Δ_1 and horizontal squeeze Δ_2 into roadway, and at the same time, the vertical stress on coal sidewall decreases and its peak value transfers into deeper position gradually, which is accompanied by the further broken and deformation of the shallow part of coal sidewall.



(a) Stress in left coal sidewall

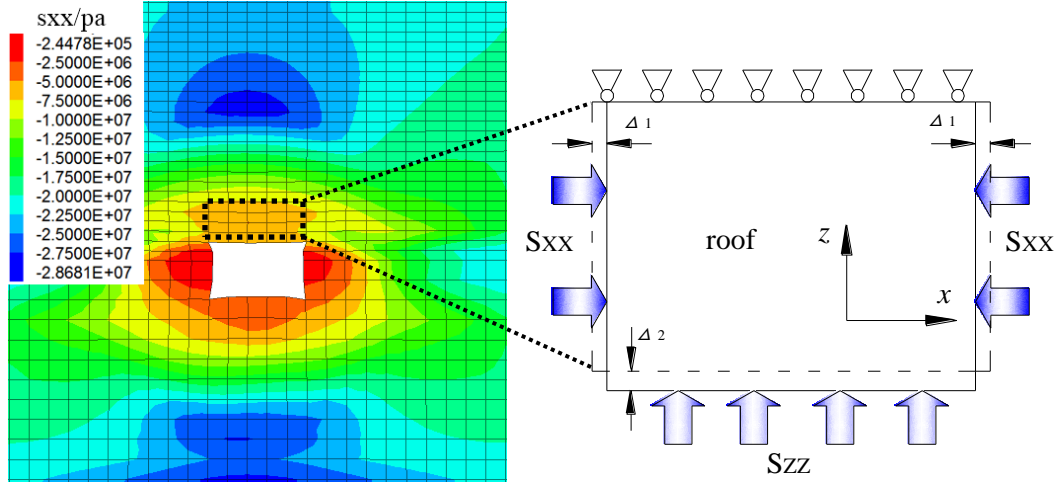
(b) Stress in right coal sidewall

Fig. 3-6 Curves of stress in the RGSG coal sidewall after roadway excavation

To value the specific disturbance of roadway excavation to the gateroad coal sidewall, exact stress in the surrounding rock were measured, as shown in Fig. 3-6. Figs. 3-6(a) and (b) represent the stress distribution in left and right coal sidewall, respectively. In left coal sidewall, vertical stress (s_{zz}) and horizontal stress (s_{xx}) in the shallow range both decrease and the horizontal stress is reduced more dramatically compared with the vertical stress. Specially, the vertical stress increases from the coal sidewall surface, reaching peak value (roughly 26.5 MPa) at a depth of approximately 7.0 m and then decreases gradually; the largest coefficient of the vertical stress concentration is found to be 1.26 (26.5 MPa/21 MPa). While, the horizontal stress increases continually from the surrounding rock surface. In right coal sidewall, stress performs similar distribution to the left one, except for the location of the peak vertical stress which is 6.0 m from the sidewall surface. It is believed that the behavior of the shallow range of coal sidewall is governed primarily by the horizontal confining stress that significantly influences the bearing capacity of surrounding rock. In right coal sidewall, two more cable bolts are installed compared with the left one, and the cable bolts can provide high confining stress to the right coal sidewall. It is the reason why the location of the peak vertical stress in right coal sidewall is shallower than that in left coal sidewall, and the deformation of right coal sidewall is less than that of left coal sidewall.

(2) Stress distribution in roadway roof and floor

Conversely, horizontal stress concentrates in roadway roof and floor, and the vertical stress releases after roadway excavation, as shown in Fig. 3-7(a). Another model is built, as shown in Fig. 3-7(b), to explain the deformation mechanism of roof and floor. After roadway excavation, the high confining stress in z direction disappears, and consequently, the bearing strength of this part of rock in roof and floor reduces considerably. As a result, the shallow part of roof and floor cannot resist the high horizontal compressive stress and experiences horizontal compression Δ_1 and vertical squeeze Δ_2 into roadway, and at the same time, the horizontal stresses in shallow part of roof and floor decrease and its peak value transfers into deeper position gradually, which is accompanied by the further broken and deformation of the shallow part of roadway roof and floor.



(a) Horizontal stress contour in roadway surrounding rock (d) Mechanical model of roof

Fig. 3-7 Curves of horizontal stress in the RGSG surrounding rock after roadway excavation

To value the specific disturbance of roadway excavation to the gateroad roof and floor, exact stress in the surrounding rock were measured. Figs. 3-8(a) and (b) represent the stress distribution in roof and floor, respectively.

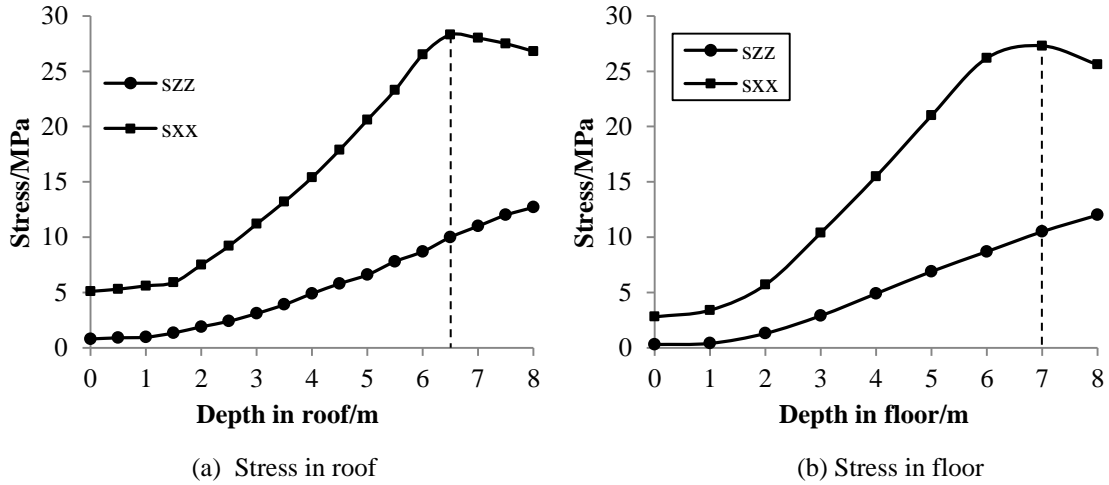


Fig. 3-8 Curves of stress in the RGSG surrounding rock after roadway excavation

Contrary to the stress distribution in coal sidewall, roadway excavation reduces the vertical stress (szz) more significantly than the horizontal stress (sxx) in roof and floor. In roof, the horizontal stress increases from the surface of surrounding rock together with the vertical stress, but with a higher speed and larger starting value. Finally, this horizontal stress reaches peak point of 28.5 MPa at a depth of 6.5 m from the roof surface. The largest coefficient of the horizontal stress concentration in roof is found to be 1.36 (28.5MPa/21 MPa). In floor, similar stress variation is experienced, and the horizontal

stress increases from the floor surface and reaches the maximum value of approximately 27.3 MPa at a depth of 7 m. And the biggest coefficient of the horizontal stress concentration in floor is 1.30 (27.3 MPa/21 MPa). Apparently, the vertical stress acts as the confining stress and controls the behavior of the shallow range of roof and floor. Because the fact that no supporting structures are installed in floor, the confining stress is provided only by its weight, and the bearing strength of this part of floor is lower than that of roof which is supported by 6 rock bolts and 4 cable bolts. It is the reason why the floor heave is larger than the roof sag during the stage of roadway excavation.

Actually, the behavior of surrounding rock of underground engineering space is controlled by its suffering stress and its bearing strength. All the geotechnics aiming to maintain the stability of rock engineering space are designed from these two aspects: reducing the stress imposed on the target surrounding rock; increasing the bearing strength of the target surrounding rock.

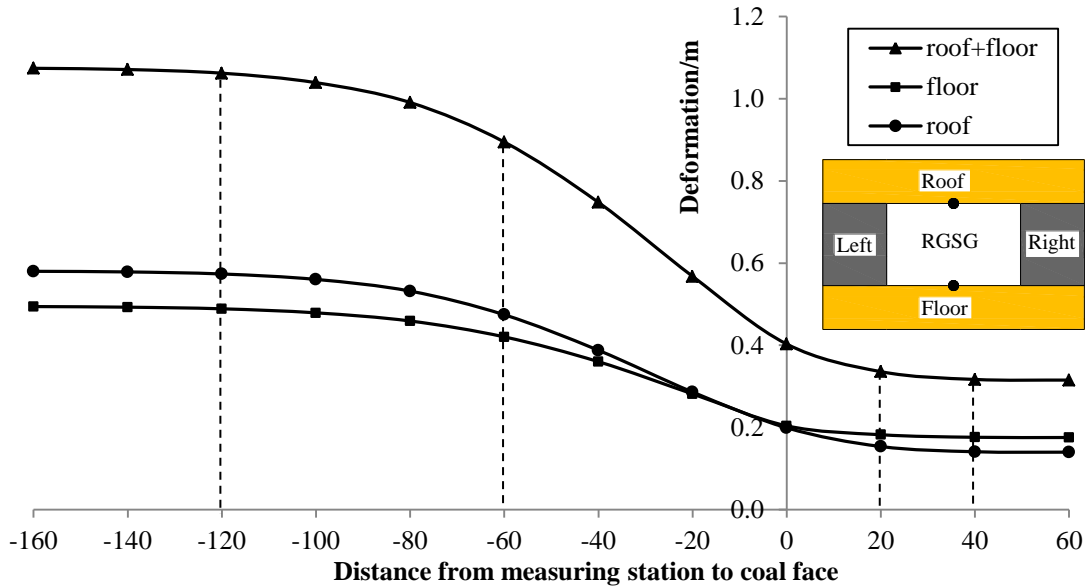
3.2.2 Basic Deformation and Stress Distribution during Coal Panel Retreating

3.2.2.1 Deformation distribution during coal panel retreating

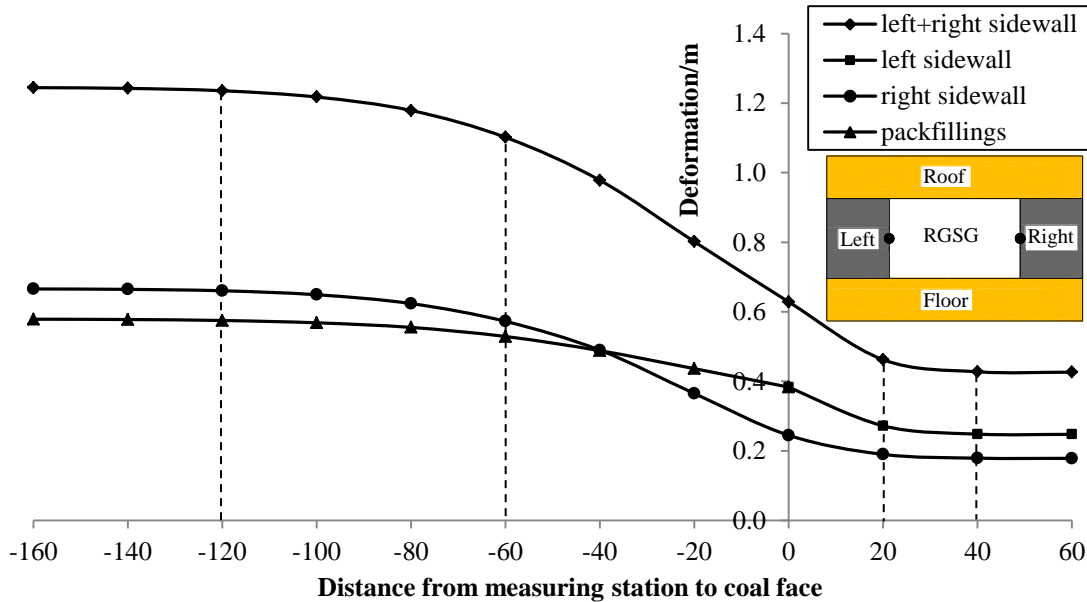
In order to understand the behavior of roadway surrounding rock during the stage of coal panel mining, deformations of the roadway surrounding rock are measured, and the results are shown in Fig. 3-9, in which the Fig. 3-9(a) represents the deformations of roof and floor and Fig. 3-9(b) represents the deformations of sidewalls. The x coordinate is relative distance from measuring station to coal face, and the positive value represents the distance ahead of coal face and negative value represents the distance behind coal face.

From the Fig. 3-9(a), we can see that roof and floor experience different deformations in different stages. Firstly, the RGSG is disturbed by roadway excavation as discussed above, and the roof sag and floor heave increase to approximately 140 mm and 173 mm, respectively, and they remain stable until 40 m away from the moving coal face. And then, the roadway roof sag and floor heave start to rise slowly to 153 mm and 182 mm when the distance to coal face reduces to 20 m from 40 m. As the coal face moves continually, RGSG roof sag and floor heave grow up quickly to 474 mm and 420 mm until 60 m behind the coal face. The roof sag exceeds the floor heave when the coal face

passes by the measuring station. After that, increasing of the roof sag and floor heave slows down and maintain unchangeable when the measuring station is 120 m away from the coal face, and at this time, the final roof sag and floor heave reach as much as 573 mm and 489 mm, respectively.



(a) Deformation of RGSG roof and floor during coal panel retreating



(b) Deformation of RGSG sidewalls during coal panel retreating

Fig. 3-9 Deformation of RGSG surrounding rock during coal panel retreating

It should be note that, larger deformation of roof than that of floor during the stage of coal panel retreating indicates that the coal panel retreating imposes severer influence

on the roof than on the floor. Last but not the least, the roof sag and floor heave achieve the largest increasing speed when the roadway is 20 m behind the coal face, which means that the movements of overlying strata including rotation and sink are most quick about 20 m behind the coal face. And these movements stop about 120 m behind the coal face.

From the Fig. 3-9(b), it can be seen that the roadway sidewalls also perform corresponding deformations under the different stress disturbances induced by coal panel retreating. Firstly, the RGSG left and right coal sidewalls achieve 248 mm and 179 mm, respectively, after experiencing the influence from roadway excavation, as discussed above. And then, they start to increase slightly to 272 mm and 190 mm when the coal face moves from 40 m to 20 m before the measuring station. When the distance to coal face reduces continually, deformations of sidewalls bolt increase quickly to 383 mm and 245 mm when the coal face passes by. After that, previous left coal sidewall is extracted and artificial packfillings is built, and the RGSG is influenced by the abutment stress behind the coal face. The deformation of right coal sidewall continually increases quickly and achieves highest increasing speed about 20 m behind the coal face, and reaches approximately 555 mm when the measuring station is 60 m behind the coal face. The increasing speed of the deformation of packfillings, however, slows down apparently after coal face passes by, and increases to 136 mm gradually about 60 m away from the coal face. The deformations of left and right sidewalls rise slowly and reach the peak value of 575 mm and 661 mm when the distance behind coal face extends to 120 m.

3.2.2.2 Stress distribution during coal panel retreating

(1) Vertical stress distribution in right sidewall

It is believed that the deformations of the RGSG surrounding rock discussed above is caused by the abutment stress around the moving coal face, which will concentrates and the concentrating zone moves together with the advancing of the coal face. To understand the distribution characteristic of this abutment stress during coal panel retreating, vertical stresses in right coal sidewall are tracked when the coal face advances, as shown in Fig. 3-10. Fig. 3-10(a) represents the vertical stresses distribution as the distance from the measuring station to the coal face changes, in which, x coordinate is the relative distance from measuring station to coal face, and the positive value represents the distance ahead of coal face and the negative value represents the distance behind coal

face. Fig. 3-10(b) represents the vertical stresses distribution as the depth inside coal sidewall increases.

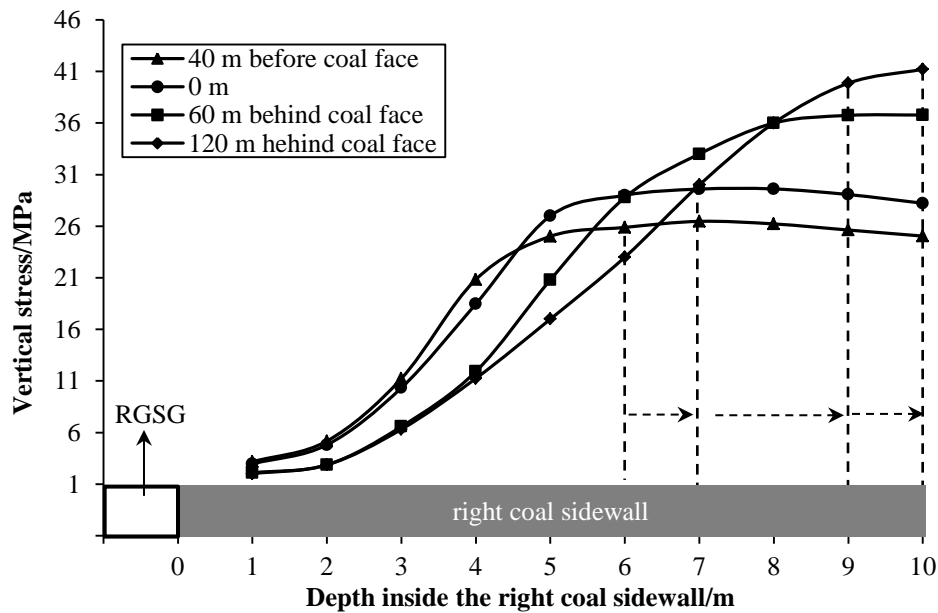
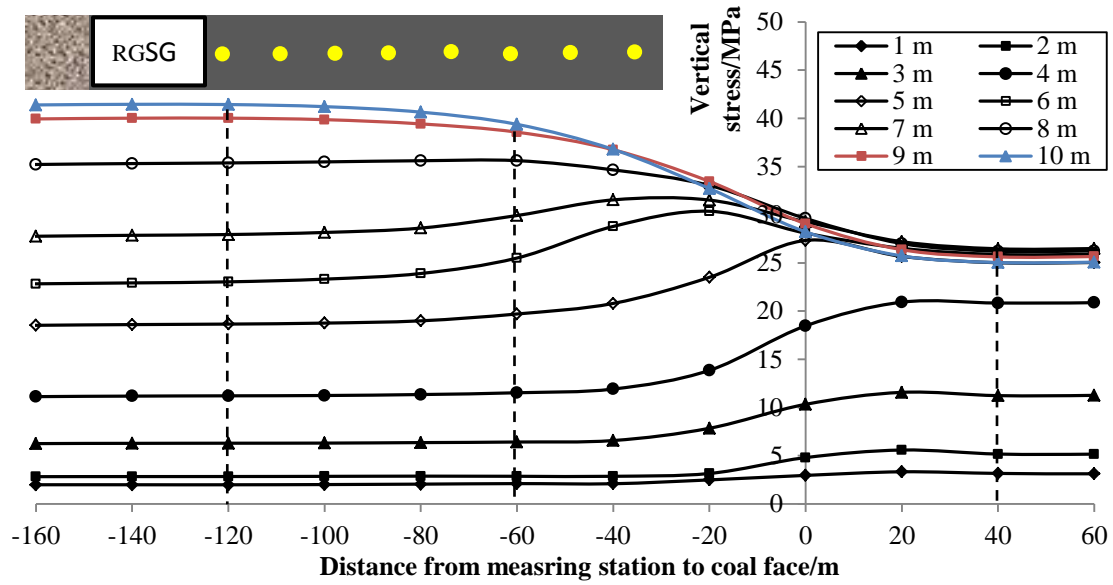


Fig. 3-10 Distribution of vertical stress in right coal sidewall during coal panel retreating

As seen from Fig. 3-10(a), the surrounding rock of the RGSG suffers different stress disturbances in different stages. Detailedly: The vertical stresses in right coal sidewall remain stable when the coal face is more than 40 m far from the measuring station. And then, the vertical stresses within the range of 4 m inside coal sidewall start to

decrease and the stresses in deeper range begin to increase. After coal face passes by, the vertical stresses at a depth of more than 6 m continually increase quickly until 60 m behind the moving coal face. During this period, the stress at depth of 5 m, 6 m and 7 m starts to decrease in succession. As the distance behind the coal face extends continually, the stresses at depth of more than 8 m continually to increase, but the increasing speed decreases obviously. Finally these stresses rise gradually to the peak value when the measuring station is 120 m away from the coal face. And then, as the coal face moves away from the measuring station continually, all the vertical stress do not change any more.

It can be concluded that, the influence of abutment stress generated by coal face moving on the right coal sidewall starts from 40 m before the coal face and finishes 120 m behind the coal face. All the influence can be divided into three stages: no influence farther than 40 m; slight influence from 40 m to 20 before the coal face and 60 m to 120 back the coal face; severe influence from 20 m ahead of coal face to 60 m back the coal face. Corresponding roadway supporting should be designed according to this kind of stress distribution characteristics.

As discussed above, the vertical stresses in shallow range of right coal sidewall decrease as the coal face moving. It is because the bearing ability of these parts of sidewall decreases due to the deteriorating influence from the stress disturbance which is generated by coal face moving. To illustrate this deterioration more clearly, distribution of vertical stress in right coal sidewall in inclination direction are measured, as shown in Fig. 3-10(b). We can see that, the peak vertical stress in right coal sidewall is located at depth of 6 m when the measuring station is 40 m before the coal face. When the coal face passes by the measuring station, this peak vertical stress transfers to 7 m inside the coal sidewall, which is accompanied by the decrement of vertical stress in shallow range. As the distance behind the coal face increases from 0 m to 60 m, this peak vertical stress continually transfers to 9 m inside the coal sidewall and with an obvious increase in value. When the coal face continually moves 120 m away from the measuring station, the peak vertical stress becomes to 10 m inside the coal sidewall, and the value also increases to 41.2 MPa.

(2) Vertical stress distribution in left sidewall

Figure 3-11 represents the distribution of vertical stresses in left coal sidewall and packfillings as the distance from the measuring station to the coal face changes, in which, x coordinate is the relative distance from measuring station to coal face, and the positive value represents the distance ahead of coal face and the negative value represents the distance behind coal face.

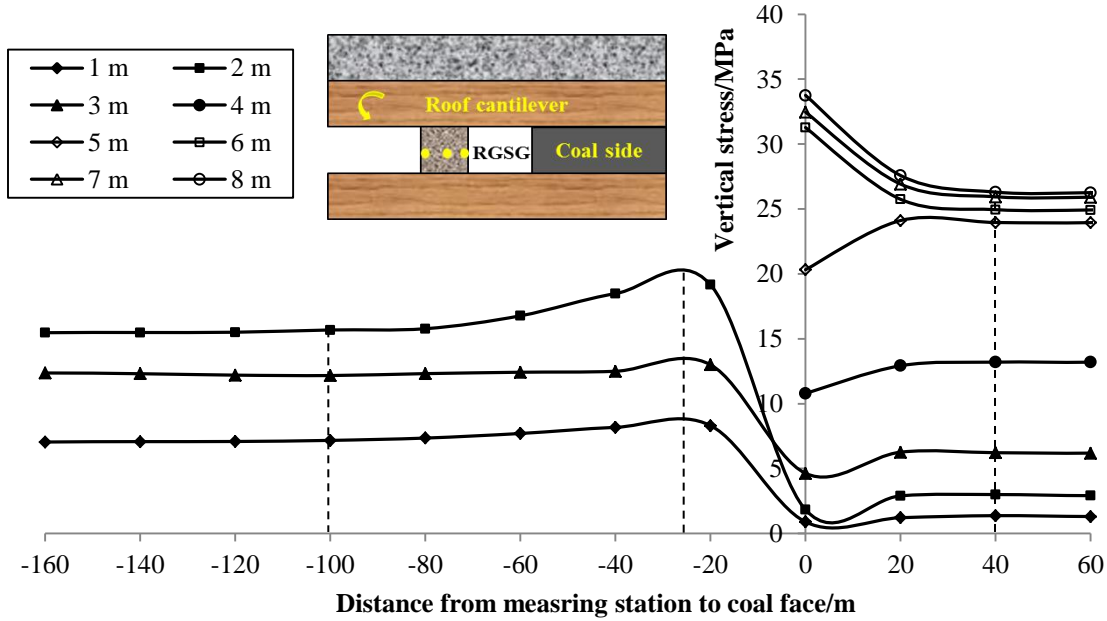


Fig. 3-11 Distribution of vertical stress in left sidewall during coal panel retreating

As shown in Fig. 3-11, the vertical stresses in left coal sidewall start to change when the coal face moves to the position about 40 m before the measuring station. Similar to the variation in right coal sidewall, shallow range within 5 m experiences stresses decrease because of strength reduces, and deeper zone more than 6 m experiences stresses increase. After coal face passes by, the entire coal panel including the left coal panel is extracted, and packfillings is built at edge of goaf where the shallow part of previous left coal sidewall located. We can see that, the vertical stresses in packfillings increase sharply once the coal face passes by, especially the stress at middle of the packfillings. About 25 m behind the coal face, the vertical stresses in packfillings reach the peak value separately. As the coal face moves further continually, the vertical stresses in packfillings decrease gradually and remain stable when the distance behind the coal face is as long as 100 m. It can be concluded that, the influence of coal face moving on the left coal sidewall is started from 40 m ahead of coal face, and the influence on

packfillings is most significant 25 m behind the coal face and finishes about 100 m away the coal face. Distribution contour of the vertical stress in the surrounding rock of the gateroad with respect to the coal face location is shown in Fig. 3-12.

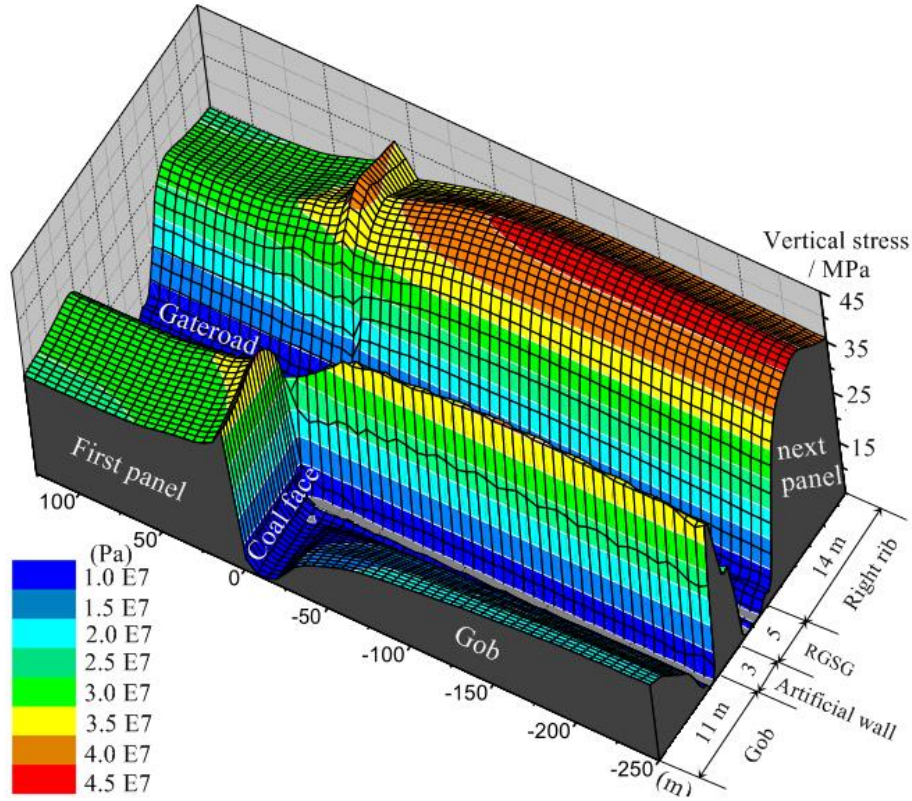


Fig. 3-12 Distribution contour of vertical stress in RGSG surrounding rock during coal panel retreating

Last but not the least, the variation of the vertical stress in packfillings also indicates that the overlying strata sink and rotate quickly about 20 m behind the coal face, and then become stable until 100 m away from the coal face. Bearing capacity of the caved rock in goaf increases gradually as the cracked rock is compacted by the overlying strata subsidence, and the increased bearing strength shares the pressure of overlying strata with the packfillings. Consequently, the vertical stress in the packfillings are smaller than those in the right rib and an obvious decrease of the vertical stress occur in the packfillings when the distance behind the coal face is more than 25 m.

3.2.3 Basic Plastic Zones Distribution during Coal Panel Retreating

It should be note that, larger deformation of right coal sidewall than that of left coal sidewall and packfillings during the stage of coal panel retreating indicates that the coal

panel retreating imposes severer influence on the right coal sidewall. Especially, behind the coal face, shallow part of right coal sidewall goes into plastic stage after experiencing these disturbances from roadway excavation and coal face m, as shown in Fig. 3-13.

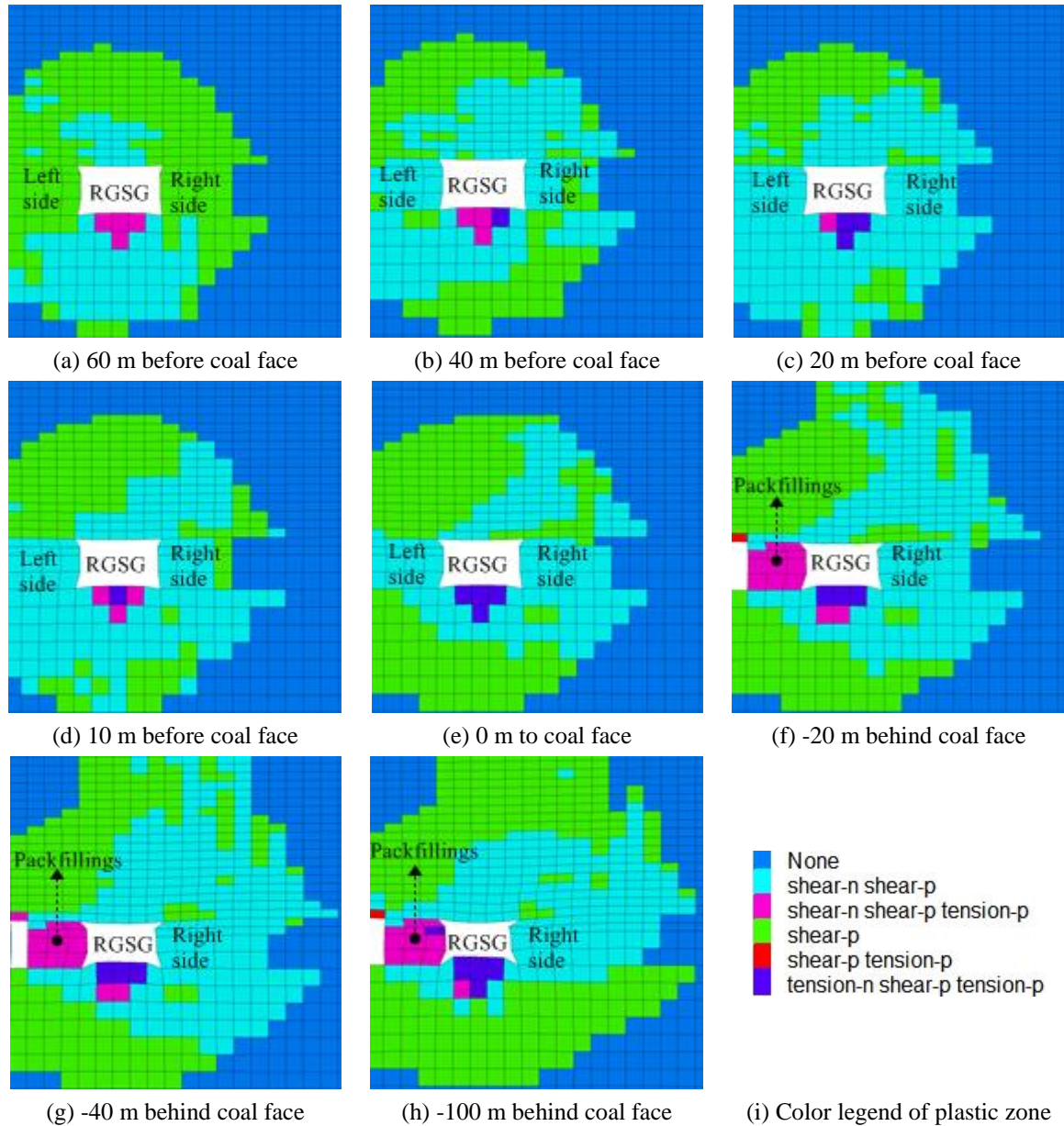


Fig. 3-13 Plastic zone distribution of the RGSG during coal panel mining

Boltability of cable bolts and rock bolts in this part of surrounding rock becomes low considerably because fissures and cracks have appeared in the shallow part of surrounding rock. Modified supporting method with longer anchoring length and higher prestress should be designed in this period.

3.3 Stress and Deformation Distribution under Different Roof Conditions

3.3.1 Different Deformation and Stress Distribution during Roadway Excavation

3.3.1.1 Deformation distribution during roadway excavation

In order to understand the behavior of roadway surrounding rock under different roof condition during the stage of roadway excavation, deformations of the roadway roof, floor and sidewalls are measured, and the results are shown in Fig. 3-14 and Fig. 3-15. The x coordinate is the computing steps after roadway excavation and the Global Mechanical Ratio Limit of this simulation is 1.0×10^{-5} .

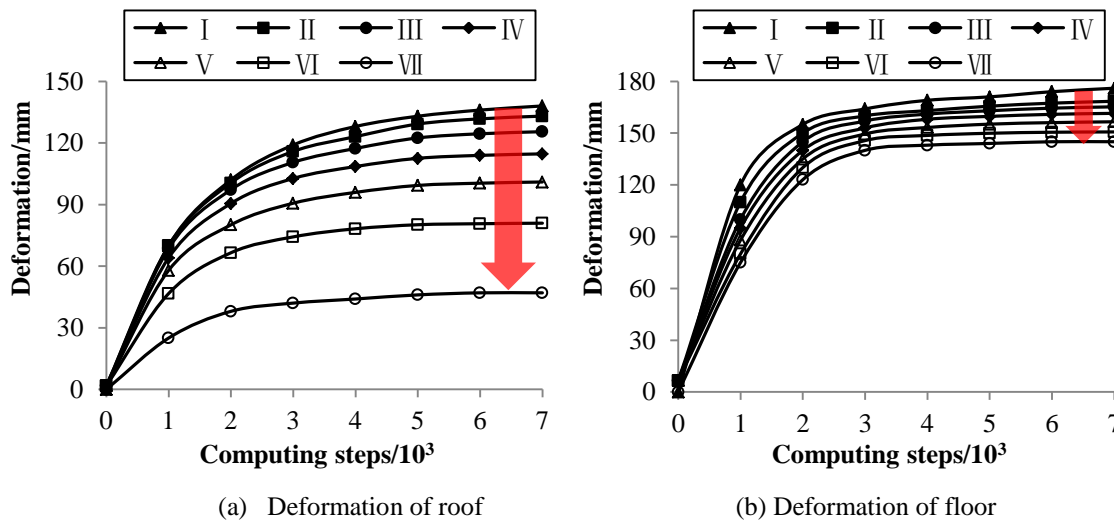


Fig. 3-14 Curves of deformation of RGSG roof and floor after roadway excavation

From the Fig. 3-14 and Fig. 3-15, we can see that the deformations of roadway surrounding rock increase sharply from beginning, respectively, until 1000 computing steps after roadway excavation. After that, the increase speed slows down, and the deformation of surrounding rock continually rises to peak value when the computing steps are 7.0×10^3 . Importantly, as the thickness of main roof increases and thickness of immediate roof decreases (from type I to VII), deformations of surrounding rock are reduced. Detailedly, roof sag decrease most obviously from 133 mm under roof condition I to 47 mm under roof condition VII; floor heave reduces from 176 mm under roof condition I to 145 mm under roof condition VII; left coal sidewall deformation reduces from 235 mm under roof condition I to 180 mm under roof condition VII; right coal

sidewall deformation reduces from 166 mm under roof condition I to 144 mm under roof condition VII.

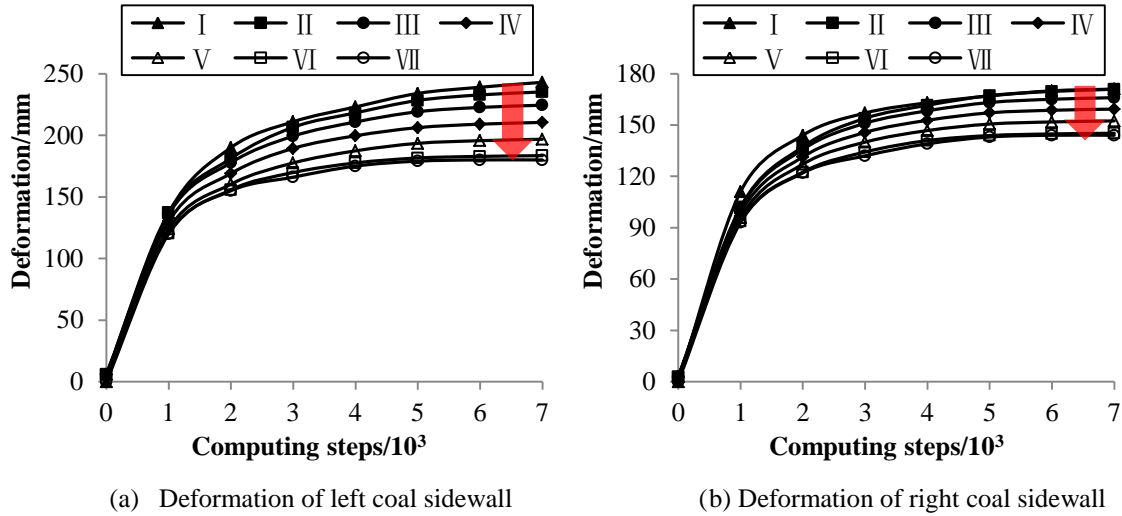


Fig. 3-15 Curves of deformation of RGSG sidewalls after roadway excavation

3.3.1.2 Stress distribution during roadway excavation

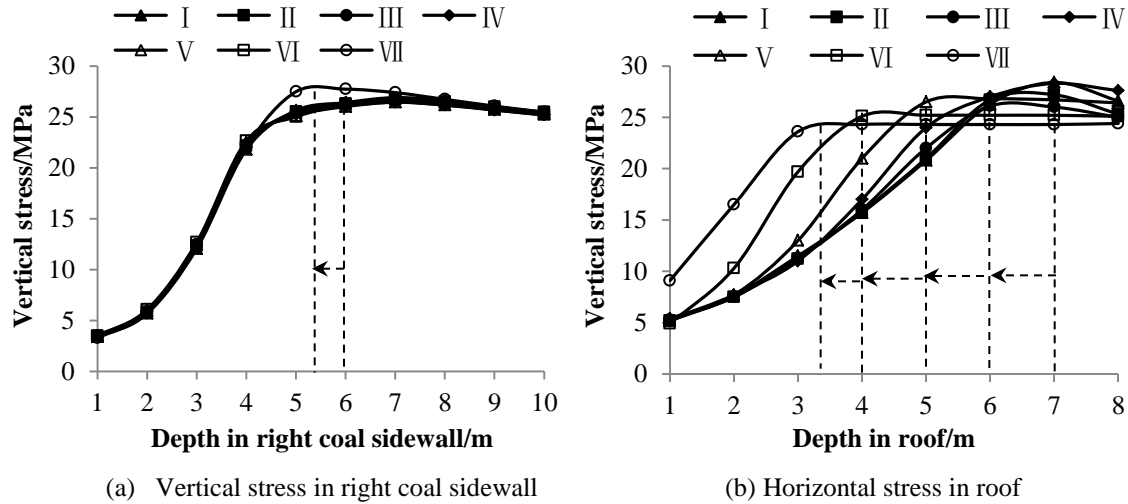


Fig. 3-16 Stress distributions in RGSG right coal sidewall and roof after roadway excavation

To reveal the influences of roadway roof variation on surrounding rock deformation during the stage of roadway excavation, stresses redistributions in roadway surrounding rock are measured, and the results are shown in Fig. 3-16. It can be seen that the distributions of the vertical stress in right coal sidewall under different roof conditions are almost same, except for the roof condition VII whose peak values is located 5.5 m away from the sidewall surface and is in value of 27.4 MPa. The peak point of the vertical

stress in right coal sidewall under other roof conditions is on the position of 6.0 m inside the coal sidewall with same value of 26.2 MPa. It can be concluded that, during roof roadway excavation, thickness increase of the main roof and thickness decrease of the immediate roof over the RGSG make little influence on the stress distribution in roadway sidewalls. Consequently, deformations of roadway sidewalls under different roofs are almost same, though some decrements are achieved.

However, in Fig. 3-16(b), we can see that the distributions of horizontal stress in roof under different roof conditions are obviously different. Generally, as the distance from roof surface increases, all the horizontal stresses increase quickly at shallow depth, and then reach maximum value at a certain depth, and finally reduce gradually to the level of in-situ stress. Specifically, the horizontal stress in roof increases more quickly from a larger point as the thickness of main roof increases, and the peak value also transfers from depth of 7.0 m under roof type I to depth of 2.5 m under roof type VII. It means that the shallow part of roof becomes stronger to bearing the horizontal stress. As a result, the deformation of roof reduces obviously. The horizontal stress contours in different roofs are shown in Fig. 3-17.

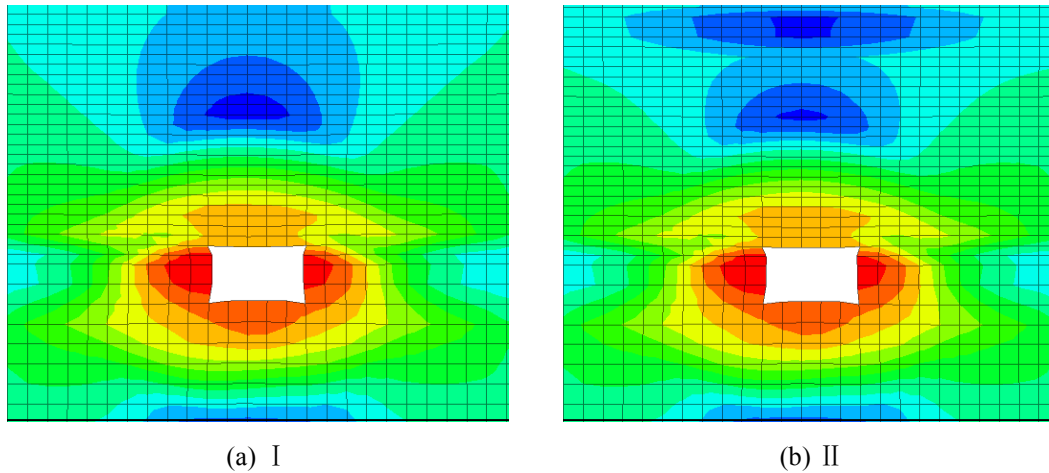


Fig. 3-17 Contour of horizontal stress in different RGSG roofs after roadway excavation

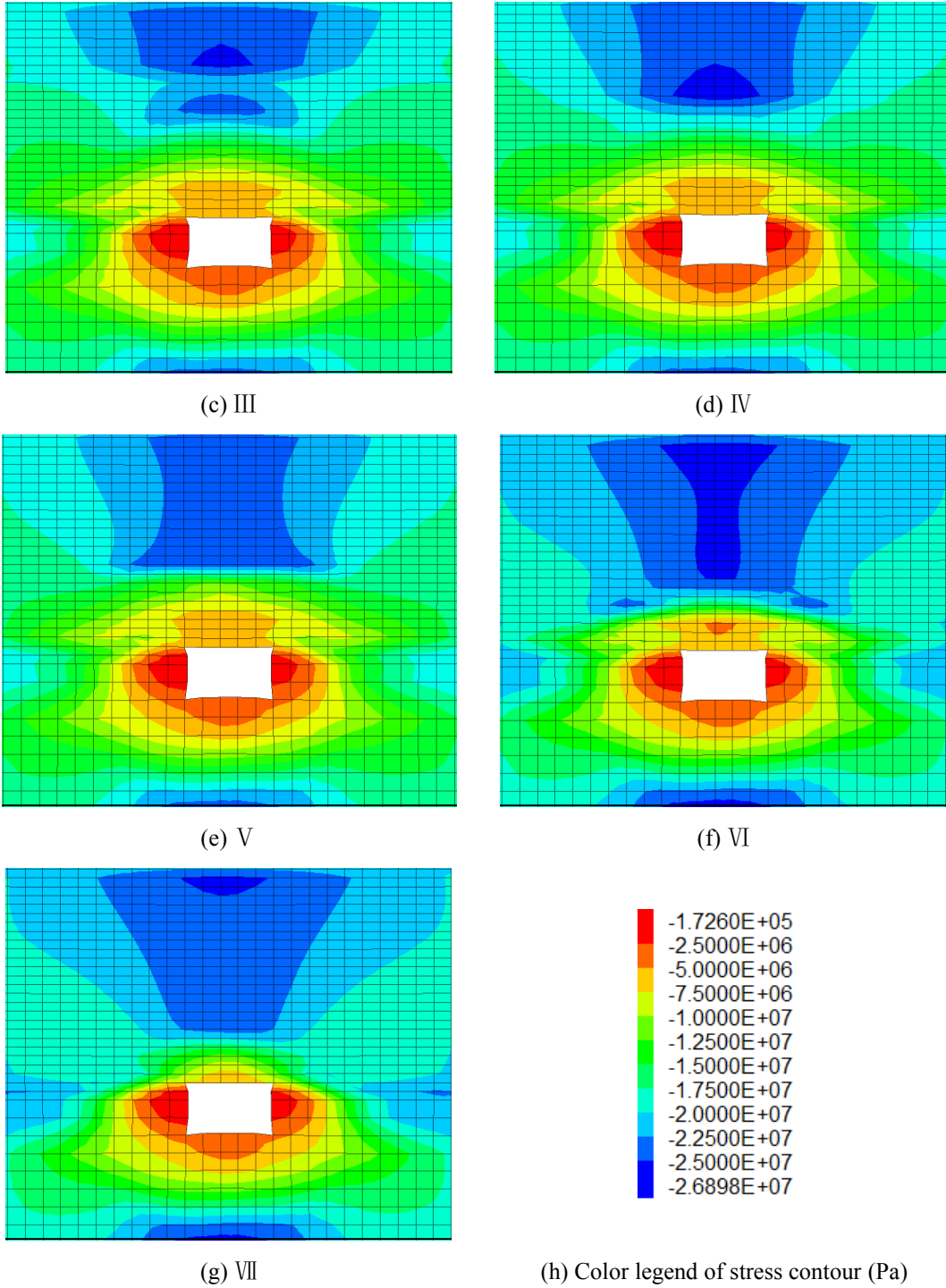


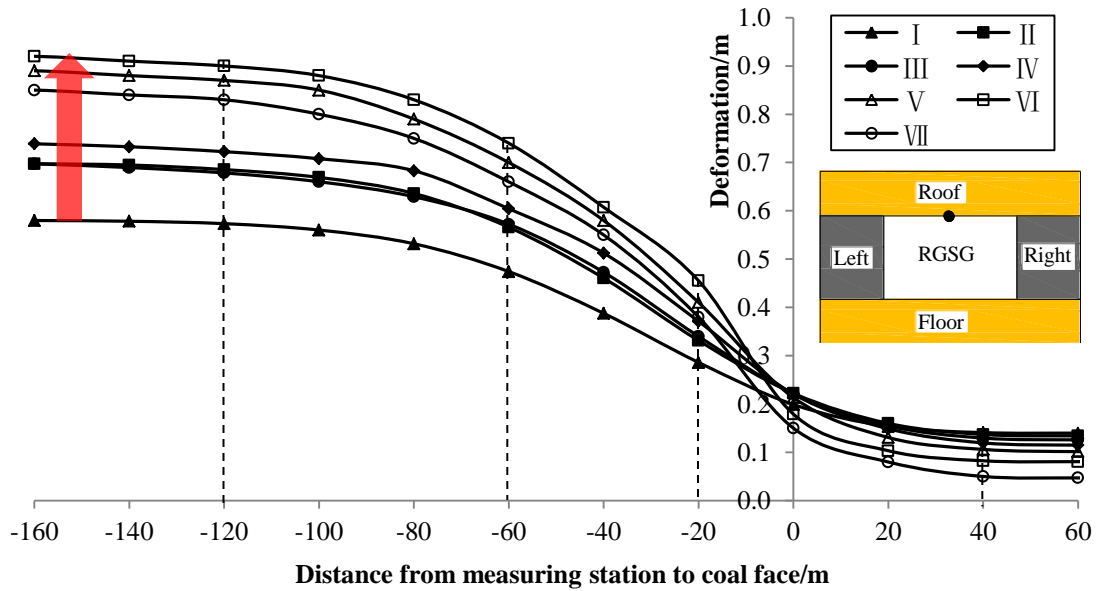
Fig. 3-17 Contour of horizontal stress in different RGSG roofs after roadway excavation

3.3.2 Different Deformation and Stress Distribution during Coal Panel Mining

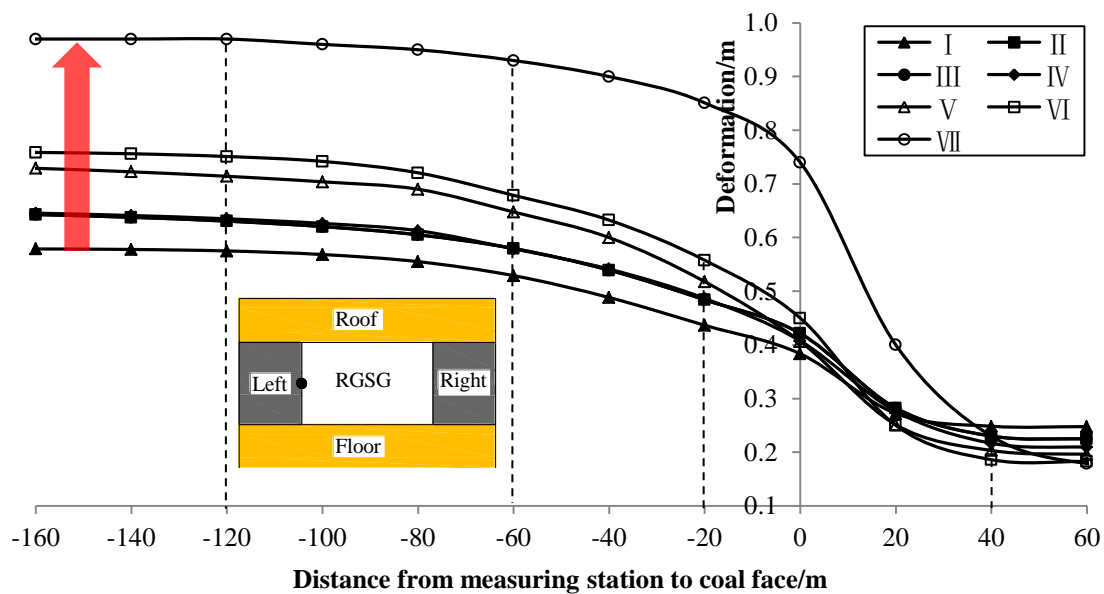
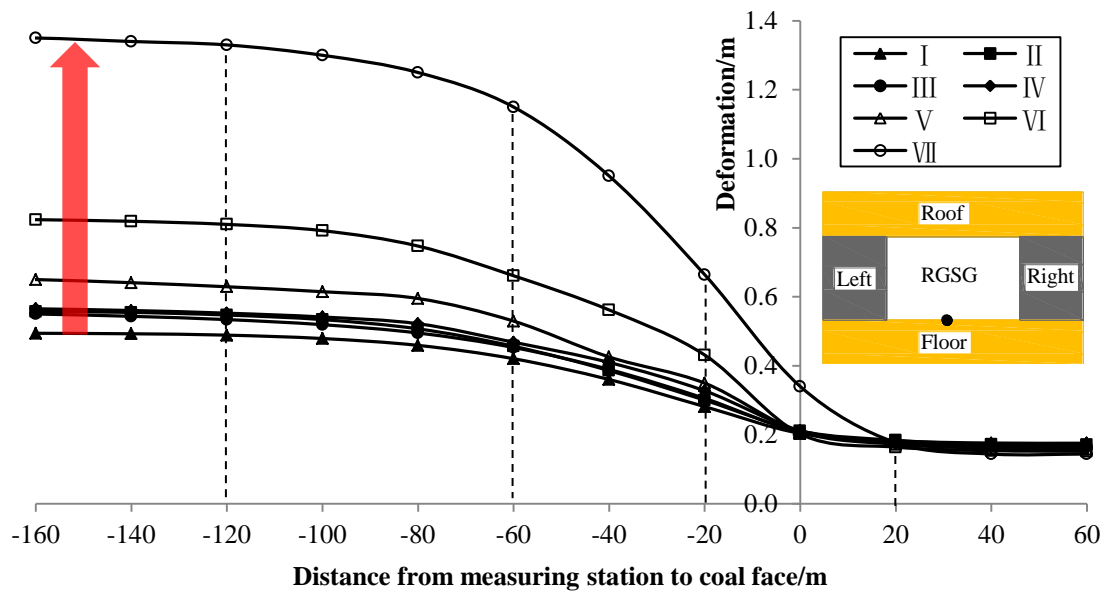
3.3.2.1 Deformation distribution during coal panel retreating

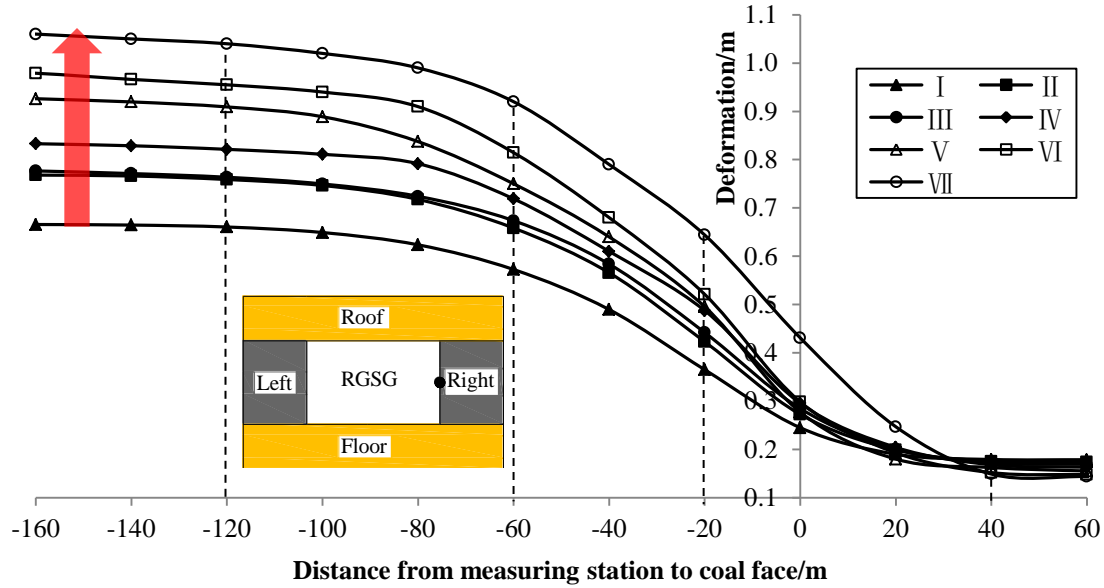
In order to understand the behavior of roadway surrounding rock under different roof conditions during the stage of coal panel retreating, deformations of the roadway roof, floor and sidewalls are measured, and the results are shown in Figs. 3-18(a), (b), (c) and (d). The x coordinate is relative distance from measuring station to coal face, and the positive value represents the distance ahead of coal face and the negative value represents the distance behind coal face. It can be seen that, contrary to the influence of the roof variations on roadway deformation during roadway excavation, the impact of roof changes on roadway stability becomes obviously serious during the stage of coal panel mining. The thicker and thinner of the main roof and the immediate roof are, the more quickly the deformations of the RGSG surrounding rock increase and the larger the maximum deformations are.

In detail, the deformation of roof (Fig. 3-18(a)) increases from 40 m ahead of the moving coal face, achieving largest increasing speed about 20 m behind the coal face and reaching maximum value approximately 120 m away from the coal face. The maximum value of roof sag increases from 580 mm in roof type I to 920 mm in roof type VII.



(a) Deformation of roof





(d) Deformation of right sidewall

Fig. 3-18 Deformation curves of RGSG surrounding rock under different roofs during coal mining

In the Fig. 3-18(b), the deformation of floor increases from 20 m ahead of the moving coal face, achieving largest increasing speed about 20 m behind the coal face and reaching maximum value approximately 120 m away from the coal face. The maximum value of floor heave increases from 495 mm in roof type I to 1,350 mm in roof type VII. It should be noted that the increment of floor heave from roof type VI (10 m main roof + 2 m immediate roof) to VII (12 m main roof + 0 m immediate roof) is obviously larger than others when roof condition changes. The floor heave has become one of the main contributions to the roadway section shrinkage. In the Fig. 3-18(c), the deformation of left sidewall except for under roof type VII increases from 40 m ahead of the moving coal face, achieving largest increasing speed when the coal face passes by and reaching maximum value approximately 120 m away from the coal face. Under the roof type VII, the roadway left sidewall starts to deform about 60 m before the coal face and deforms most quickly about 20 m ahead of the coal face. The maximum value of left sidewall deformation increases from 579 mm in roof type I to 970 mm in roof condition VII. It should be note that the increment of left sidewall from roof type VI (10 m main roof + 2

m immediate roof) to VII (12 m main roof + 0 m immediate roof) is apparently larger than others when roof condition changes.

In the Fig. 3-18(d), the deformation of right sidewall increases from 40 m ahead of the moving coal face, achieving largest increasing speed about 20 m behind the coal face and reaching maximum value approximately 120 m away from the coal face. The maximum value of the right sidewall deformation increases from 667 mm in roof type I to 1,070 mm in roof type VII. The deformation contours of the RGSG when 0 m, -60 m and -120 m from the coal face under different roof conditions are shown in Fig. 3-19.

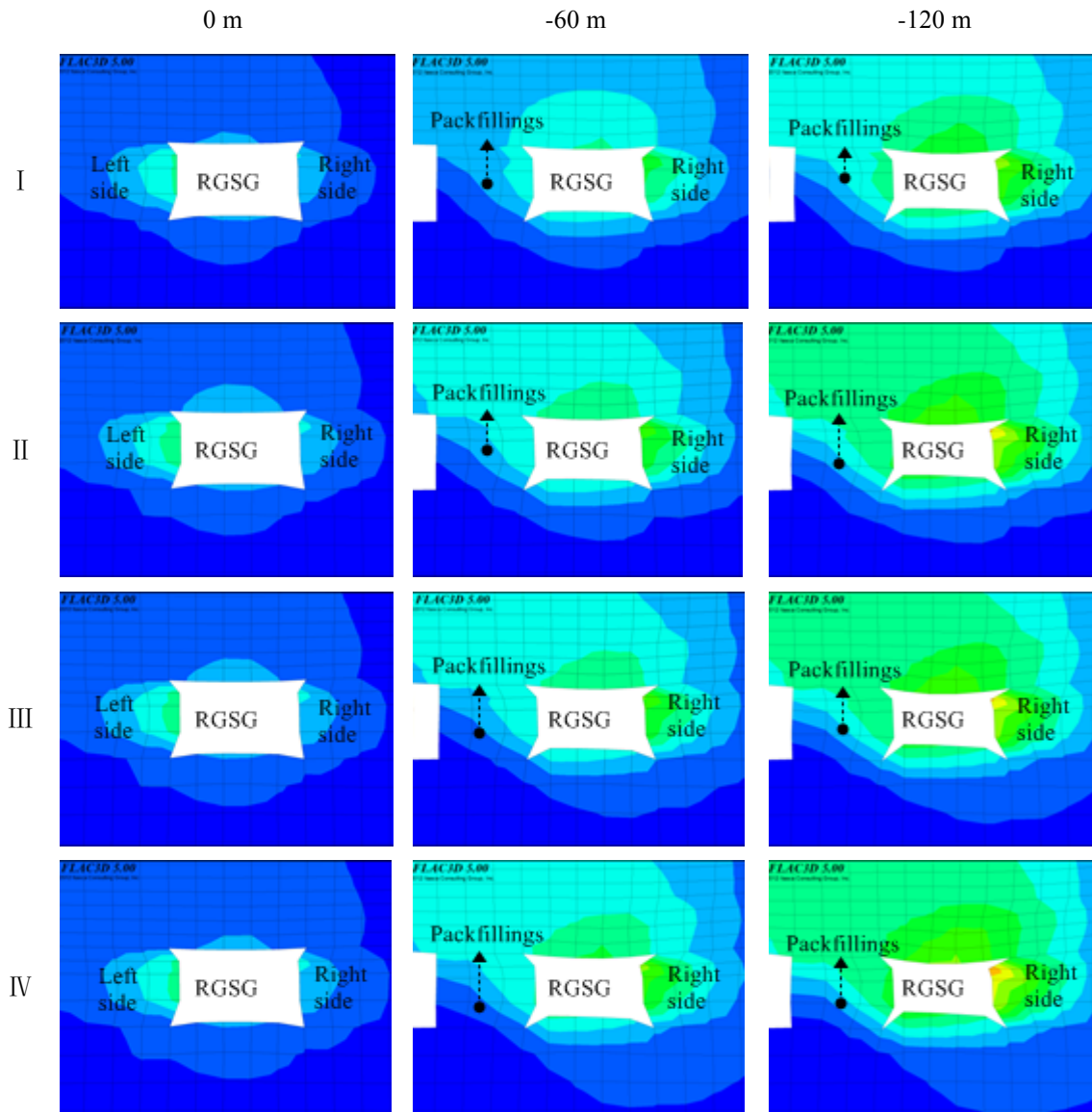


Fig. 3-19 Deformation contour of RGSG surrounding rock under different roof during coal mining

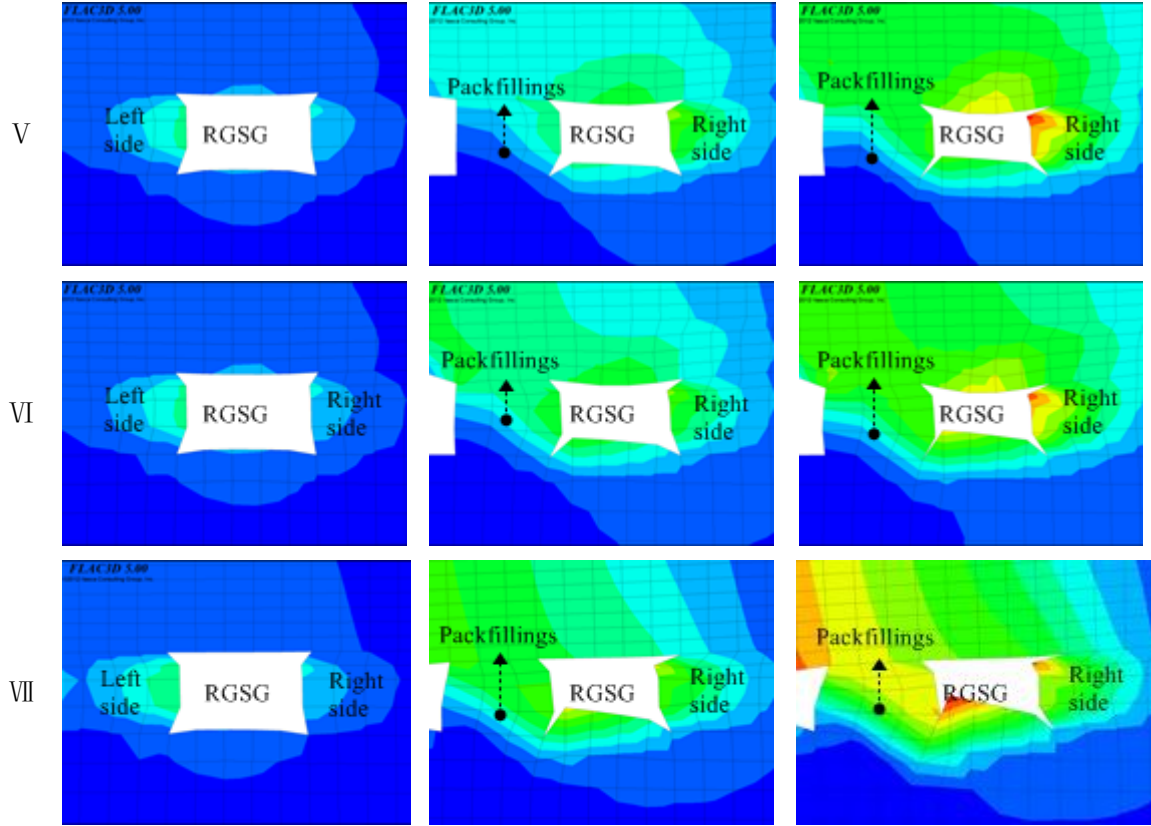


Fig. 3-19 Deformation contour of RGSG surrounding rock under different roof during coal mining

3.3.2.2 Stress distribution during coal panel retreat

To understand the reason why the RGSG surrounding rock behaviors like that under different roof conditions during coal panel mining, vertical stresses in right coal sidewall are tracked when the coal face advances, as shown in Fig. 3-20, in which, x coordinate is the relative distance from measuring station to coal face, and the positive value represents the distance ahead of coal face and the negative value represents the distance behind coal face.

From the Fig. 20, we can see that the variations of vertical stress in right coal sidewall under different roof conditions are similar to the basic one that has been discussed in Section 3.2. Generally, this abutment stress starts to increase from a certain distance ahead of coal face, achieves the highest increasing speed at a certain distance behind the coal face and finally reaches the largest value when the roadway is enough away from the coal face.

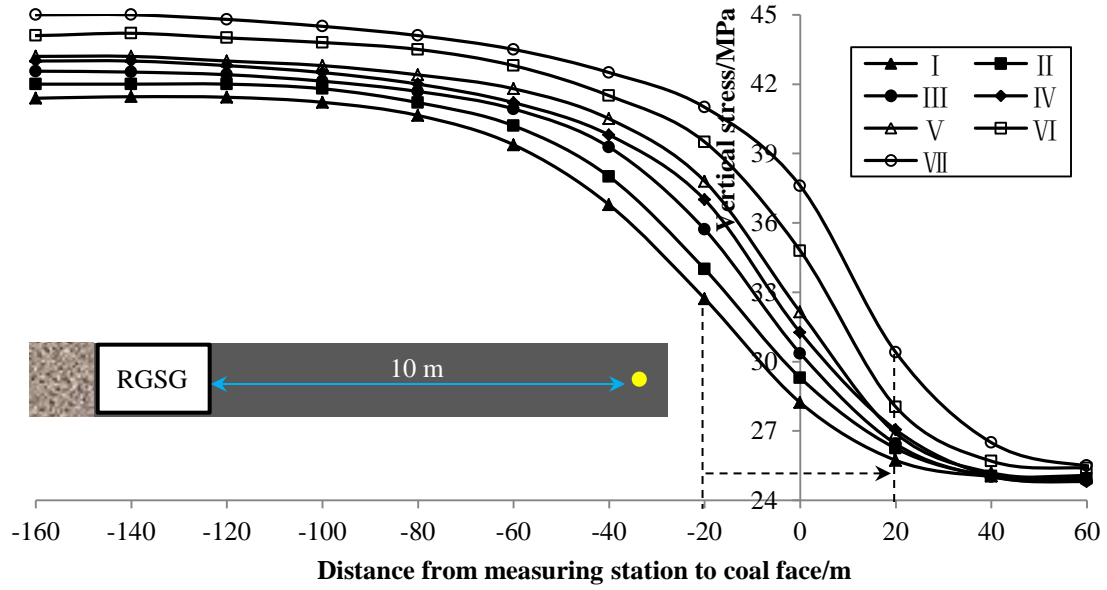


Fig. 20 Vertical Stress in RGSG right sidewall under different roofs during coal panel mining

Specially, when the thickness of the main roof increases and that of the immediate roof decreases, the position where the vertical stress induced by the coal face moving in right coal sidewall starts to increase become further from the coal face. For example, the vertical stress under roof type I starts to increase about 40 m ahead of coal face, and while, the vertical stress under roof type VII begins to rise approximately 60 m before the coal face. The position where the vertical stress achieves the largest increasing speed also transfers forward as the roof condition changes. For instance, the vertical stress achieves highest increasing speed about 20 m behind the coal face when under roof type I. When the roof type changes from VII, the vertical stress increases most quick about 20 m before the coal face. It means that the influence induced by the coal panel mining on RGSG become earlier when the main roof become thicker and the immediate roof becomes thinner. Last but not the least, the vertical stress value also increases when roof type changes from I to type VII. For example, the vertical stress in sidewall 20 m before coal face increases from 25.7 MPa to 30.4 MPa, the vertical stress in sidewall when coal face passes by increases from 28.2 MPa to 37.6 MPa, the vertical stress in sidewall 20 m behind coal face rises from 32.7 MPa to 41.0 MPa, and the vertical stress in sidewall 40 m behind coal face rises from 36.8 MPa to 42.5 MPa when the roof type change from I

to type VII. It indicates that influence of coal face moving on the RGSG become severer when the main roof becomes thicker and the immediate roof becomes thinner.

3.4 Summary

In order to analyze the accurate stress and deformation distribution in the surrounding rock of the RGSG with different roof conditions, a representative 3D numerical model is built using the FLAC3D software in this chapter. Simulation results show that RGSG suffers the stress disturbances from roadway excavation and coal panel retreating, and as a result, roadway surrounding rock perform different deformations in different period. The variation of roof thickness over the RGSG makes different influences on the RGSG surrounding rock during roadway excavation stage and coal panel retreating stage. The detailed conclusions are as follows:

(1) A representative numerical model is built to analyze the accurate distribution stress and decoration in the RGSG surrounding rock using FLAC3D software. In this simulation, a vertical stress as much as 19.7 MPa is applied at the top of model to simulate the weight of overburden of 940 m thickness; Immediate roof is excavated together with coal seam, and the excavation is filled with soft elastic material, to model the caving activity of the immediate roof and supporting function of the caved rock mass to the overlying strata; Coal seam, mudstone strata are set as strain softening constitutive materials to simulate the softening behavior of these weak rock mass in deep mining environment; Roadway supporting is also installed in these simulations according to the present criterion applied in the underground coal mines in Eastern China; Measuring station set to monitor the stress and deformation distribution in roadway surrounding rock as the distance from coal face to measuring station changes.

(2) RGSG suffers the stress disturbances from roadway excavation and coal panel mining, and as a result, roadway surrounding rock performs different deformations in different period. During roadway excavation, the confining stress normal to surface of roadway surrounding rock decreases considerably and the bearing strength of shallow part of surrounding rock reduces reasonably. Consequently, the shallow part of surrounding rock breaks and deforms towards roadway space. At end of this period, the

deformations of roadway roof, floor, left and right sidewalls are 138 mm, 176 mm, 243 mm and 171 mm, respectively.

During coal panel mining, the influence of abutment stress induced by coal face moving can be divided into three stages: no influence farther than 40 m; slight influence from 40 m to 20 before the coal face and 60 m to 120 back the coal face; severe influence from 20 m ahead of coal face to 60 m back the coal face. At end of this period, the deformations of roadway roof, floor, left and right sidewalls increase up to 560 mm, 479 mm, 575 mm and 649 mm, respectively.

Boltability of cable bolts and rock bolts in the shallow part of surrounding rock becomes low considerably because fissures and cracks have appeared in the shallow part of surrounding rock. Modified supporting method with longer anchoring length and higher prestress should be designed in this period.

(3) Variations of the thickness of roof makes different influence on the RGSG surrounding rock during roadway excavation and coal panel retreating. During roadway excavation, deformations of RGSG surrounding rock decrease as the thickness of the main roof increases and the thickness of the immediate roof decreases. During coal panel mining, however, deformations of roadway surrounding rock increase considerably when the main roof becomes thicker and the immediate roof becomes thinner. When the coal seam is beneath the hard main roof of 12 m, the deformations of RGSG roof, floor, left sidewall and right sidewall reach the maximum value of 880 mm, 1,330 mm, 960 mm and 1,070 mm, respectively.

Reference

- D. Zhu (1987) Breakage law of the main roof over longwall face and its application, Chinese university of mining and technology press, Xuzhou.
- H. Sun, B. Zhao (1993) Theory and application of the gob-side entry retaining, China Coal Industry Press, Beijing.
- F. Gao, M. Qian, X. Miao (2000) Mechanical analysis of the immediate roof subjected to given deformation of the main roof, Chinese journal of rock mechanics and engineering, Vol.19, pp.145-148.
- Yan S, Bai JB, Wang XY et al. (2013) An innovative approach for gateroad layout in highly gassy longwall top coal caving. Int J Rock Mech Min Sci 59, 33-41.

- Mortazavi A, Hassani FP, Shabani M (2009) A numerical investigation of rock pillar failure mechanism in underground openings. *Comput Geotech* 36, 691–697.
- Itasca Consulting Group Inc (2012) *Fast Lagrangian Analysis of Continua in 3 Dimensions. Constitutive Models*. USA, 54-57.
- N. Mohammad, D.J. Reddish, L.R. Stace (1997) The relation between in-situ and laboratory rock properties used in numerical modelling. *Int J Rock Mech Min Sci* 34, 289-297.
- Brook N (1997) Estimating the triaxial strength of rocks. *Int. J. Rock Mech. Min. Sci* (16), 261–264.

CHAPTER 4

STABILITY MAINTAINACE TECHNOLOGY OF THE DEEP RGSG

4.1 Basically Staged Supporting Strategy to the RGSG

According to the results concluded above, the stress distribution in the surrounding rock of the gateroad has different characteristics in different mining stages. A staged supporting strategy is proposed to deal with the various disturbances.

4.1.1 Strategy during Gateroad Excavation

The results of the stress distribution after gateroad excavation imply that the confining stress of the sidewall, roof and floor are much lower than the primary stress, resulting in decreasing of bearing capacity of the surrounding rock. From this point of view, a prestressed bolting system aiming at providing high lateral confining stress is proposed in the first supporting stage. This pre-stressed bolting system consists of rock bolts with a high strength (i.e., yield strength >600 MPa), steel plates and an M-straps with a high stiffness (Zhang 2004). Prestress is imposed on the surface of the surrounding rock through the steel plates and M-straps by tightening the nuts at the end of rock bolts. The high-strength bolt rod contributes to the high prestress, and the high-stiffness plate and M-strap widen the range of the prestress.

4.1.2 Strategy during Panel Extraction

The results of the stress distribution during panel retreating illustrate that the influence of abutment pressure ahead of the coal face on the gateroad increases gradually as the distance to the coal face decreases. Therefore, a secondary supporting to the gateroad is required within the range influenced by this abutment pressure. To fix the anchor structures into reliable strata, cable bolt system with larger length is better than rock bolt system in this stage due to the loose and broken range of the surrounding rock widening. Additionally, behind the coal face, the vertical stress in the surrounding of the gateroad increases continually, a third supporting to the gateroad is required. Considering the technical and economic feasibility and the gradually rising pressure on the artificial packfillings, constructing material of the artificial packfillings is required to perform

appropriate strength at right time and right place, rather than acquiring a high strength at beginning. Thus, the requirements of the material are lowered and the cost can be reduced. Lastly, it is predicted that the roof strata over the artificial packfillings will become broken after experiencing the influence of roadway and panel excavation, to pre-reinforce this broken zone over the artificial packfillings, a gap is excavated ahead of the coal face.

4.2 Improvement of Hard Roof Structures over RGSG by Pre-Split Technology

As analyzed in above Chapters 2 and 3, as the main roof becomes thicker and the immediate roof becomes thinner, deformations of the RGSG surrounding rock increase sharply. For example, the roof sag, floor heave, left sidewall and right sidewall of the RGSG under roof condition VII (12 m hard main roof) are as much as 880 mm, 1,350 mm, 960 mm and 1,070 mm, respectively, and the roadway section shrinkage rate is up to 82.5%. Roadway deformations are too large to serve for next coal panel mining. Most importantly, large deformation increases the risk of roadway instability accidents like roof caving, sidewall collapsing and packfillings toppling. In addition, large floor heaving hampers the transportation of minerals, miners and machines.

4.2.1 Numerical Model

Actually, the large deformations of the RGSG surrounding rock are caused by the hard main roof of 12 m thickness in type VII. In above Chapter 2, roof pre-split technology is proposed to resolve this problem. In order to verify this technology, another numerical model is built based on previous one in roof type VII. In the new model, an interface is set in the main roof along the goaf side to reduce the influence of the hard main roof caving on the RGSG surrounding rock, as shown in Fig. 4-1.

In Fig. 4-1(b), an interface is installed in hard main roof to simulate the weakening of pre-split. This interface is located along one edge of the packfillings that near goaf. All the rock parameters in this modified model are same as the previous model in roof type VII. The parameters of interface in this new model are listed in Table 6.

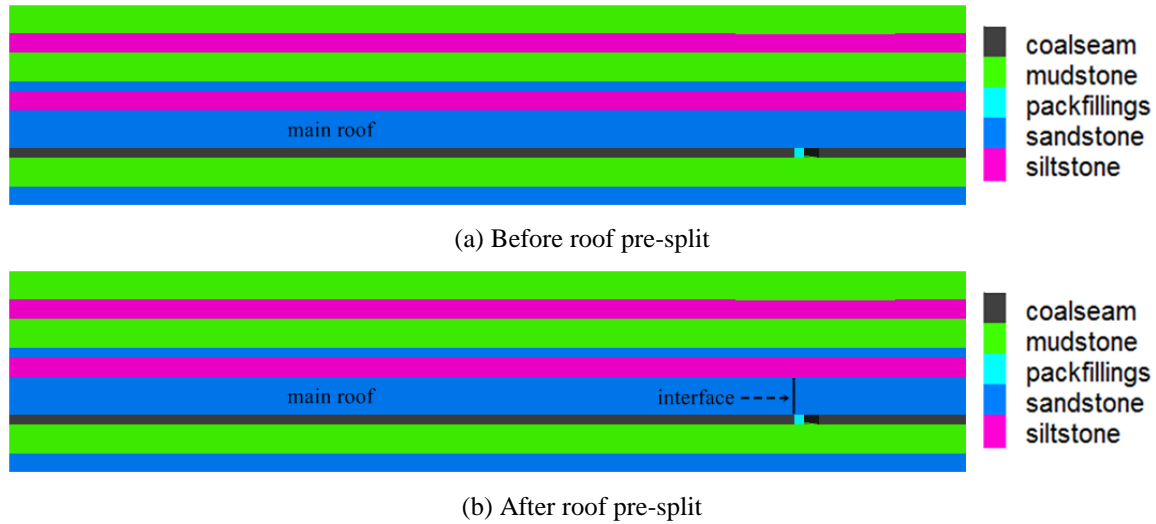


Fig. 4-1 Numerical model of improvement of hard roof structure over the RGSG

Table 6 Parameters of the interface in the modified numerical model

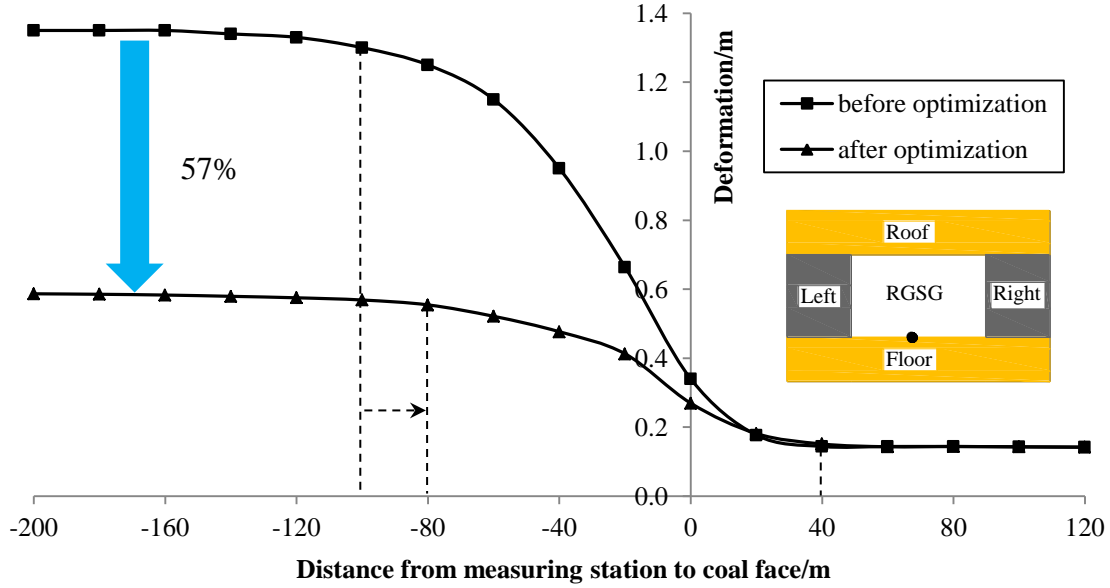
Kn (Pa/m)	Ks (Pa/m)	Friction (°)	Cohesion (Pa)	Tension (Pa)
1.0×10^{12}	1.0×10	30	0	0
Rcohesion (Pa)	Rfriction (°)	Rtension (Pa)	Bslip	Sbratio
0	20	0	on	1

4.2.2 Deformation of the RGSG Surrounding rock after Improvement

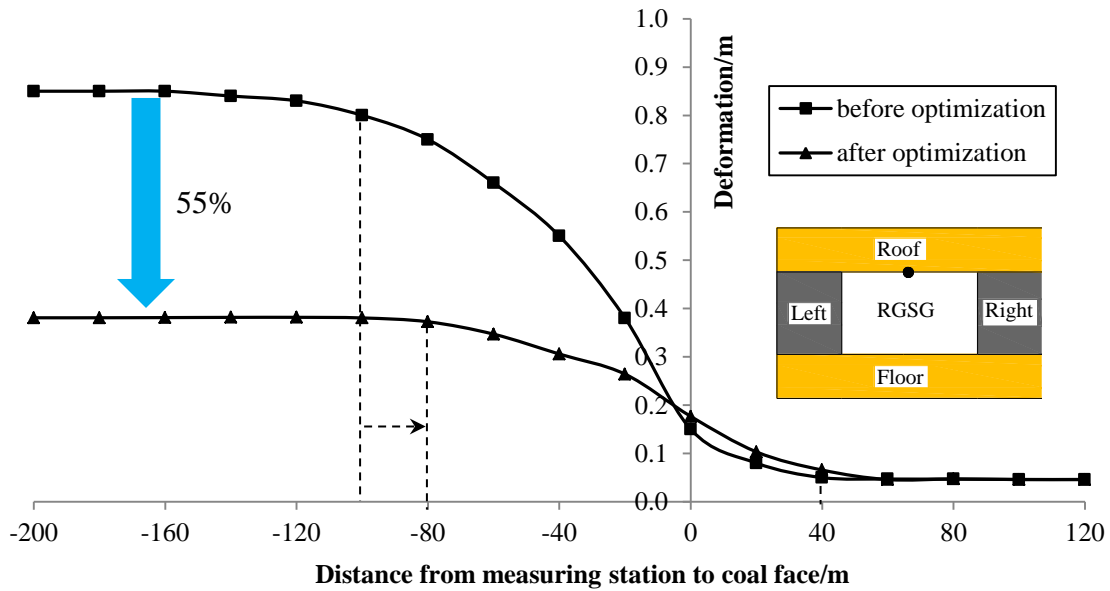
Figs. 4-2(a), (b), (c) and (d) represent the detailed deformations of the RGSG floor, roof, and sidewalls after coal face passes, without roof pre-split and with roof pre-split. It can be seen that there is no much change about the position where the roadway surrounding rock start to increase. For example, roadway floor heaves both start to increase about 40 m before coal face before and after roof pre-split, and roadway roof sags both begin to rise about 60 m ahead of coal face, and roadway left sidewall deformations both start to grow 60 m before coal face, and roadway right sidewall deformations both begin to increase 60 m ahead of coal face.

The positions where the deformations of RGSG surrounding rock stop increasing before and after roof pre-split are changed obviously. For example, roadway floor heave stops increasing about 80 m behind the coal face when roof pre-split is applied, while, the roadway floor heaves stops rising about 100 m behind the coal face when roof pre-split is

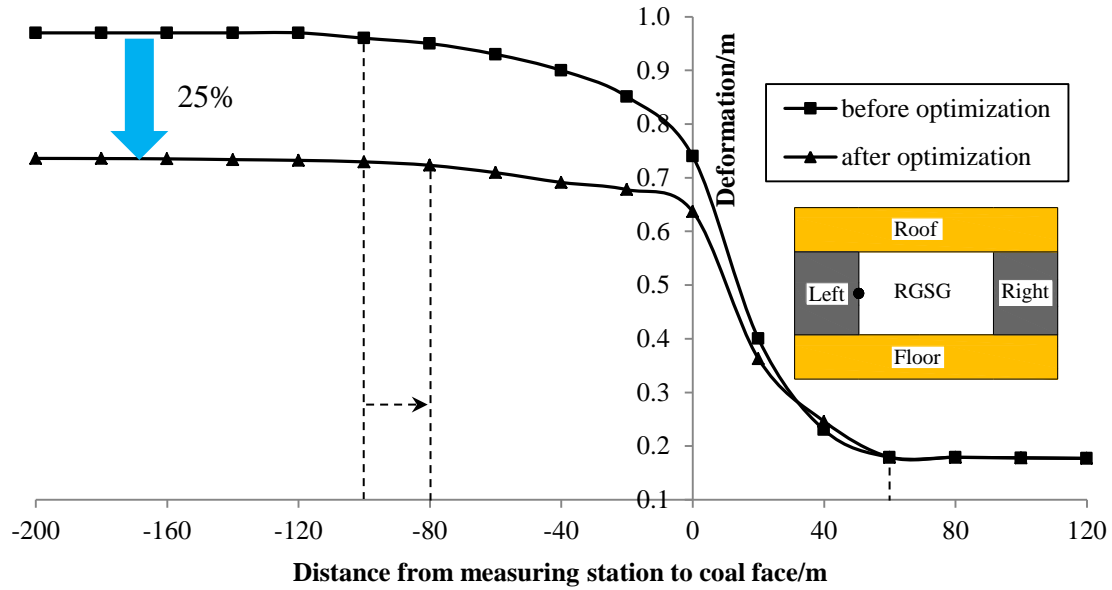
not employed. Same situation happens to roadway roof. The roof sag before roof pre-split maintain stable about 100 m back the coal face, and after roof pre-split however, that position moves to 80 m behind the coal face.



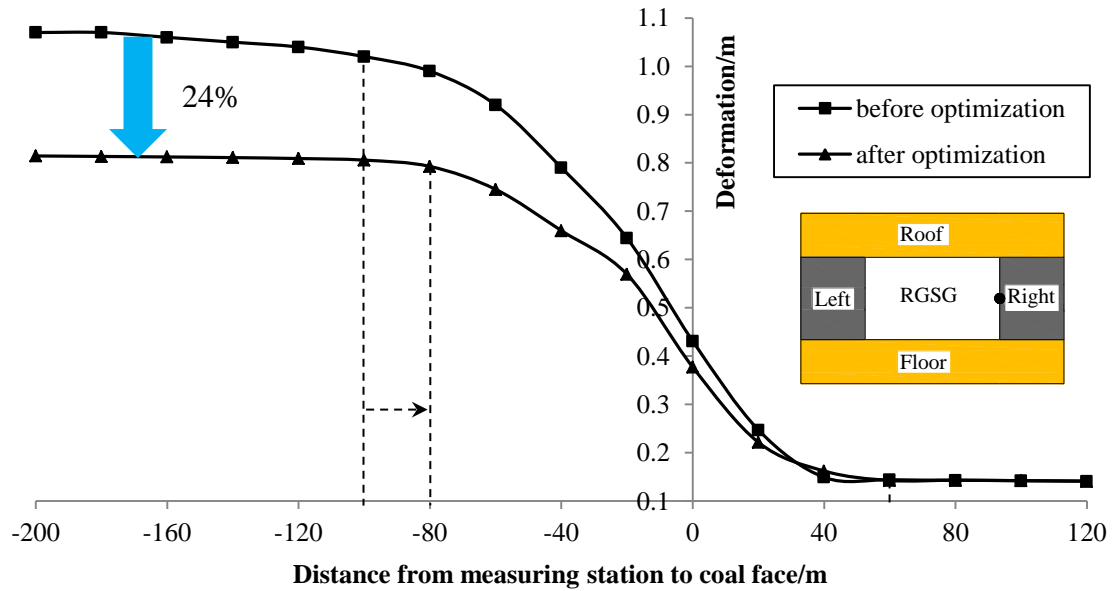
(a) Deformation of floor



(b) Deformation of roof



(c) Deformation of left sidewall



(d) Deformation of right sidewall

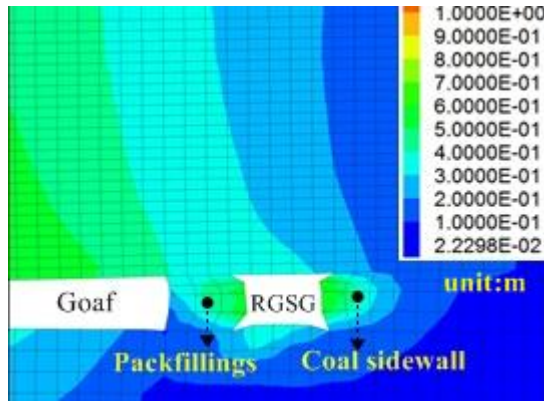
Fig. 4-2 Curves of deformations of RGSG surrounding rock with and without roof pre-split

The deformation value of the RGSG surrounding rock also reduces considerable, as expected. The RGSG floor heave decreases most obviously by 57% with 767 mm decrement, followed by the roof sag reduced by 55% with 469 mm decrement. The third significant improvement is the left sidewall deformation, with 235 mm decrements accounting for 25% of the previous value. Lastly, the coal sidewall convergence decreases by 24% with 257 mm decrement, ranking forth.

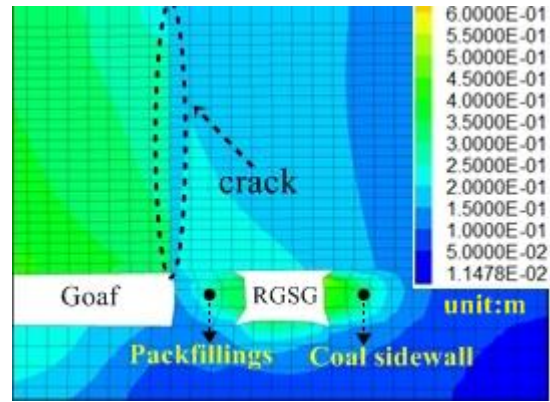
4.2.3 Deformation Mechanism before and after Hard Roof Pre-Split

In order to explain above descriptions about overlying strata movements, the deformation contour of roadway surrounding rock within 100 m behind the coal face is presented in Fig. 4-3. Before roof pre-split (Fig. 4-3(a)), it is found that the primary movement of the roof cantilever at the edge of goaf is rotation, and this kind of movement can transfer to the roof over RGSG, leading to significant compression to roadway surrounding. As a result, the RGSG experiences severer convergence, especially the floor. The strength of the floor is lowest compared with other parts of roadway because it is not supported. When the hard main roof sinks, large compression is imposed on packfillings and right coal sidewall. Consequently, two results are produced. Firstly, the packfillings and right coal sidewall deform in vertical direction and horizontal direction. Secondly, one part of the compression stress induced by hard roof sink is transferred to weak floor strata through relative strong packfillings and right coal sidewall. As a final result, large floor heaving occur due to the compression from packfillings and right coal sidewall at two edges. After roof pre-split (Fig. 4-3(b)), vertical sink plays the leading role in the movements of roof beside the roadway, and importantly, this sink movement cannot transfer to the adjacent roof over RGSG, due to pre-split crack. As a consequence, roadway surrounding rock suffers little compression from hard roof sink, and roadway stability is improved considerably.

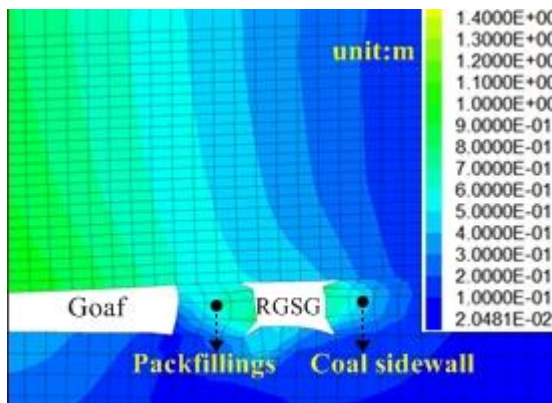
In addition, the position where roadway surrounding rock deformations stop moves closer to coal face after roof pre-split. It is because the deformations of the RGSG surrounding rock are generated by the movement of overlying strata, and the roadway deformations start once the coal panel is extracted and finish when the overlying strata movements stop. From the following pictures, it can be found that the sink of the overlying strata is quicker after pre-split, for example, the cracked main roof near the RGSG has already touched the goaf floor 40 m behind the coal face, and the same part of the main roof before roof pre-split is still sinking. It means that the influencing period of the main roof movements on RGSG surrounding rock is reduced after the main roof is cracked along the goaf edge, and the corresponding time of roadway surrounding rock deforming is shortened. Before coal face, the influencing time is not changed because the roof pre-split is not conducted at that time.



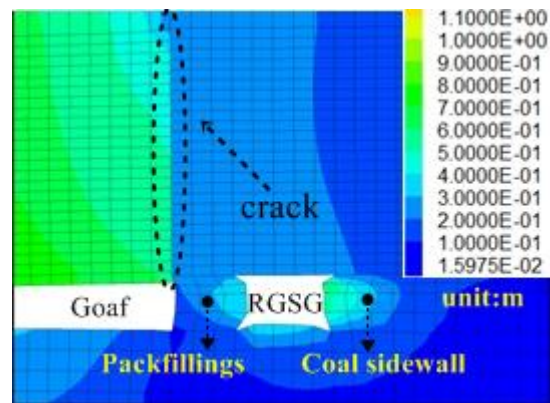
8 m behind coal face



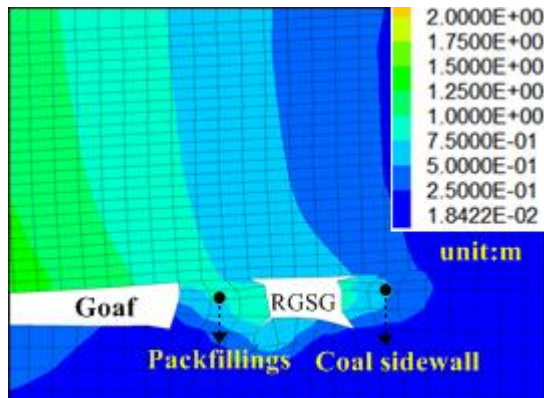
8 m behind coal face



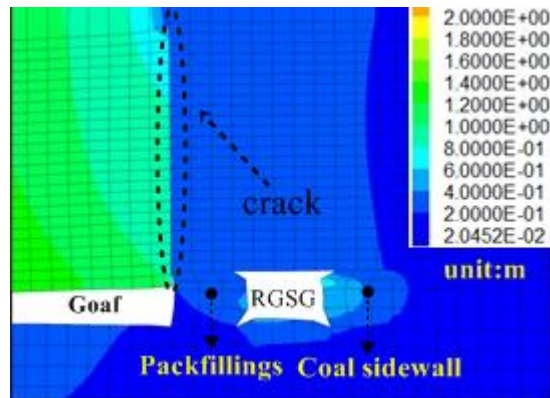
16 m behind coal face



16 m behind coal face



24 m behind coal face



24 m behind coal face

Fig. 4-3 Contour of deformation of RGSG under hard main roof before and after roof pre-split

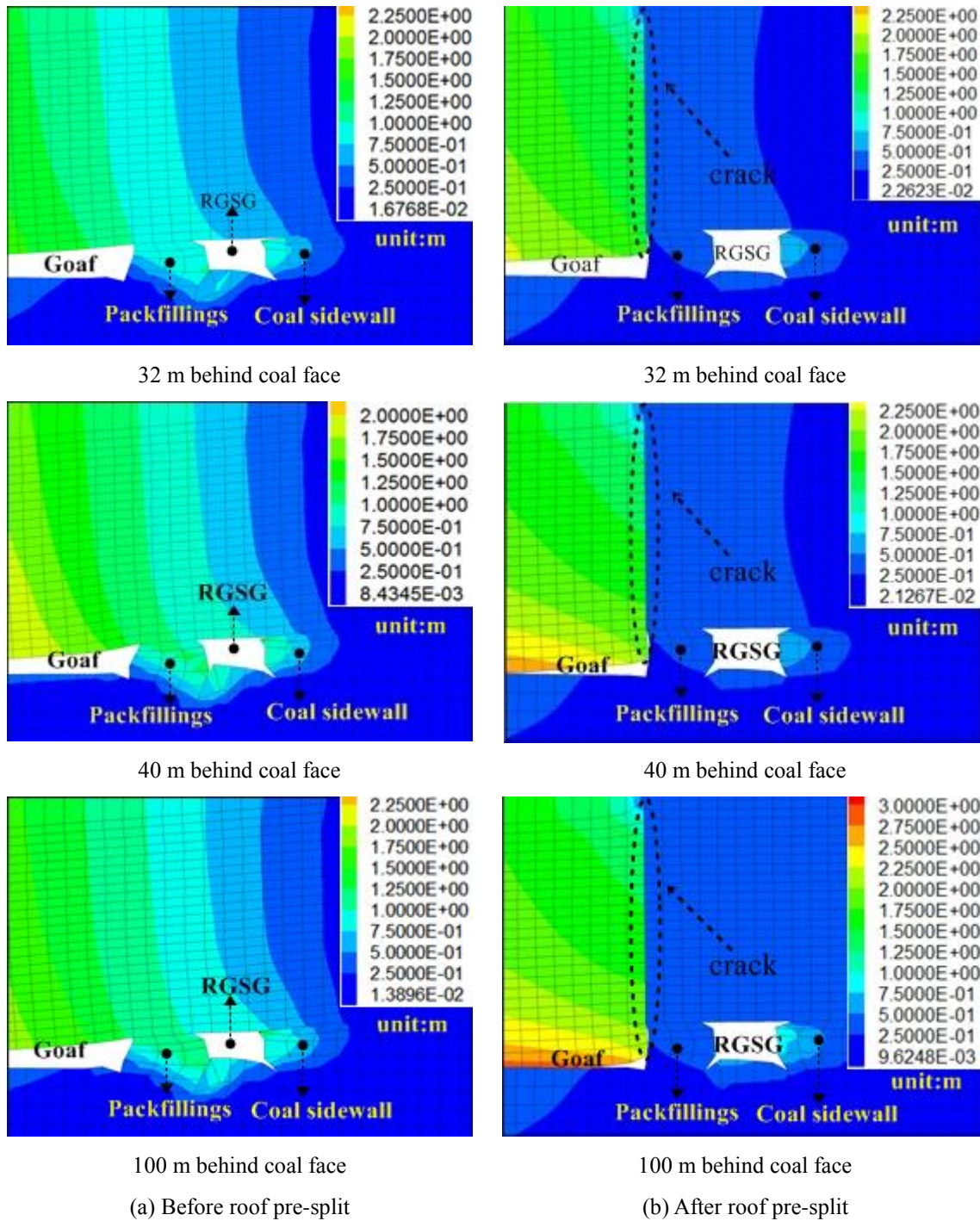
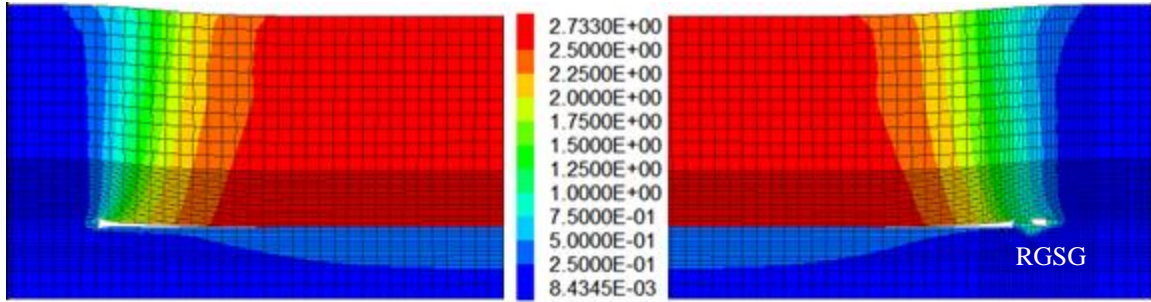
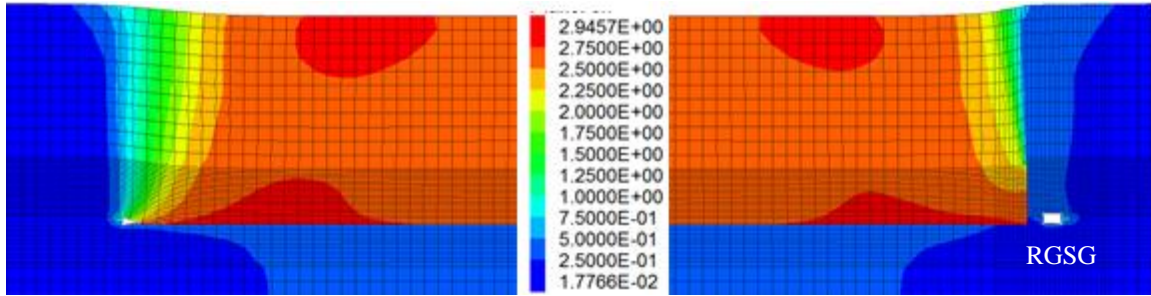


Fig. 4-3 Contour of deformation of RGSG under hard main roof before and after roof pre-split

Last but not the least, the pre-split technology can only changes the regional roof structure near RGSG, and the roof structure far from the RGSG will not be changed obviously, as shown in Fig. 4-4. Therefore, the pressure on supports at coal face cannot be improved.



(a) Deformation contour of the goaf overlying strata before pre-split



(b) Deformation contour of the goaf overlying strata after pre-split

Fig. 4-4 Deformation contour of the goaf overlying strata before and after roof pre-split

4.3 Improved Grout Bolting Technology to Control the RGS Sidewalls

According to above analyses, the roof pre-split technology can only improve the stability of the RGS after coal panel is mined (behind the coal face), and the deformations of roadway surrounding rock before coal face cannot be reduced obviously. The final deformations of the RGS sidewalls are still very large although some improvements have been achieved through roof pre-split. It has been mentioned above, the shallow part of sidewall goes in to plastic stage after roadway excavation, and this plastic zone enlarges when suffering from the disturbances of coal face moving, and at same time cracks also develop in this plastic zone, which triggers sidewall collapse easily. To reduce the deformation of cracked sidewalls of RGS under hard main roof, a modified grout bolting technology (including grouting cable bolt and grouting rock bolt) that is capable of providing confining stress and grouts injection to the surrounding rock simultaneously is proposed, as shown in Fig. 4-5. This roadway supporting technology should be installed before the roadway suffering from the disturbance of front abutment stress of moving coal face.

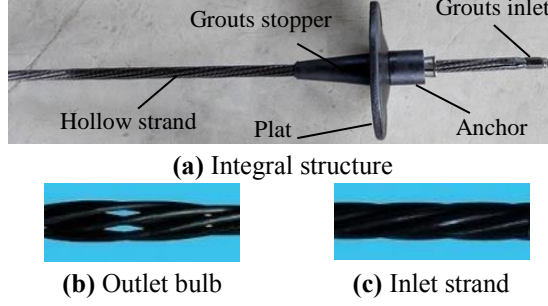


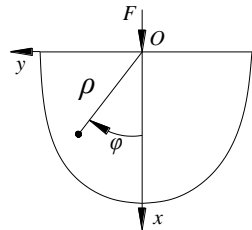
Fig. 4-5 Structures of the grouting cable bolt

4.3.1 Improvements of the Grout Bolting Technology

In order to understand the controlment of the grout bolting technology to the large deformed roadway surrounding rock with developed cracks, improvements of the grouting cable bolt in different installation stages are studied.

4.3.1.1 During the installing stage

Usually, preforce is installed by a special tension jack after the cable bolt is anchored by resin. The confining stress induced by preforce plays an important role in the controlling large deformed surrounding rock with cracks. Without cracks, distribution of the additional stress in the surrounding rock can be simplified as the stress transfers in an elastic body under the condition that a half-plane suffers a focus normal force. The stress at any position inside the rock can be calculated according to the following Equations (Xu 1978):



$$\left. \begin{aligned} \sigma_x &= -\frac{2F \cos^3 \varphi}{\pi \rho} \\ \sigma_y &= -\frac{2F \sin^2 \varphi \cos \varphi}{\pi \rho} \\ \tau_{xy} &= -\frac{2F \sin \varphi \cos^2 \varphi}{\pi \rho} \end{aligned} \right\} \quad (6)$$

In Equation (6), F equals to the preforce (100 kN); confining stress σ_x is in inverse proportion to the distance (ρ) to the point O . It means that the confining stress σ_x in surrounding rock generated by preforce F decreases gradually as the distance to surrounding rock surface increases. Adversely, the cracks in plastic zone also weaken this transfer of confining stress into deep side of surrounding rock. The space in cracks is usually filled with water, air and powdery rock, resulting in the normal stiffness of the cracks being much smaller than that of the solid rocks. Consequently, the passage of

stress transfer is blocked. The precondition of the stress transfer from one side of a crack to the other is that the crack must be compressed to close. During the installation of preforce, the cracks in the shallow range of surrounding rock are compressed to close gradually. In the deeper side, however, the confining stresses reduce severely because of the natural attenuation and the weaken action of cracks. As a consequence, the cracks in deeper side achieve little confining force at the end of this stage.

4.3.1.2 During the grouting stage

(1) Control the cracks more effectively. As analyzed above, the cracks found in a shallow range of roof strata are closed during the installation of preforce, whereas the cracks in deeper side are preserved. To resolve this problem, grouting is conducted through a predesigned hollow grouting pipe. Mechanical models of the grouting cable bolt with and without grouting are shown in Fig. 4-6. Cable bolt is considered to be one type of passive support method and the confining stress is activated by the deformation of the rock mass between its two ends (Hagan 2004). As shown in Fig. 4-6(a), when the space of one crack experiences an enlargement of Δm , the cable bolt will produce a confining force F_1 through the steel plate on the surface of surrounding rock.

$$F_1 = K \times \Delta h_1 \quad (7)$$

Where, K is the tension stiffness of the cable bolt; Δh_1 is the effective extension of the cable bolt. Notably, $\Delta h_1 \leq \Delta m$, because some part of the Δm produced by one crack may be offset by the close of another crack. Then this confining force F_1 transfers from surrounding rock's surface and experiences the natural attenuation and the weaken action of cracks, and finally acts on the target crack with an even smaller confining force than F_1 .

In Fig. 4-6(b), however, the cracks and cracks in rock strata are filled with grouts, which bond the surrounding rock with the cable bolt along the whole length of rod. Consequently, the cable bolt is more sensitive to the deformation of surrounding rock. When the space of one crack experiences an enlargement of Δm , the cable bolt will produce a confining force F_2 immediately through the grouts to the target crack.

$$F_2 = K \times \Delta h_2 \quad (8)$$

Where, Δh_2 equals to the Δm . It means that the target crack will get a bigger confining force with a shorter time compared with that in the situation without grouting.

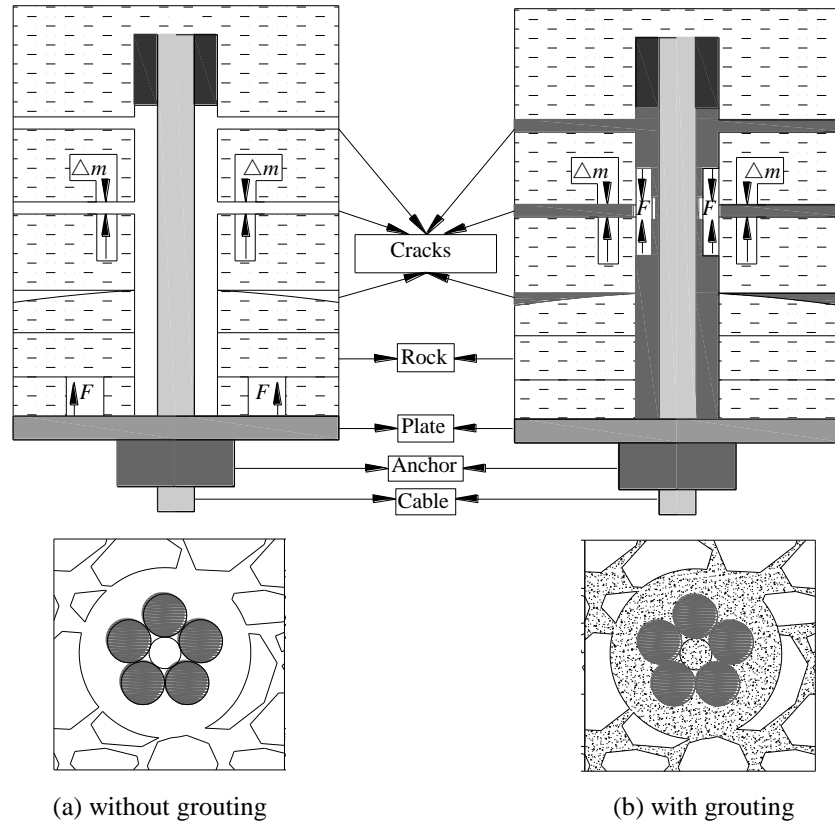


Fig. 4-6 Mechanism of the cable bolt in cracked rock with and without grouting

(2) Large bearing capacity. Bearing capacity of the grout bolting also increases considerably due to full anchorage resulting from grouting. Bearing capacity is a valuable parameter to evaluate reinforcement of a cable bolt to the rock engineering. In order to compare the bearing capacity between the grout bolting technology and conventional bolting technology, numerical pull out tests of these two geotechnics in coal are conducted, using FLAC3D software. Conventional cable bolt has resin anchorage of 3.0 m, and grouting cable bolt has resin anchorage of 3.0 m plus cement anchorage of 3.0 m. Conventional rock bolt has resin anchorage of 1.0 m, and grouting rock bolt has resin anchorage of 1.0 m plus cement anchorage of 1.5 m. Detailed parameters used in this simulation are listed in Table 7, and the simulation results are shown in Fig. 4-7. The peak pull out force of the grouting cable bolt in coal is 1.9 times (335 kN / 174 kN) larger than that of conventional cable bolts, and the maximum bearing capacity of grouting rock bolt is 2.6 times (160 kN / 60 kN) larger than the conventional rock bolt. Larger bearing

capacity indicates that higher force can be generated to confine the deformations of surrounding rock, and that the tension strength of cable bolt rod (≥ 580 kN) and rock bolt rod (≥ 220 kN) can be used more efficiently.

Table 7 Parameters of the pull out tests of rock bolt and cable bolt in RGSG sidewall

Supporting name	E_{mod} (N/m ²)	Y_{tens} (N)	X_{carea} (m ²)	Gr_{coh} (N/m)	Gr_k (N/m ²)	Anchorage length (m)
Conventional cable bolt	8×10^{10}	5.8×10^5	3.7×10^{-4}	9×10^4	2×10^7	3.0
Grouting cable bolt	8×10^{10}	5.8×10^5	3.7×10^{-4}	9×10^4	2×10^7	6.0
Conventional rock bolt	2×10^{10}	2.5×10^3	3.7×10^{-4}	9×10^4	2×10^7	1.0
Grouting rock bolt	2×10^{10}	2.5×10^3	3.7×10^{-4}	9×10^4	2×10^7	2.5

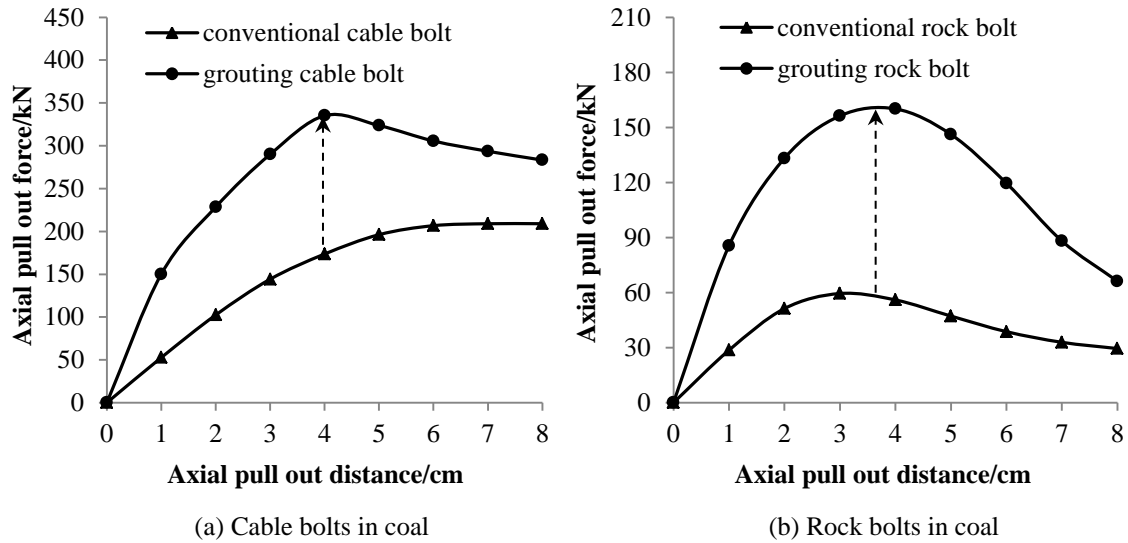


Fig. 4-7 Results of the pull out tests of rock bolt and cable bolt in RGSG sidewall

4.3.2 Mechanism of the Grouting Technology in RGSG Sidewall

According to the analyses of stress distribution, a plastic zone appears in the shallow range of the coal sidewall where the most of sidewall conveyance comes from. This plastic zone is widened gradually by several stress disturbances, especially the one generated by the strata movements behind the coal face. Behind the coal face, overlying strata of the RGSG will break, and then sink and rotate along with the compaction of the caved rock in goaf. The structure model of the RGSG surrounding rock behind the coal face is built, as shown in Fig. 4-8.

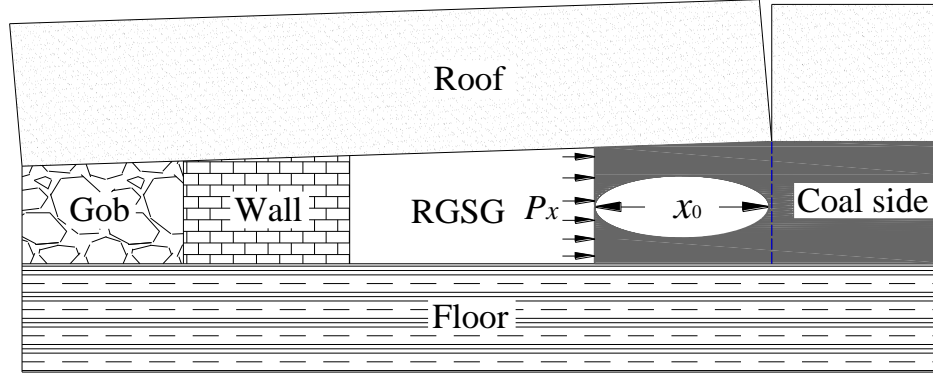


Fig. 4-8 Structure model of the RGSG surrounding rock behind the coal face

As shown in Fig. 4-8, the width of plastic zone x_0 can be calculated as following (Bai, 2006):

$$x_0 = \frac{m\lambda}{2 \tan \varphi_0} \ln \left(\frac{k\gamma H + \frac{C_0}{\tan \varphi_0}}{\frac{C_0}{\tan \varphi_0} + \frac{P_x}{\lambda}} \right) \quad (9)$$

Where, m is the mining height; λ is the lateral stress coefficient; k is the coefficient of vertical stress concentration; γ is the volume-weight of overburdens; H is the thickness of overburdens; C_0 is the cohesion of the coal; φ_0 is the friction angle of coal; P_x is the confining force of the coal sidewall. As shown in Equation (9), the volume-weight and thickness of overburdens, mining height, coefficient of vertical stress concentration and lateral stress coefficient are consistent respect to a certain geological condition. Hence, the width of the plastic zone is governed only by the friction angle, cohesion and confining stress and these parameters can be improved by appropriate geotechnical methods. It is believed that the mechanical parameters of surrounding rock are mainly determined by weak planes in it (Brady and Brown, 1993; Singh et al., 2002; Verma et al., 2010). Grouting cable bolt performs obvious superiorities in these aspects. First, the bearing capacity of the grouting cable bolt has been found to be larger than that of a conventional cable bolt, providing high confining stress P_x to increase the bearing capacity of the reinforced surrounding rock. Second, the grouts injected into cracked surrounding rock displaces the air and water overlying the cracks and fissures, and then fills and cements the surface of cracks and fissures, thereby increasing the stability of the weak planes. Third, some micro-cracks and fissures that are too small to interact with grouts will be closed due to the compaction from high grouting pressure. Consequently, mechanical parameters like friction angle and cohesion are improved and the width of the

plastic zone is decreased. Last but not the least, the length of the roof cantilever can be decreased by reducing the plastic zone, which decreases the heavy load exposed on the artificial packfillings.

4.3.3 Effectiveness of the Grout Bolting Technology on RGSG Sidewalls

4.3.3.1 Numerical simulation schemes

In order to verify the effectiveness of the grouting bolting technology on RGSG sidewalls, the numerical model previous Chapter 4.2 is employed. All the conventional rock bolts and cable bolts installed in roadway sidewalls (Fig. 4-9(a)) are replaced by the grouting rock bolts and grouting cable bolts (Fig. 4-9(b)) to model the fully anchorage improvement after grouting and the parameters of grouting cable bolts and grouting rock bolts are set according to the above Table 7. The residual cohesion and friction angle of the RGSG coal sidewall within anchorage range are improved according to the following Table 8 to model the improvement of rock mechanics of RGSG sidewalls by grouts injection.

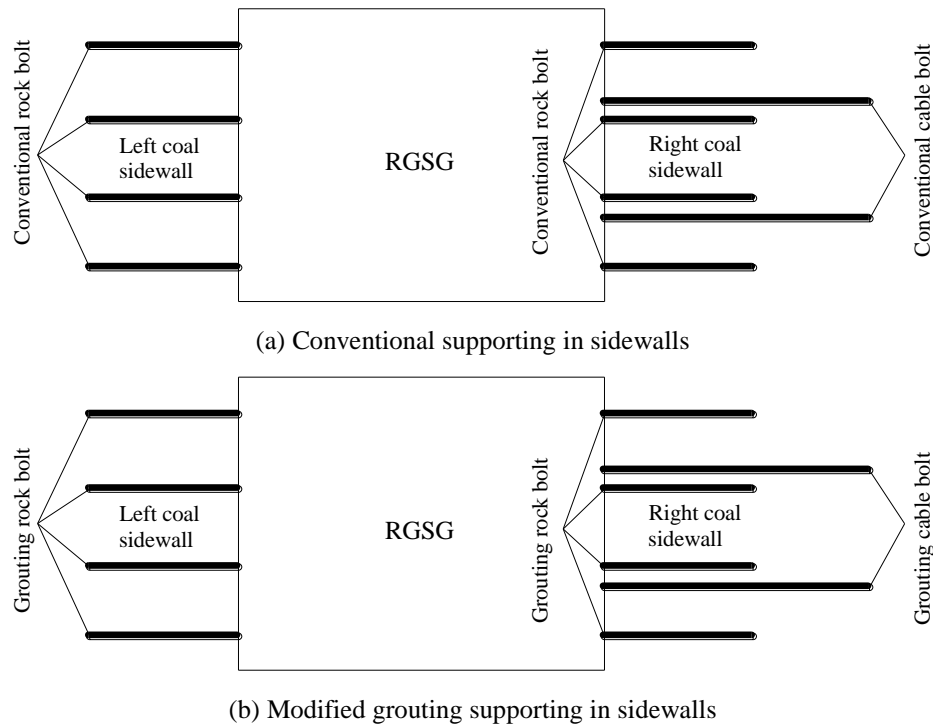


Fig. 4-9 Conventional and modified supporting in RGSG sidewalls

Table 8 Residual cohesion and friction angle of coal sidewall after grouting

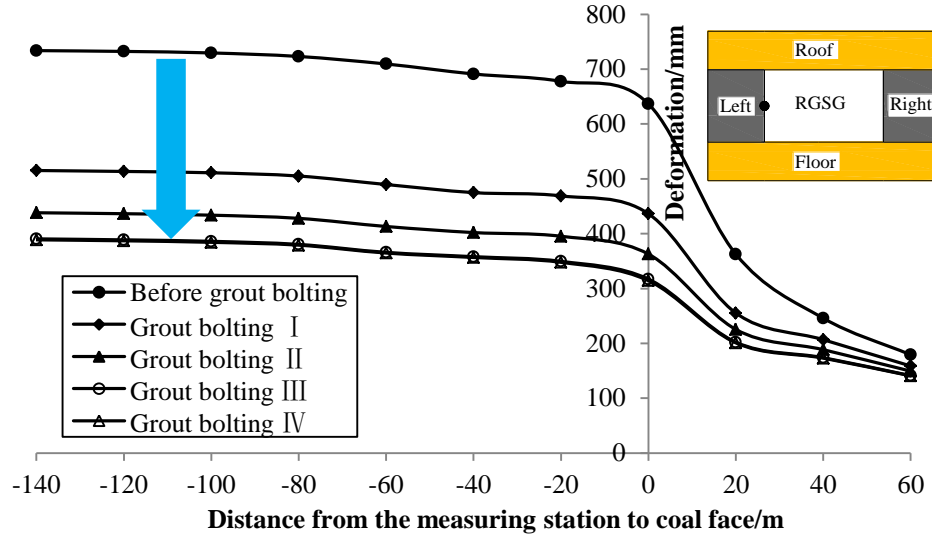
Simulation schemes	Residual cohesion (MPa)	Ratio of residual to original cohesion (MPa)	Residual friction angel (°)
Before grout bolting	0.08	10%	21.0
Grout bolting I	0.16	20%	21.5
Grout bolting II	0.24	30%	22.0
Grout bolting III	0.32	40%	22.5
Grout bolting IV	0.40	50%	23.0

4.3.3.2 Simulation results analyses

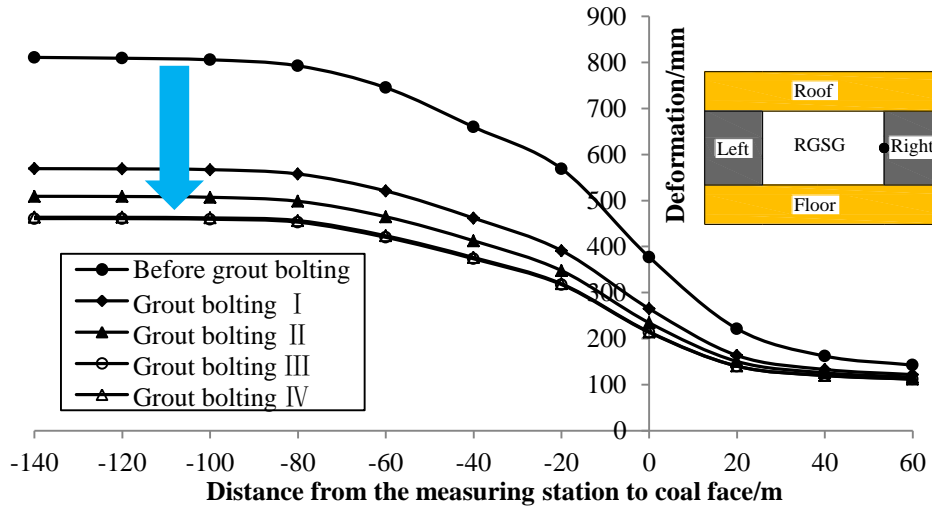
After the RGSG is supported by the modified grout bolting technology in coal sidewalls, roadway deformations are measured and the results are shown in Fig. 4-10, in which the previous roadway deformations without grout bolting technology are also added.

Fig. 4-10(a) represents the RGSG left sidewall deformation during coal panel mining. We can find that the left sidewall deformation before coal face passing by makes the main contribution the whole sidewall deformation, and the one behind the coal face, however, is very limited because the strength of the packfillings is larger than coal sidewall and the fact that compression stress is released by roof pre-split. After the coal sidewall is supported by the grouting rock bolts and accompanied grouts injection, the deformation of the left coal sidewall is reduced considerably. The more the residual cohesion and friction angle are improved, the more the decrement of coal sidewall deformation is. Sidewall deformation is reduced to 356 mm when the coal sidewall is reinforced by the grout bolting technology with grouting scheme III, and at this time, the residual cohesion is 40% of original one. Fig. 4-10(b) represents the RGSG right sidewall deformation during coal panel mining. We can find that both of the deformations before and behind coal face are reduced significantly after applied of the grout bolting technology. When the right coal sidewall is supported by the grouting cable bolts and grouting rock bolts with grouting scheme III, its deformation can be decreased to 456 mm from 792 mm. It should be note that when the grout bolting scheme is changed from III to IV, the deformations of coal sidewalls are not reduced any longer. It means that grout

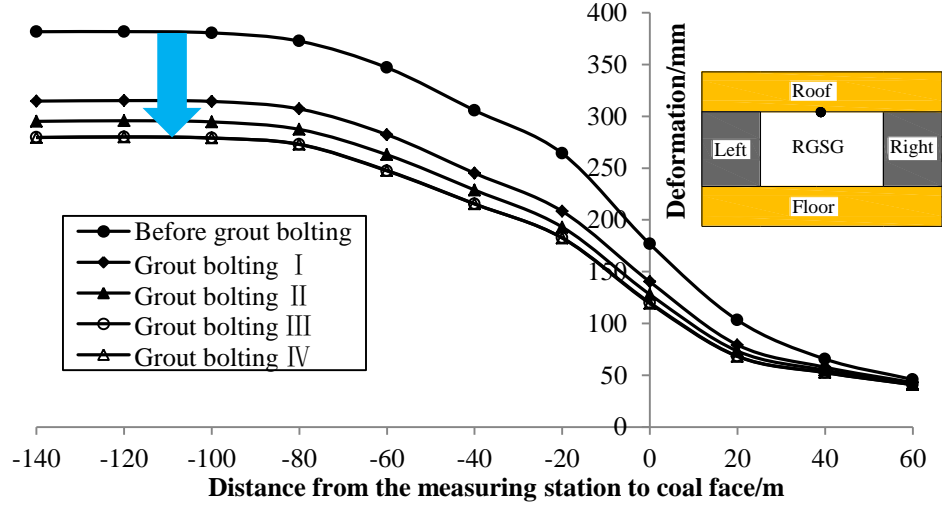
bolting technology accompanied by the increment of 40% of the residual cohesion of the coal sidewall is enough for stability maintainance of the RGSG coal sidewalls.



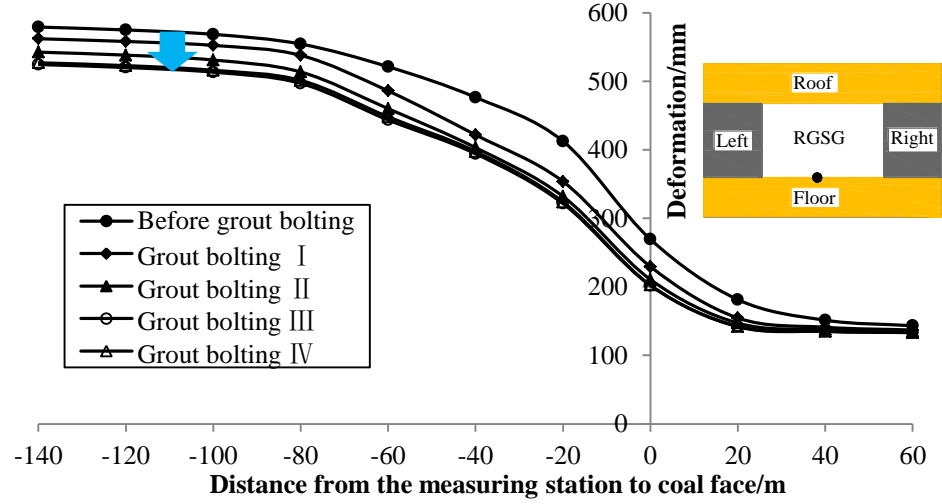
(a) Left sidewall deformation



(b) Right sidewall deformation



(c) Roof sag



(d) Floor heave

Fig. 4-10 RGSG deformations after sidewalls are supported by grout bolting technology

According to the results in Fig. 4-10(c) and (d), it can be seen that the deformations of roadway roof and floor are also reduced, although only the coal sidewalls are supported by the grout bolting technology. It means that the deformations of roadway different surrounding rock are in mutual coordination and the stability of roadway coal sidewall can promote the stability of roof sag and floor heave to same extent.

In addition, the plastic zone in the RGSG surrounding rock after different grout bolting reinforcement to coal sidewalls is also measured when the first coal panel mining finishes and the results are shown in Fig. 4-11. Accompanying the deformation reduce of the roadway surrounding rock, breaking style is also changed, especially to the roadway sidewalls. In left sidewall, shear broken zone is reduced considerably and replace by

strength recovery one, which is the reason why the above mentioned deformation decrease are achieved after application of this kind of reinforcement to roadway sidewalls.

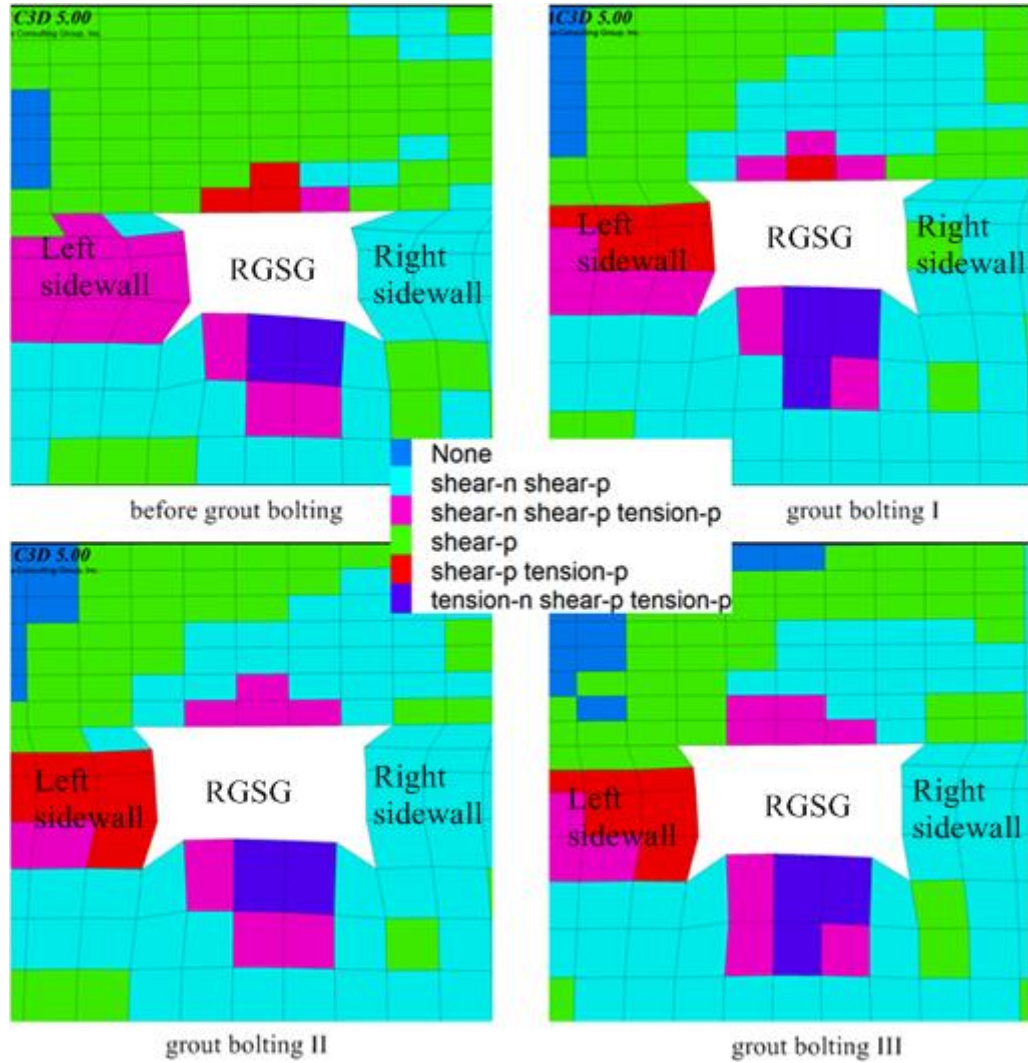


Fig. 4-11 Plastic zones distribution in RGSG surrounding rock after grout bolting to sidewalls

4.4 Grouting Reinforcement to Control the Large Heaved Floor

As mentioned above, the surrounding rock of RGSG preforms corresponding deformations after experiencing the stress disturbances from roadway excavation and coal panel mining. The deformations of RGSG surrounding rock increase as the main roof becomes thicker and the immediate roof becomes thinner and reach the largest value when the RGSG is beneath 12 m hard main roof. At this time, the large compression of the long roof cantilever makes the main contribution to the roadway section shrinkage. Thereby, roof pre-split technology is proposed to resolve this problem by shortening the

length of hard roof cantilever over the RGSG. As expected, the deformations of RGSG surrounding rock are reduced considerably, especially the roof and floor. After roof pre-split, the deformations of roadway sidewalls turn to the main contribution to the roadway section shrinkage, and grout bolting technology is proposed and is verified to be effective. After the RGSG sidewalls are controlled by the grout bolting technology, the deformation of floor that is not supported plays the leading role in roadway section shrinkage again. Actually, the large floor heaving is attributed to the weak rock mechanics of mudstone and large compressive stress from movements of long roof cantilever. As for the long hard roof cantilever, roof pre-split technology has been proposed and verified to be effective in previous Section 4.2. In this chapter, the weak mechanics of the floor strata is put into mind by employing grouting technology to reduce the large floor heaving.

4.4.1 Mechanism of the Floor Heaves During Coal Panel Mining

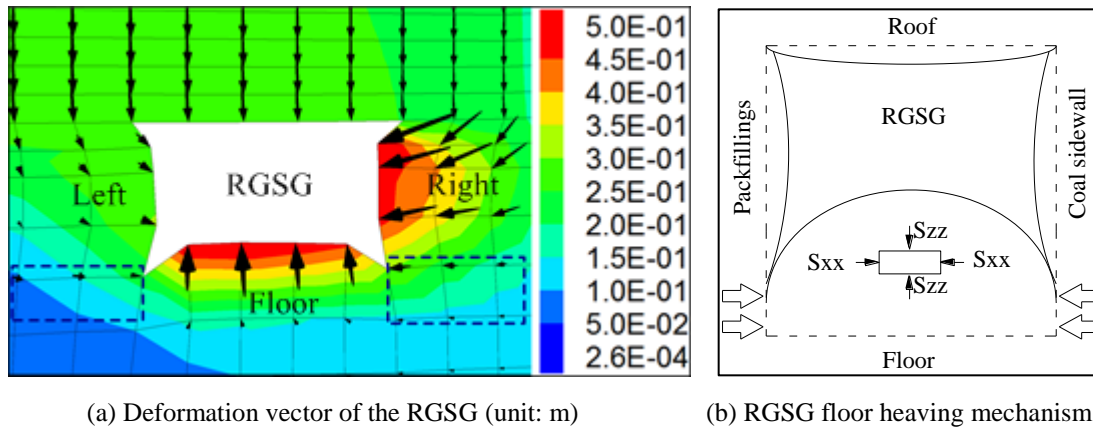


Fig. 4-12 Deformation vector and mechanism of the RGSG floor heaving before floor grouting

Fig. 4-12(a) represents the final deformation of the RGSG when roof pre-split technology and sidewall grout bolting technologies are applied. It can be seen that the moving directions of the rock masses adjacent roadway floor strata are almost horizontal. It implies that this floor heave is mainly attributed to the horizontal compression of neighbouring rock mass. As mentioned in above Section 3.2.1, the confining stress normal to the roadway surrounding rock surface is reduced considerably, which makes the strength decrease of the roadway surrounding rock and leads to the surrounding rock deformations. For roadway floor, vertical stress acts as the confining stress and the horizontal stress plays the role of compressive stress, and the floor heave is the final

result of interaction of these two kinds of stress and the floor strength. In light of this fact, a mechanical model is built, as illustrated in Fig. 4-12(b), and the vertical stress and horizontal stress in floor strata are monitored during coal panel retreating based on the FLAC3D model in above Section 4.3 with grout bolting III, and the results are shown in Fig. 4-13.

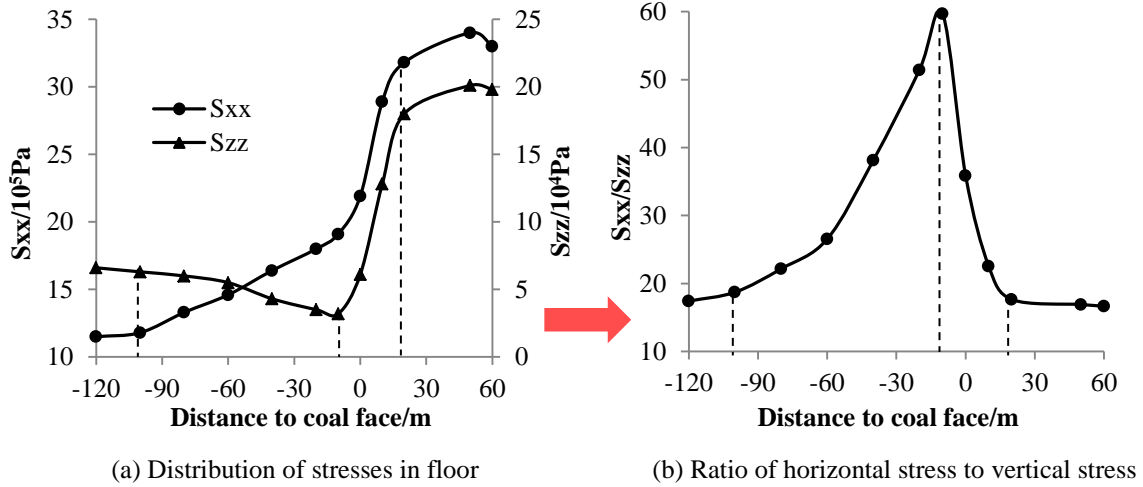


Fig. 4-13 Distribution of the stresses in RGSG floor during coal face moving

In Fig. 4-13(a), horizontal stress and vertical stress both decrease quickly about 20 m ahead of the coal face, and the vertical stress reduces to the lowest value of 3.2×10^4 Pa when the roadway is 20 m behind the coal face. When the distance to coal face enlarges to 100 m, the horizontal stress and vertical stress do not change any more. Consequently, the ratio of the horizontal stress to vertical stress (Fig. 4-13(b)) that influences the strength of roadway floor strata significantly experiences corresponding variation during coal face moving. In detail, the ratio starts to increase when the measuring station is 20 m before the coal face, and then rises sharply to the maximum value of 60 when the measuring station is 15 behind the coal face. After that, this ratio decreases quickly until 100 m away from the coal face.

During the coal panel retreating, the deformations at different depths of the floor strata are also measured, and the results are shown in Fig. 4-14. It has been illustrated that the floor heave begins to increase about 20 m before the coal face and archives the largest increasing speed at a distance of 15 m behind the coal face. Finally, the heaving of floor surface reaches largest value of approximately 523 mm about 100 m back the coal face. It should be note that the variation of the roadway floor heave is in consistent with the

variation of the ratio of horizontal stress to vertical stress in floor. It means that the root reason of the roadway floor heaving is that the ratio of horizontal stress to vertical stress is changed under the disturbance of coal panel retreating. In addition, the heaving within 1 m of the floor strata accounts for 72% of whole floor heaving, and at a depth of more than 3 m, there is little floor heaves.

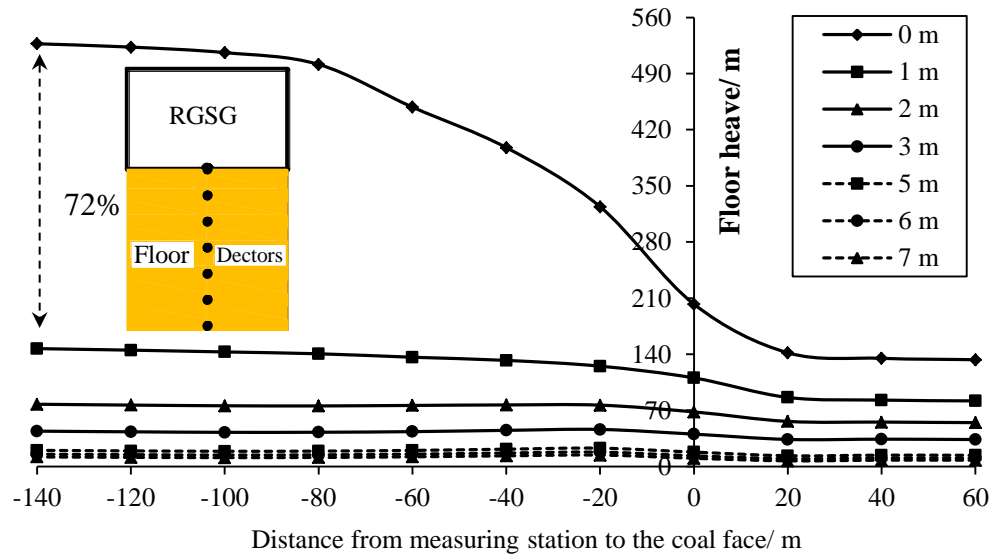


Fig. 4-14 Distribution of the floor heave of the RGSG at different depth during coal face moving

4.4.2 Grouting Reinforcement of the Floor Heave

Over the last few decades, grouting technology has been widely applied in various geotechnical engineering for the purposes of strengthening or making them impermeable (Arvind et al 1993; ISRM 1996; Zhang 2004; Huang et al. 2007; Liao et al. 2011). Poor rock conditions and severe stress disturbances are the main causes of the large floor heave of the RGSG in deep underground coal mine. As for the former issue, grouting reinforcement performs its incomparable advantages by improving the mechanical parameters of the weak surrounding rock fundamentally (Lee et al. 2000; Utsuki 2013; Zolfaghari et al. 2015).

4.4.2.1 Floor grouting schemes

Because of the high stress and low strength in deep mining environment, the shallow part of roadway surrounding rock yields and breaks in a short time after excavations, and then makes contributions to roadway section shrinkage and even

instability. Therefore, for a long time during roadway serving life, this kind of surrounding rock reacts to external load with its residual strength. Additionally, the grouting reinforcement is carried out after roadway excavation in the field, only the residual strength is anticipate to be improved compared with that before grouting reinforcement. From the viewpoint of these, 4 grouting schemes are simulated, in which only the residual cohesion and friction angle are increased, as shown in Table 9.

Table 9 Residual cohesion and friction angle of floor strata after grouting

Simulation schemes	Residual cohesion (MPa)	Ratio of residual and original cohesion (MPa)	Residual friction angel (°)
Before grouting	0.12	10%	24.0
Grouting I	0.36	30%	24.5
Grouting II	0.60	50%	25.0
Grouting III	0.84	70%	25.5
Grouting IV	0.108	90%	26.0

4.4.2.2 Uniaxial compressive testes of Grouted Rock

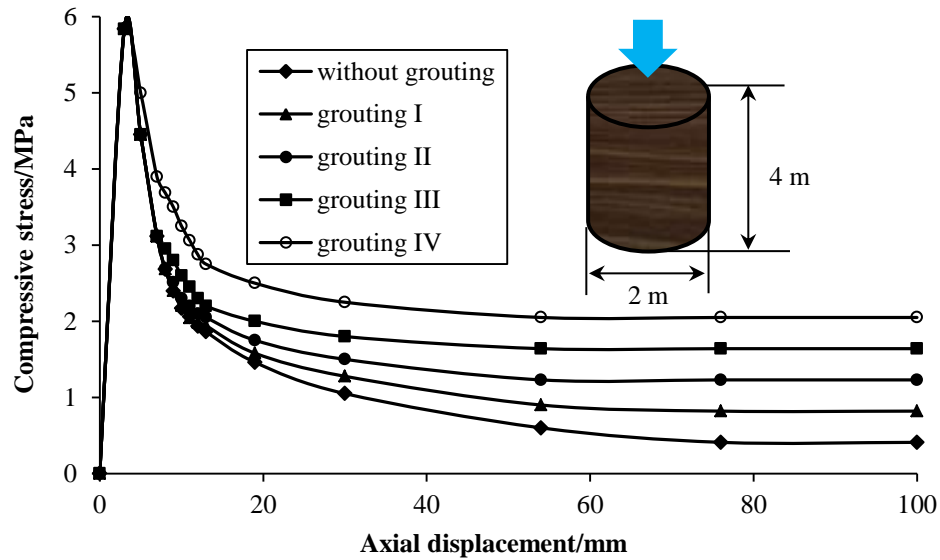


Fig. 4-15 Stress-strain curves of mudstone sample after reinforced by grouting

As mentioned in Section 2.1, the mudstone in floor is set as strain softening constitutive material to model the soft rock mechanics of weak surrounding rock. In order to prepare for the next effectiveness evaluation of the grouting technology on the RGSG floor reinforcement, the exact relationship between these mechanical parameters and

uniaxial compressive strength (UCS) of mudstone are studied, using numerical uniaxial compressive tests. In simulation, a representative cylinder-shaped rock sample having a diameter of 2 m and a height of 4 m are employed, and the cohesion and friction angle of the rock sample are changed to model the improvements of different grouting schemes, and the residual strength of the rock sample is selected as a reference indicator to identify different grouting schemes. The simulated stress-strain curves of these grouting schemes are shown in Fig. 4-15.

It can be seen that the strength of mudstone decreases gradually after yielding and maintains a certain value finally with a large displacement, rather than dropping significantly to zero once yield occurs. This behavior characteristic performs a crucial role in the stability maintenance of the RGSG in response to the special mining conditions in deep environment. Detailedly, 1) Without grouting, the residual strength is 0.41 MPa which is equivalent to 6.8% of the peak strength; 2) with grouting I, the residual strength is 0.82 MPa accounting for 13.7% of the peak strength; 3) with grouting II, the residual strength is 1.23 MPa equaling to 20.5% of the peak strength; 4) with grouting III, the residual strength is 1.64 MPa which accounts for 27.3% of the peak strength; 5) with grouting IV, the residual strength is 2.05 MPa which accounts for 34.2% of the peak strength.

4.4.2.3 Effectiveness of the grouting reinforcement on the RGSG floor heave

As analyzed in Section 4.4.1, the deformations within 1 m depth of the floor strata make the main contributions to the whole floor heave. Therefore, only the rock mechanical parameters within 1 m depth of the floor strata are improved during coal panel retreating (Fig. 4-16), and the other settings are same as the model in Section 4.3 in which the roadway coal sidewalls are reinforced with grout bolting technology III. The simulation results are shown in Fig. 4-16, it can be seen that the floor heaves are reduced considerably by 40% from 516 mm to 273 mm when it is reinforced by the grouting scheme I. When the residual cohesion and friction angle of the floor are increased from the scheme I to II and III, the floor heaves are reduced continually to 202 mm, and 194, respectively. As the parameters of the floor strata are increased furtherly, however, floor heave is not reduced obviously any more.

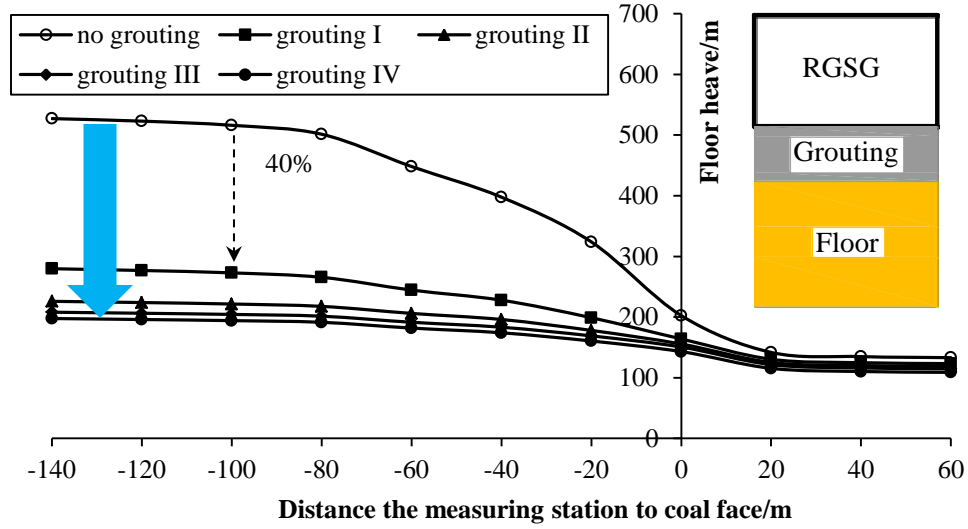


Fig. 4-16 Deformations of the RGSG floor after reinforced by floor grouting

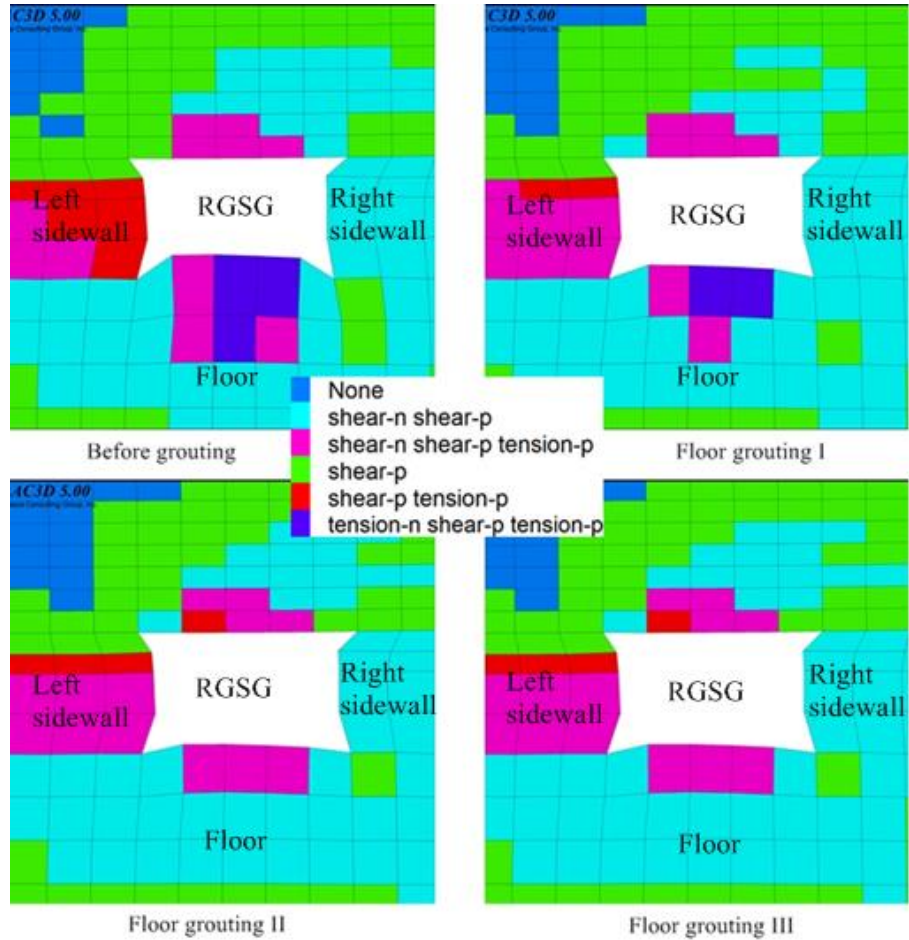


Fig. 4-17 Plastic zones distribution in RGSG surrounding rock after different grouting to floor

During coal panel retreating, plastic zones where the most of deformations comes from, under different grouting conditions are also measured in the floor strata and the

final results are shown in Fig. 4-17. Without grouting reinforcement, it can be seen that the plastic zone in floor strata is biggest of 2 m high and 3 m wide, and this part of floor strata are destroyed mainly because of tension. After grouting, the plastic zone is effectively reduced and the rock failure mechanisms become to shear failure partly. It is, therefore, beneficial to the stability maintenance of floor strata because the shear strength of rock mass is usually larger than the tension strength.

4.5 Summary

In this chapter, four roadway supporting technologies are proposed to maintain the stability of the RGSG according to the different characters of stresses and deformations distribution in the RGSG surrounding rock concluded in chapter 3. These roadway supporting technologies are basically staged supporting strategy, hard roof pre-split technology, sidewalls improved grout bolting technology, and floor grouting reinforcement. The detailed conclusions are as follows:

(1) Basically staged supporting strategy is proposed to maintain the stability of the RGSG. In the first supporting stage, a prestressed bolting system aiming at providing high lateral confining stress is proposed to maintain the stability of the RGSG during roadway excavation. In the second supporting stage, cable bolt system with larger length is suggested within the range influenced by coal face abutment pressure, considering the loose and broken range of the surrounding rock widening. In the third supporting stage, packfillings with gradually increasing strength and reinforcement to the roof over packfillings should be put into mind because of the continually increasing abutment stress behind the coal face.

(2) Deformations of the RGSG under hard main roof are reduced considerably after application of roof pre-split technology. Because the fact that the roadway section shrinkage rate is up to 82.5% when the RGSG suffers the influence of long roof cantilever of hard main roof with thickness of 12 m. Pre-split technology is applied to reducing this influence by shortening the length of roof cantilever, and an interface is set in simulation to model the pre-split cracks. The deformations of the RGSG surrounding rock are reduced considerable, as expected after roof pre-split. The RGSG floor heave decreases most obviously by 57% with 767 mm decrement, followed by the roof sag

reduced by 55% with 469 mm decrement. The third significant improvement is the left sidewall deformation, with 235 mm decrements accounting for 25% of the previous value. Lastly, the coal sidewall convergence decreases by 24% with 257 mm decrement, ranking forth.

(3) Improved grout bolting technology is proposed to control the large deformations RGSG sidewalls. The final deformations of the RGSG sidewalls are still very large (more than 700 mm) although some improves have be achieved through roof pre-split. To control the large deformed sidewalls with developed cracks, a modified grout bolting technology is proposed. This modified technology not only can provide higher confining stress at the stage of installation, but also controls the cracks more effectively and has larger bearing capacity during the followed grouting stage. These advantages promote the stability of the RGSG sidewalls effectively. After application of this technology to the RGSG sidewalls, the deformations of left and right coal sidewall can be reduced to 356 mm, and 456 mm from 729 and 792 mm, respectively.

(4) Grouting reinforcement is proposed to control the large heaved floor. After applications of pre-split to roof and grout bolting technology to coal sidewalls, the deformation of RGSG floor not supported plays the leading role in roadway section shrinkage again. Roadway floor heaving is in direct proportion to the ratio of horizontal stress to vertical stress in floor strata. Grouting reinforcement is proposed to reduce the floor heaves by considering the weak rock mechanics of the mudstone, and only 1 m within the floor is grouted because the heaving within 1 m of the floor strata accounts for 72% of whole floor heaving. When the residual cohesion is increased to 30%, 50% and 70% of the original one and residual friction angle is increased to 24.5° , 25° and 25.5° , respectively, floor heaves are reduced considerably to 273 mm, 202 mm, and 194 mm from 516 mm. As the parameters of the floor strata are increased furtherly, floor heave is not reduced obviously any more. After grouting, the plastic zone is effectively reduced and the rock failure mechanisms become to shear failure partly.

Reference

- Zhang N and Gao MS (2004) High-strength and pretension bolting support of coal roadway and its application. *J. Chin. Univ. Min. Technol* (33), 524–527.
- Xu ZL (1978) *Elasticity*. Higher Education Press. Beijing, 81-3.

- Hagan PC (2004) Variation in load transfer of a fully encapsulated rockbolt. 23rd International conference on ground control in mining. Morgantown, USA
- Bai JB (2006) Surrounding rock control of entry driven along nest goaf. Xuzhou: Press of China University of Mining and Technology 22-36.
- Brady B.G, Brown ET (1993) Rock mechanics for underground mining. Chapman & Hall, London, 85-139.
- Singh M, Rao KS, Ramamurthy T (2002) Strength and deformational behavior of a jointed rock mass. *Rock Mech Rock Eng* 35, 45-64.
- Verma AK, Singh TN (2010) Modeling of a jointed rock mass under triaxial conditions. *Arab J Geosci* 3, 91-103.
- Arvind VS, Dhananjay LS (1993) Grouting Technology in Tunneling and Dam Construction. 2ed ed. India: Aa Balkema; February.
- ISRM (1996) International society for rock mechanics commission on rock grouting. *Int J Rock Mech Min Sci Geomech Abstr* 33, 803–847.
- Zhang N (2004) Theory and practice of surrounding rock control by delayed grouting of roadway. Xuzhou: China University of Mining and Technology press, 14-38.
- Huang CL, Fan JC, Yang WJ (2007) A study of applying microfine cement grout to sandy silt soil. *Sino-Geotech* 111, 71–82.
- Liao KW, Fan JC, Huang CL (2011) An artificial neural network for groutability prediction of permeation grouting with microfine cement grouts. *Comput Geotech* 38, 978–986.
- Lee JS, Bang CS, Mok YJ, Joh SH (2000) Numerical and experimental analysis of penetration grouting in jointed rock masses. *Int J Rock Mech Min Sci* 37, 1027–1037.
- Utsuki S (2013) In-situ experimental studies on improvement of deformability of rock masses by grout treatment. *Jpn Comm Rock Mech*, 9, 7–8.
- Zolfaghari A, Sohrabi Bidar A, Maleki Javan MR, Haftani M, Mehinrad A (2015) Evaluation of rock mass improvement due to cement grouting by Q-system at Bakhtiary dam site. *Int J Rock Mech Min Sci*, 74, 38–44.

CHAPTER 5

FIELD APPLICATIONS

5.1 Application of Staged Supporting Method in RGSG with Depth of 900 m

5.1.1 Geological Condition

Zhuji coal mine is a new mine in Huainan, Anhui Province of China, with a designed productive capacity of 4 million tonnes per year. Geological columnar section stratigraphy of this coal mine is shown in Fig. 5-1.


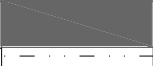

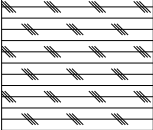

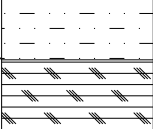
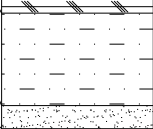


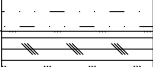
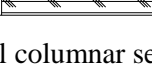
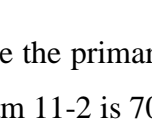
Thickness/ m	Figure	Rock name and nature
6.9		Mudstone: gray-gray; massive, dense, brittle
4.1		11-3 coal seam: simple coal seam structure; weakly metallic luster
9.7		Mudstone: gray-gray; massive, dense, brittle
18.2		Siltstone: gray-dark gray; massive, dense, brittle; with plant fossils
8.7		Mudstone: gray-gray; massive, dense, brittle
9.9		Siltstone: gray-dark gray; massive, dense, brittle; with plant fossils
11.3		Mudstone: gray-gray; massive, dense, brittle
3.1		Fine sandstone: light gray-gray, dense, with plant fossil debris
9.9		Mudstone: gray-gray; massive, dense, brittle
1.2		11-2 coal seam: mainly massive and fragmental
13.1		Mudstone: gray-gray; massive, dense, brittle
6.9		Siltstone: gray-dark gray; massive, dense, brittle; with plant fossils

Fig. 5-1 Geological columnar section stratigraphy of Zhuji coal mine

Seams 11-2 and 11-3 are the primary mineable coal seams, with a thickness of 1.2 m and 4.1 m, respectively. Seam 11-2 is 70~75 m below Seam 11-3. These two seams are both high in gas content ($37.4 \text{ m}^3/\text{min}$) and low in gas seepage coefficient ($0.0011 \text{ m}^2/$

MPa 2d), which impedes gas drainage from surface prior to coal extraction (Liu 2014). Furthermore, the gas with high pressure and large quantity can trigger the outburst as well as gas overrun easily, endangering the mining safety. In addition, Seam 11-2 is buried at a depth of approximately 910 m, large coal pillars will likely be required to support the weight of overlying strata, not only decreasing the resource recovery but also contributing to the outburst resulting from high stress concentration. To resolve the gas emission challenge and improve the coal recovery, a mining system that is capable of achieving simultaneous extraction of gas and coal pillars is put forward.

5.1.2 Simultaneous Extraction of Coal and Gas

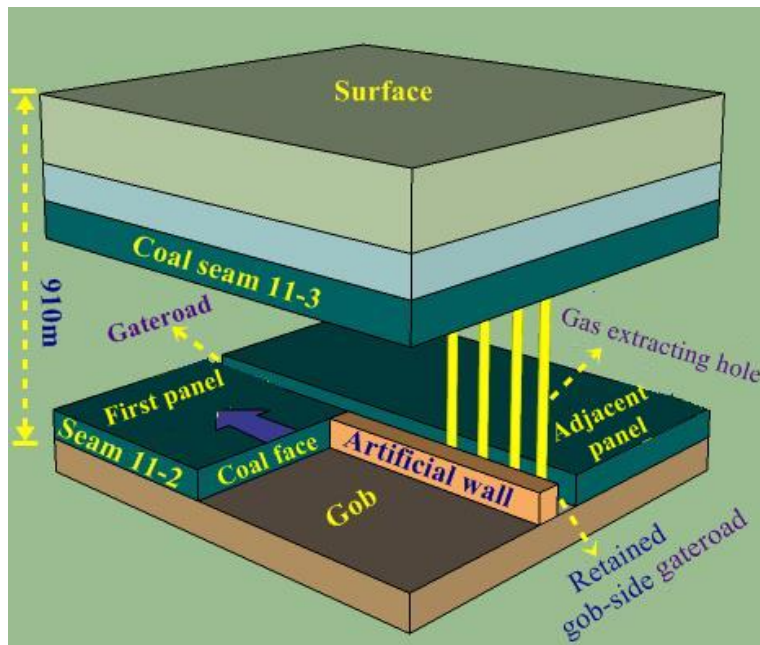


Fig. 5-2 Simultaneous extraction system of coal and gas in Zhuji coal mine

It is believed that gas pressure and permeability can be reduced and increased, respectively, by decreasing the stress in strata (Valliappan et al. 1996; Jia et al. 2013; Si et al. 2015). Coal seam excavation can trigger the movement and breakage of overlying strata, in which in-situ stress redistributes, forming a relatively destressed and cracked region (Leigh 1963; Malone 1965; Qian 1982; Colin 1986). As a result, gas drainage in this region becomes possible, and outburst risk can be eliminated and the coal seam can be extracted safely. RGSG is a longwall gateroad which has been maintained available by constructing an artificial packfillings along the gob side when the coal face advances.

Utilizing the above strata control method and roadway retaining method, a system focused on extracting coal and gas simultaneously is proposed based on the geological characteristics of the Zhuji coal mine, as shown in Fig. 5-2. The Seam 11-2 is chosen for extracting firstly because its outburst potential is relatively lower compared with that of the Seam 11-3. After the Seam 11-2 being extracted, stress relief and fracture propagation can be expected in Seam 11-3, facilitating gas drainage in the Seam 11-3 and creating the possibility for future mining in the Seam 11-3. In addition, the resulting space provided by RGSG in the Seam 11-2 could be used as an access to extract the gas released from the Seam 11-3.

5.1.3 Construction Process and Parameters

According to the staged supporting strategy described above, corresponding construction parameters and process are designed for the RGSG in the Zhuji coal mine when the first coal panel mines, as shown in Fig. 5-3.

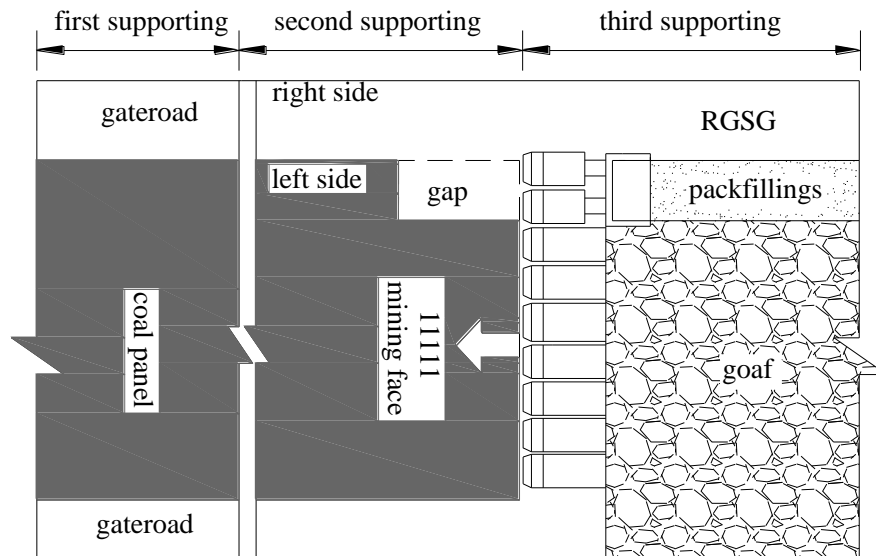


Fig. 5-3 Staged supporting system designed for the RGSG in Zhuji coal mine

5.1.3.1 First Supporting System

The first supporting system consists of steel meshes, rock bolts, cable bolts, steel straps and steel channel beams, as shown in Fig. 5-4. Detailed construction sequences are described as follows: (i) after the gateroad excavation, boreholes for rock bolts and cable bolts are drilled; the rock bolts and cable bolts are then pushed into the boreholes, meanwhile resin capsules are placed at the end of boreholes; the rock bolts and cable

bolts are then revolved and anchored into the surrounding rock; (ii) steel meshes, M5# steel straps (rock bolts), 20# steel channel beam (cable bolts), and steel plates are then placed on the surface of the surrounding rock successively; finally prestress the rock bolts and cable bolts to designed value: 60 kN for rock bolts and 120 kN for cable bolts. This supporting system is constructed as soon as possible after gateroad excavation.

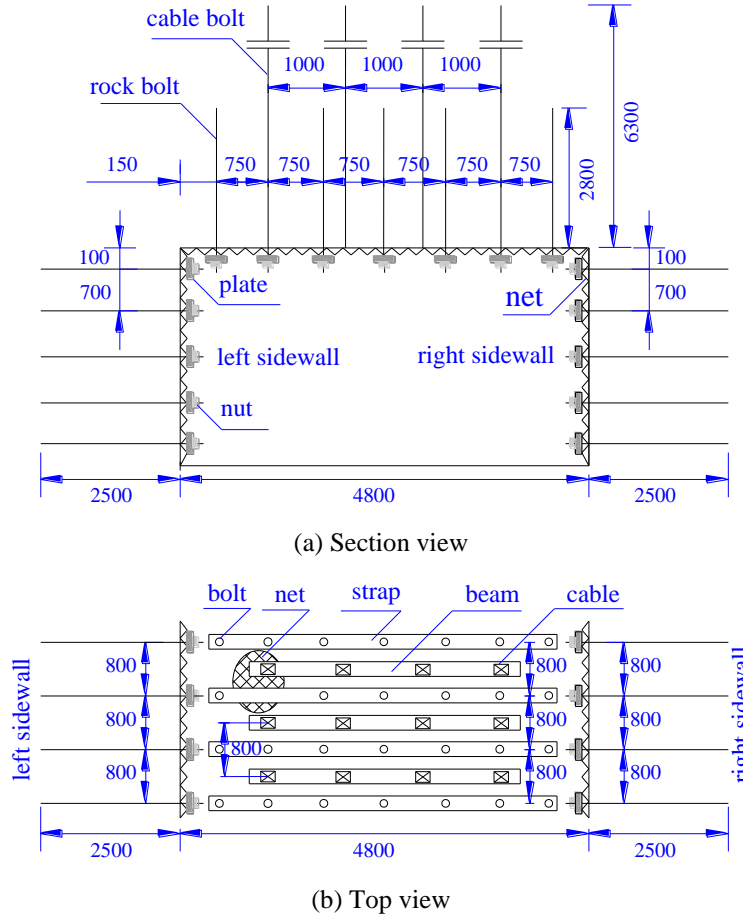


Fig. 5-4 First roadway supporting parameters during roadway excavation (mm)

5.1.3.2 Second Supporting System

To resist the disturbance of the abutment pressure ahead of the coal face, a cable bolts-based reinforcing system (full line in red) is proposed, as shown in Fig. 5-5. Based on the first supporting system (dotted line in black, only cable bolts are illustrated), three rows of cable bolts accompanied by steel channel beams are installed in the roof along the length of gateroad, two rows are installed in the right sidewall. Prestress installation is same as first supporting system. Cable bolts are not installed in the left sidewall considering the influence of cable bolts on the coal cutting shearer. This enhancing

system is constructed 100 m ahead of the coal face where the influence of coal face on the gateroad is triggered.

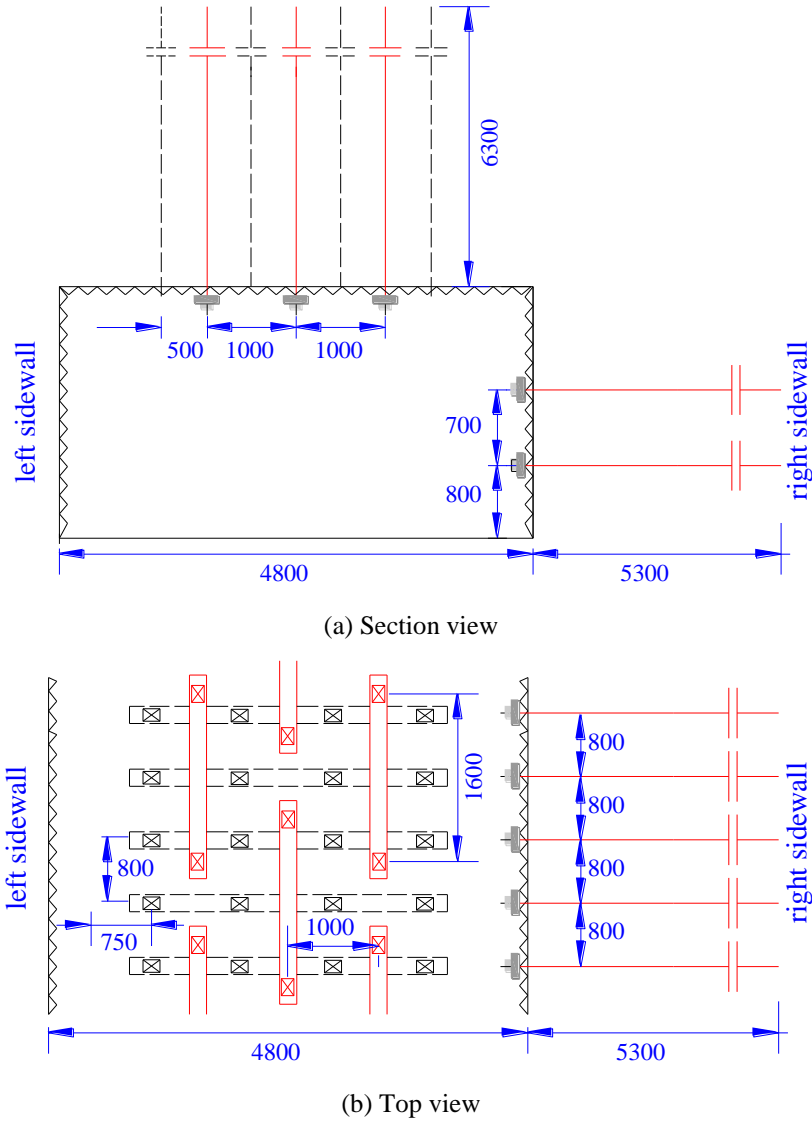
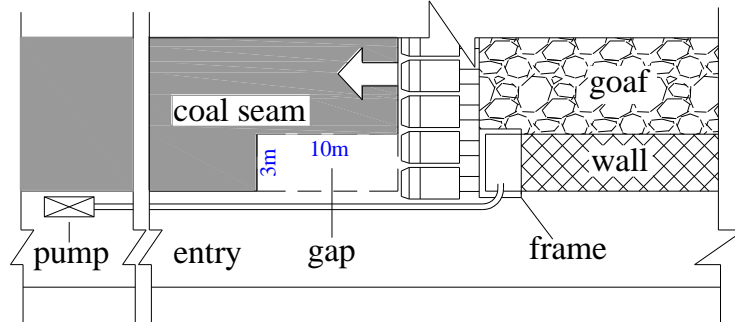
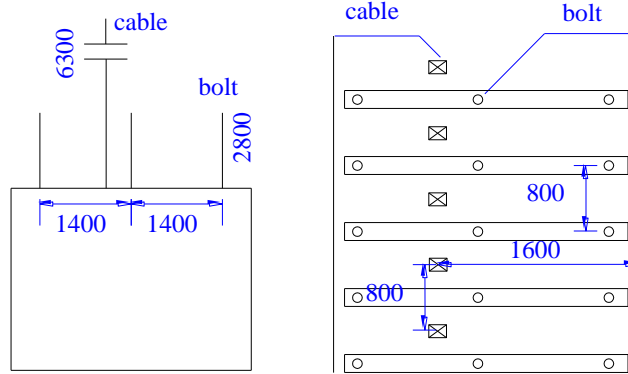


Fig. 5-5 Second roadway supporting parameters before coal face (mm)

To reinforce the cracked roof strata over the artificial packfillings and reduce the preparation time for packfillings constructing, a special gap is excavated ahead of the coal face to provide space for roof reinforcement, as shown in Fig. 5-6(a). The width and length of this gap is 3 m and 10 m, respectively, and the supporting parameters are shown in Figs. 5-6(b) and (c). Furthermore, within the significant influence range (55 m to 0 m) ahead of the coal face, assistant supporting system comprised by hydraulic props and articulated roof beams are installed to increase the safety factor of the gateroad.



(a) Location of the gap before coal face



(a) Section view of supporting (b) Top view of supporting

Fig. 5-6 Second supporting parameters to the gap before coal face (mm)

5.1.3.3 Third Supporting System

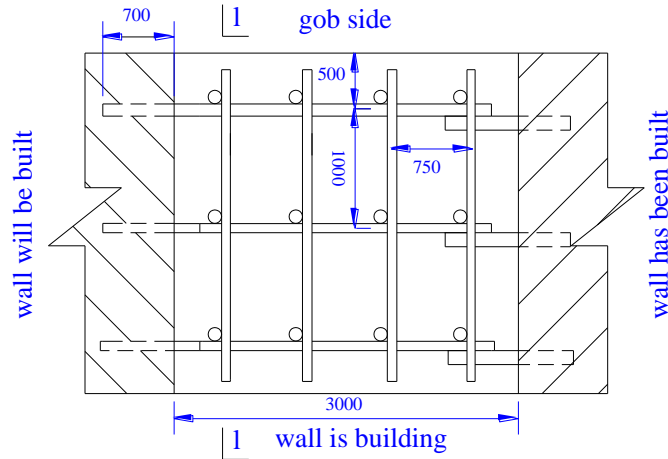
(1) Artificial wall Constructing material

Performance of the constructing material affects the RGSG technically and economically. As analyzed before, the stress in the artificial wall increases gradually from a relatively low level rather than remaining at a high level once the coal seam is extracted. From this point of view, a mixed constructing material with increasing strength is designed. This material is composed of cement 23%, fly ash 8%, gravel 45%, sand 23% and 1% chemical additives by weight, and the ratio of water to cement is 0.5. The testing uniaxial compressive strength of this constructing material is 15.6 MPa (1 day), 25.6 MPa (3 day), 30.5 MPa (7 day) and 37.0 MPa (28 day), respectively, which meets the strength requirements of artificial wall.

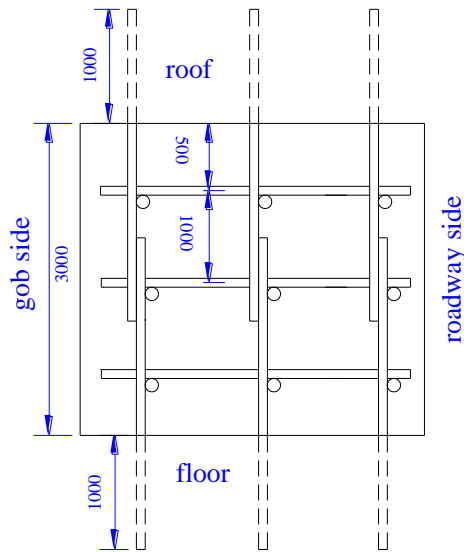
(2) Reinforcing steel rebar

To resist the continually increasing pressure on the artificial wall, reinforcing steel rebar is designed as shown in Fig. 5-7. The reinforcing steel rebar in each unit overlaps

by 700 mm to prevent the relative movements between wall units. Vertical reinforcing steel rebar is inserted into the roof and floor strata by 1,000 mm to prevent relative movements between the wall and adjacent strata. Old rock bolts collected during gap excavation can be reused as rebar to reduce costs.



(a) Top view



(b) Section view

Fig. 5-7 Parameters of the reinforcing steel rebar in wall during third supporting stage (mm)

(3) Construction process

As shown in Fig. 5-3, roof of the gap is supported firstly. Then, the powered roof supports are moved ahead, and the reinforcing steel rebar is settled in the frame. At this time the hydraulic link between the powered roof support and frame is extended. Then, the mixed materials are pumped into the frame. After the fluid constructing materials

solidifies, the frame hydraulically advances itself. At this moment, the hydraulic link is shortened to prepare for the next circle.

Additionally, the original hydraulic prop supporting system installed during the second supporting construction is retained after the coal seam passing by to maintain the long-term stability of the RGSG, resulting from the stress redistribution caused by the coal panel excavation becomes stable until 120 m behind the coal face.

5.1.4 Field Measurements and Discussions

Deformations of ribs, roof and floor were measured until excavation of the first panel finished. Distributions of these deformations are divided into 4 stages, as shown in Fig. 5-8. The x-coordinate represents the serving time of the gateroad. According to the Fig. 5-8, the following laws can be concluded with the combination of stress distribution analyzed before:

(1) During the stage 1, the gateroad is influenced by roadway excavation. Relative deformations of rib-to-rib and roof-to-floor increase quickly within the first 10 days, and then increase relative slowly to approximately 200 mm (right rib convergence accounts for 56% with 113 mm) and 450 mm (floor heave accounts for 56% with 260 mm), respectively. A roadway profile at the end of this stage is shown in Fig. 5-9(a).

(2) During the stage 2, gateroad is influenced by the stress concentration before the coal face. Even though the influence time is shorter than that during stage 1, the influence is much severe, with deformations of rib-to-rib and roof-to-floor up to approximately 701 mm (right rib convergence accounts for 64% with 453 mm) and 1,460 mm (floor heave accounts for 65% with 960 mm). A roadway profile at the end of this stage is shown in Fig. 5-9(b).

(3) During the stage 3, gateroad is influenced by the stress redistribution behind the coal face. The deformations of rib-to-rib and roof-to-floor increase significantly up to 1,171 mm (right rib convergence accounts for 69% with 813 mm) and 1,859 mm (floor heave accounts for 78% with 1,460 mm). A roadway profile at the end of this stage is shown in Fig. 5-9(c).

(4) During the stage 4, apparent creep deformations (Malan 1999; Dawson et al. 1983) appear. Although the stress does not change any more in this stage, the deformations of rib-to-rib and roof-to-floor increase continually to 1,315 mm (right rib

convergence accounts for 73% with 993 mm) and 2,200 mm (floor heave accounts for 77% with 1,701 mm), with stable speed of 1.2 mm/d and 2.27 mm/d, respectively. The lateral deformation of the artificial wall increases only to 110 mm and then remains stable, verifying the effectiveness of the artificial wall designing. A roadway profile at the end of this stage is shown in Fig. 5-9(d).

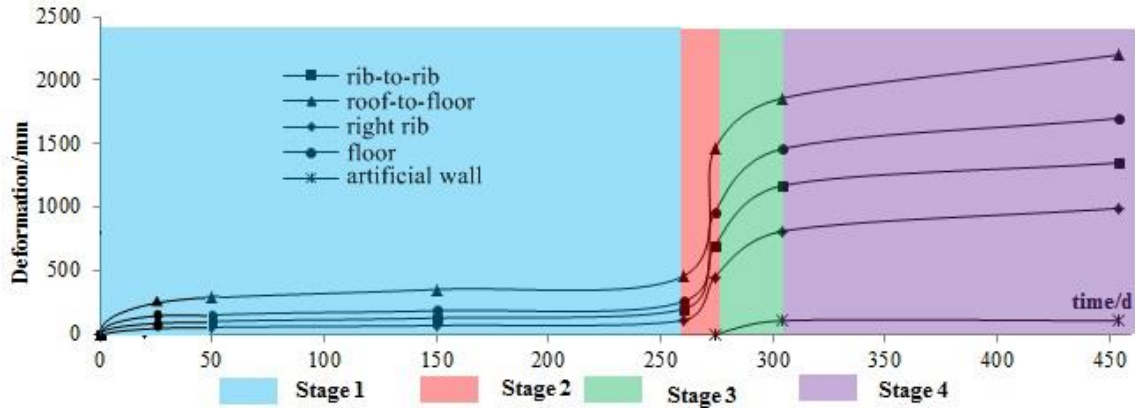


Fig. 5-8 Deformations curves of the RGSG surrounding rock during first coal panel mining



(a) At the end of stage 1



(b) At the end of stage 2



(c) At the end of stage 3



(d) At the end of stage 4

Fig. 5-9 Profiles of the roadway section in different mining stages

5.1.5 Roadway Maintenance for the adjacent Coal Panel Extraction

As shown in Fig. 5-8 and 5-9, the deformations of the roadway in the stages 1, 2 and 3 are controlled effectively, and gas extracting could be carried out at the end of the stage 3 as designed. While the section at the end of the stage 4 is too small to serve for the adjacent panel extraction, there is a need to conduct maintenance to this gateroad.

5.1.5.1 Considerations before maintenance

(1) Stability of the roof strata. After coal seam excavation, the roof strata over the RGSG fracture, rotate and sink. With the compaction of caved rock in gob area, these movements weaken and stop eventually, forming a balanced structure that acts as a protective shield beam for the roadway. Stability of this structure is the precondition of the maintenance. Starting from this perspective, the Borehole Imaging was carried out in roof and right sidewall to check the integrity of surrounding rock. Results of the Borehole Imaging are shown in Fig. 5-10. The depth of fractured region of roof and right rib are about 1.5 m and 1.2 m, respectively, indicating that the fractured region in the surrounding rock is controlled effectively by the staged supporting, and the rock in deep side of the surrounding rock are intact, and the balanced roof structure is stable.

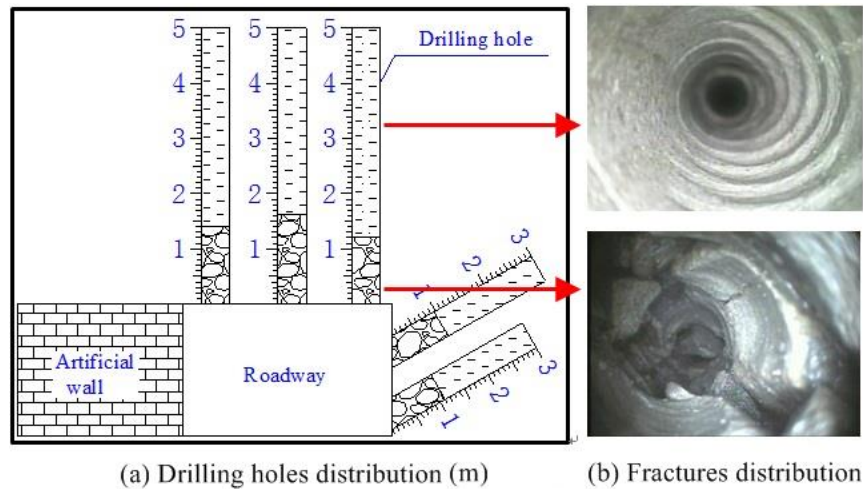


Fig. 5-10 Results of the drilling imaging in RGSG roof and right sidewall

(2) Supporting function of the right rib. As shown in Fig. 5-8, the deformations of the floor and right rib are the primarily contributions to the section shrinkage of the RGSG. Considering the maintenance costs, efficiency and stability control to the roof structure, only the squeezed portions of the floor and right rib are cleared during the maintenance. In order to get a deep insight of the disturbance of the maintenance to the

stability of the balanced roof structure, the supporting role of the squeezed portion of the right rib to the roof strata is analyzed. It is known that the shallow part of the right rib undergoes deformation and breakage after experiencing disturbances of gateroad and panel excavation, forming a Limit Equilibrium Zone, in which the vertical supporting stress can be calculated using the following Equation (Hou 1989):

$$\sigma(x) = \left(\frac{C_0}{\tan \varphi_0} + \frac{Px}{A} \right) e^{\frac{2x \tan \varphi_0}{m\lambda}} - \frac{C_0}{\tan \varphi_0} \quad (10)$$

Where, φ_0 and C_0 are the internal friction angle and cohesion of coal; Px is the confining stress on the surface of the right rib; λ is the lateral pressure coefficient; x is the depth inside the right rib; m is the mining height.

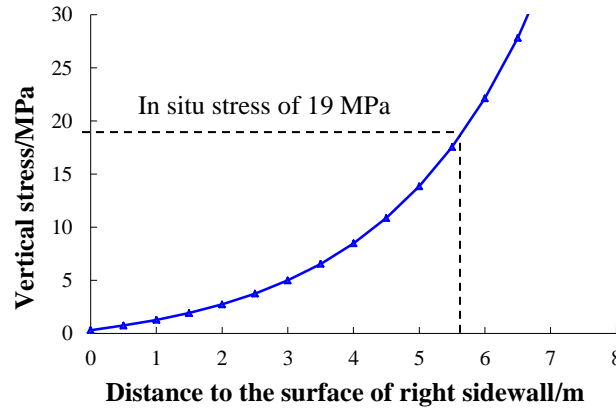


Fig. 5-11 Vertical stress in shallow part of RGSG right rib

According to statistical field measurements, the average internal cohesion and friction angle are 0.3 MPa and 20 degree; the lateral pressure coefficient is 1; the mining height is 1.8 m; and the confining stress of right rib is 0.35 MPa. The calculating results are shown in Fig. 5-11. The supporting stress in the shallow region of right rib grows exponentially from the surface. A stress relaxation zone (roughly 5.6 m wide) appears, in which the supporting stress is lower than the in-situ vertical stress (19 MPa), which indicates that the supporting of the squeezed part (of 815 mm in width) that will be cleared to the roof strata is very limited, and following widening operation makes little disturbance to the stability of the roof structure.

5.1.5.2 Maintenance implement

Firstly, integrity of the artificial wall is checked, and the cracks and fissures on the wall surface are filled to prevent water and gas in the gob area flowing into the roadway

space during maintenance. Then, dinting is carried out to provide the working space for the following operations. After that, the squeezed part of right rib is cleared, and the exposed portion of the rock bolts and cable bolts due to widening are cut off and the retained portion inside the surrounding rock are prestressed again. After maintenance, the roadway section is $4,500 \text{ mm} \times 2,500 \text{ mm}$ (width \times height) that satisfies the requirements of the adjacent panel excavation. Roadway profiles during different processes of section enlarging are shown in Fig. 5-12.

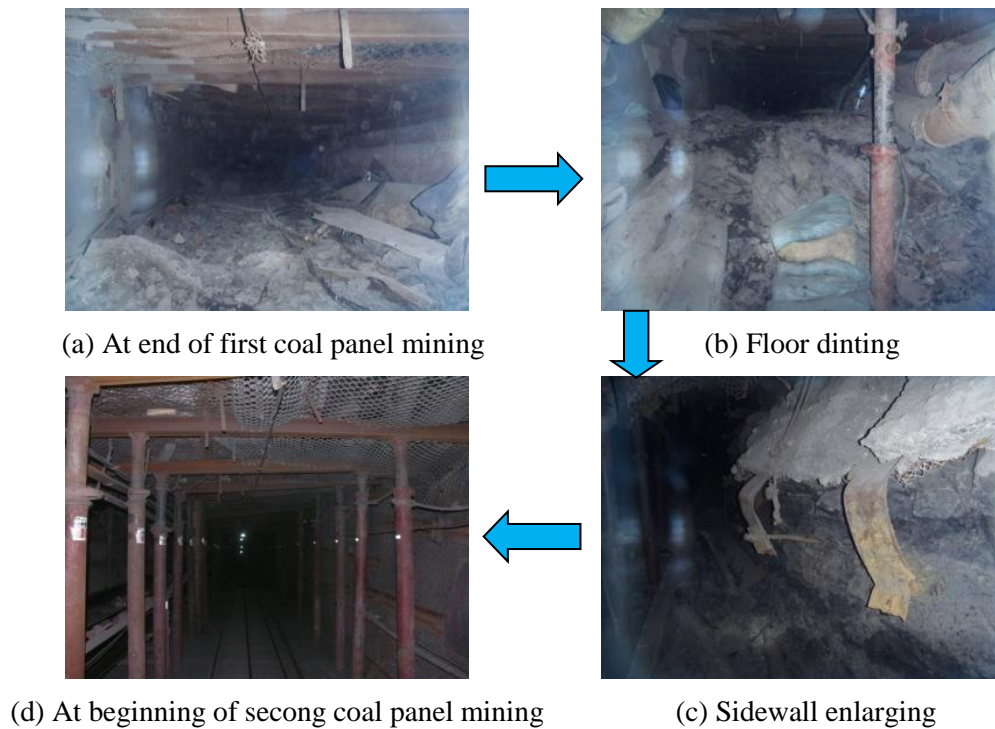


Fig. 5-12 Profiles of the RGSG in different processes of section enlarging

5.2 Application of Grout Bolting Method in RGSG with Depth of 850 m

5.2.1 Geological Condition

Pan Yidong coal mine, located near Huainan in Anhui Province, China, is chosen resulting from the following considerations. Firstly, this coal mine has the typical geological conditions in the eastern China, where the RGSG is widely applied. Its primarily minable coal seam is buried at a depth of 850 m, with relative gas content of 26.33 m³/t and a thickness of 3.0 m. According to the results of in-situ stress measurements with the stress relief method, the maximum and minimum principal stresses are nearly horizontal, and are 36.7 MPa and 18.1 MPa, respectively, and the

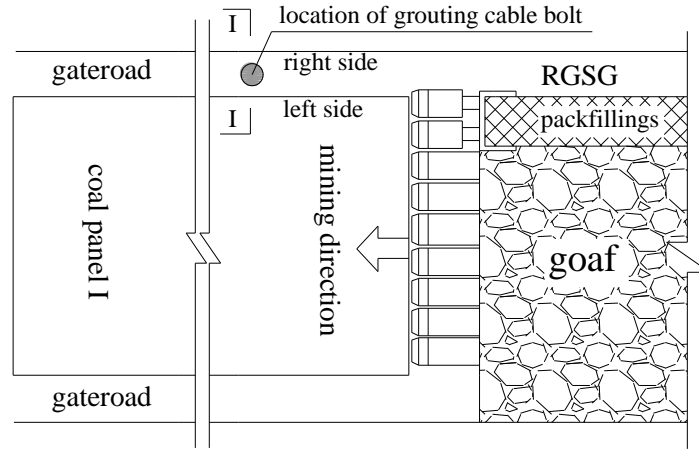
middle principle stress is nearly vertical, and is up to 19.8 MPa. It should be noted that the maximum principle in-situ stress is almost parallel to the orientation of the roadway axis, which indicates that only the middle and minimum principle in-situ stress that perpendicular to the roadway axial direction, makes mainly contributions to the RGSG instability. Empirically, more than 4 gateroads (2 gateroads responsible for fresh air flowing in and others for dirty air returning) are needed to account for the high gas emission, and large coal pillars wider than 15 m between adjacent gateroads are required to resist the high in-situ stress, when using the conventional U type mining system. In order to eliminate the risk of gas explosion due to high gas accumulation and heavy coal resources loss results from large coal pillars, Y type mining system based on the RGSG is employed in this coal mine. Research results of this study can provide valuable scientific reference for other coal mines of similar geological conditions. Secondly, this coal mine is a newly built one and the supporting criterion and parameters are lack, which cannot be satisfied by simply copying the supporting techniques from other coal mines. Particularly, the immediate roof stratum over the minable coal seam in the Pan Yidong is typically composed of multilayer weak mudstone with small thickness by each, and the whole height is approximately 9.0 m. Appropriate roadway stabilizing method should be designed according to the special geotechnical conditions of the Pan Yidong coal mine.

5.2.2 Construction Process and Parameters

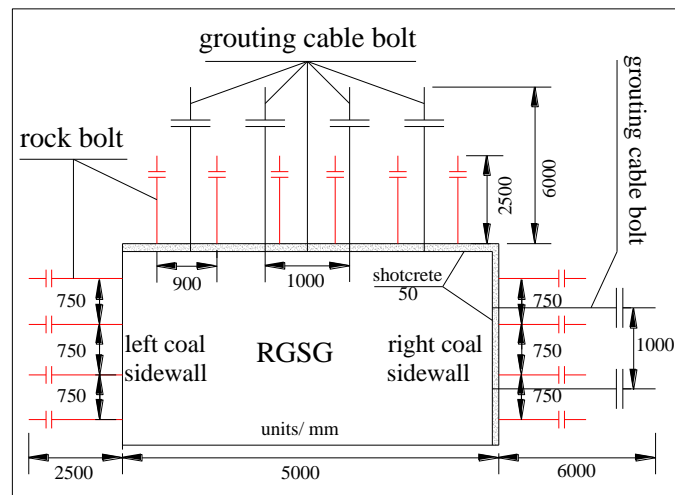
During roadway excavation, the first supporting system was installed. In detail, rock bolts with a diameter of 22 mm and a length of 2,850 mm were installed in two coal sidewall and roof, with an inter-row space of 0.75 m×0.8 m; conventional cable bolts with a diameter of 22 mm and a length of 6,300 mm were installed only in roof strata, with an inter-row space of 1.0 m×1.6 m.

As shown in Fig. 5-13, according to the construction time and process, a series of the hollow grouting cable bolts (in red) were constructed based on the first supporting system (in black). The hollow grouting cable bolts with a diameter of 22 mm and a length of 6,300 mm were installed in the space of original supporting system, 4 sets in roof and 2 sets in the right coal sidewall, and no hollow grouting cable bolts were installed in the left coal sidewall considering the impediments of cable bolt to the coal cutting shearer. Two resin capsules and one steel plate were needed for every cable bolt set, and the

designed prestress was larger than 60 kN. Grouts have a ratio of cement (425#) to water of 0.5, a chemical additive (ACZ—I) of 8% by weight; grouting pressure was 2~3 MPa; grouting time was 3~5 minutes and the thickness of cement lining was 50 mm.



(a) Location of the grouting cable bolt installation in the RGSG



(b) Parameters of the grout bolting (Section view I-I)

Fig. 5-13 Position and parameters of the grouting cable bolts in RGSG

5.2.3 Field Measurements

5.2.3.1 Improvement of the integrity of surrounding rock

To reveal the effectiveness of cement grouting on the integrity of cracked surrounding rock, the distribution of cracks in the roof strata before and after the installation of hollow grouting cable bolt were measured using borehole imaging equipment. The results are shown in Fig. 5-14. Many horizontal separations and vertical cracks were found within 6 m in the surrounding rock before reinforcement. These

damages have resulted from disturbances from the roadway and coal seam excavations, as well as the drilling process. After the hollow grouting cable installation and followed grouting, all the separations and cracks in the surrounding rock were sealed. Consequently, the integrity and boltability of the surrounding rock were improved.

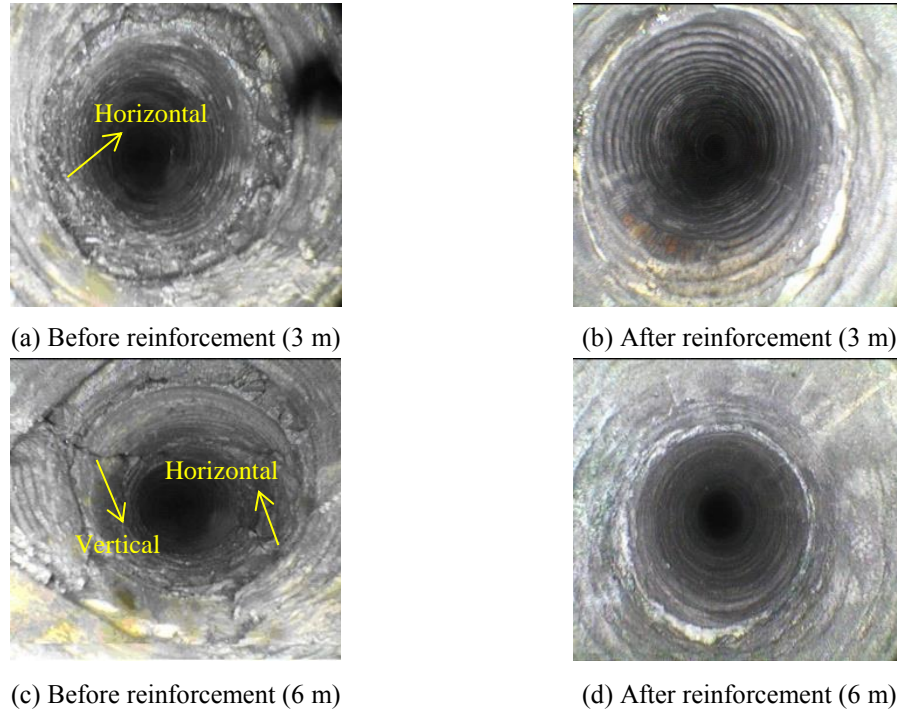


Fig. 5-14 Integrity of the roof strata before and after the installation of hollow grouting cable

5.2.3.2 Control of the separations in roof strata

The axial force of the hollow grouting cable bolt and the separations of the reinforced roof strata were measured after the hollow grouting cable bolt installation, to verify the effectiveness of this type of supporting on the separations in the RGSG. The results are shown in Fig. 5-15. The separations in roof strata increase slowly when the coal face moves closer to the measure station from 60 m to 20 m, and then rise rapidly up to 215 mm when the coal face moves to the position 50 m behind the measure station, and finally remain roughly stable as the coal face moves farther. The axial force of the hollow grouting cable bolt follows a trend that is similar to that observed about the separations, increasing slowly at first and then rising to a peak value of 161 kN approximately 48 m behind the coal face; in this case, however, there is a subsequent decrease in axial force at great distances, rather than leveling off. The similar trends

observed with the separations and cable bolt axial force verify that the hollow grouting cable bolt have a positive and rapid action on the enlargements of all the separations in the roof, and that the separations can be controlled to a relatively low level after the serious disturbances of coal seam excavation. According to the field observations, however, the shallow surrounding rock was still broken and cracked approximately 60 to 80 m behind the coal face. Hence, the possible reason of the gradual decrease of the bearing force of the hollow grouting cable bolt after reaching its peak value is that the shallow surrounding rock broken results in the release of the elastic energy stored in cable bolts.

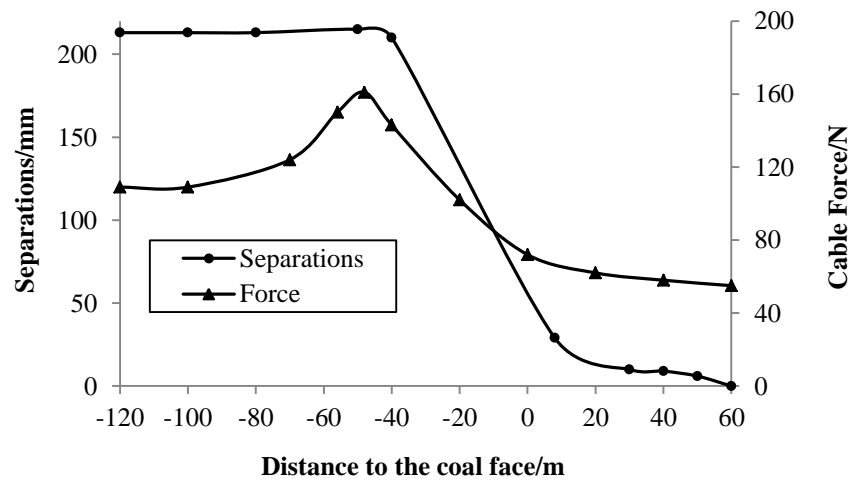


Fig. 5-15 Curves of the cable force and roof separations

5.2.3.3 Maintenance of roadway profile

The significant features of the RGSG are that it serves as an outlet for dirty air during the first longwall panel mining and as the inlet for the clean air during adjacent longwall panel excavation. Maintaining a sufficient roadway section is a precondition of these goals achievements.

Figure 5-16 represents the deformations of the RGSG, which can be divided into 4 stages according to the different increasing rates: (i) > 60 m, in which the influence of the stress disturbances induced by coal face advancing is activated, and the deformations begin to increase; (ii) $60 \sim 30$ m, in which the influence of the coal face advancing on the gateroad increases slightly and the deformations are still small; (iii) $30 \sim -140$ m, in which, the gateroad is influenced significantly by the severer stress concentration and the deformations increase quickly as well; (iv) < -140 m, increase of the deformations slows

down obviously and finally remains stable, which illustrates the influence of the coal face advancing recedes, and the movements of the over strata induced by coal seam excavation weakens and then stops. After experiencing the stress disturbances of roadway and the first coal panel excavation, the width and height of the RGSG is maintained up to 4,000 mm and 2,800 mm, respectively, and the surrounding rock including roof, coal sidewall and artificial wall are entirely stable. Parameters of this RGSG satisfy all the requirements of safe mining. The final profile of the RGSG in the Pan Yidong coal mine is shown in Fig. 5-17.

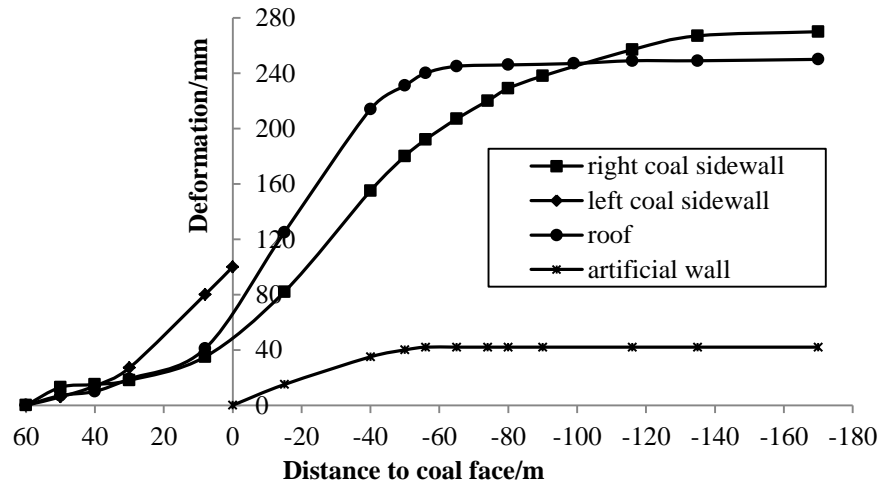


Fig. 5-16 Deformation curves of the roadway's surrounding rock



Fig. 5-17 Profiles of the RGSG 100 m behind the mining face

5.3 Application of Hard Roof Pre-Split in RGSG with Depth of 1100 m

5.3.1 Geological Condition

Pingdingshan No.12 colliery is located in Pingdingshan city, Henan Province, China. Its mineable coal seam is buried at an average depth of 1,100 m, with an average thickness of 2.0 m and an average dip angle of 5.5° . The target coal panel 14-31010 is 570 m along the strike and 150 m along the dip. The immediate roof is sandstone with an average thickness of 18 m and an average Protodikonov's Hardness Coefficient of more than 7.3, as shown in Fig. 5-18.

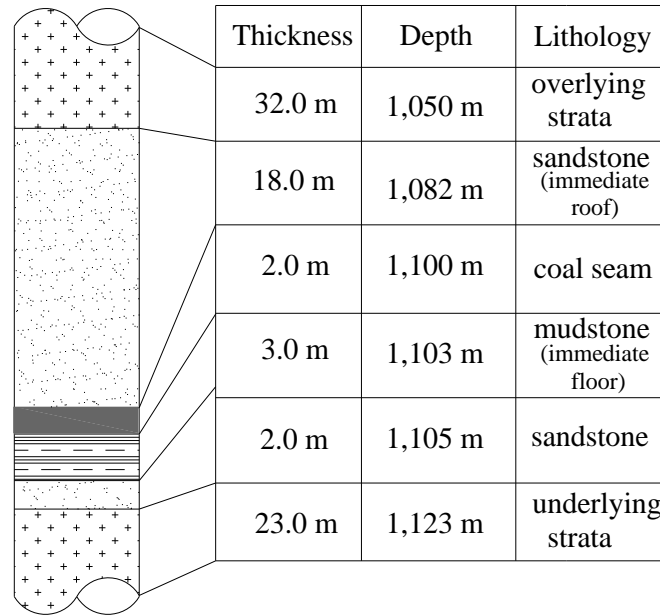


Fig. 5-18 Geological columnar section stratigraphy of Pingdingshan coal mine

5.3.2 Construction Process and Parameters of Roof Pre-Split Blasting

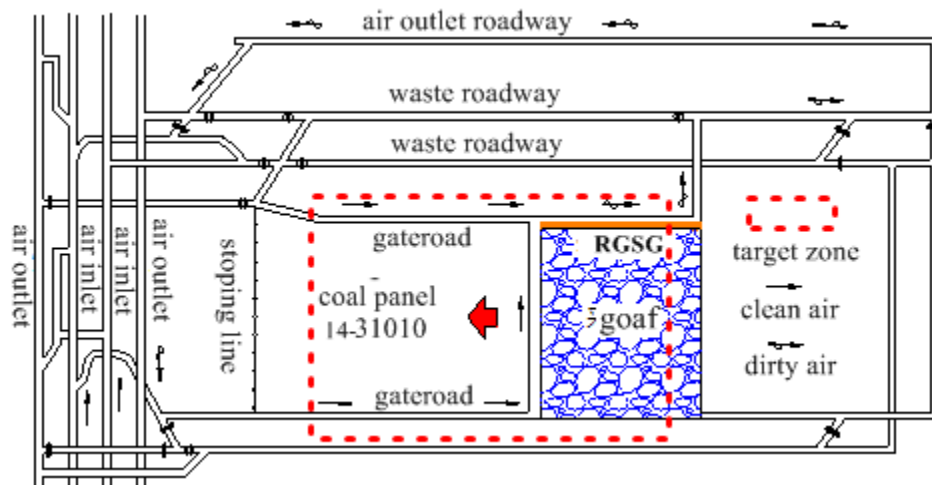


Fig. 5-19 Layout of the coal face and RGSG in Pingdingshan coal mine

In order to reduce the additional abutment stress generated by the immediate sandstone roof stratum, pre-split blasting technology was applied in the longwall panel 14-31010. Drill sites with length of 5 m and width of 4 m were excavated in solid coal panel approximately 120 m before the coal face, to provide working space for blasting holes drilling. The layout of the coal face and RGSG in this coal mine is shown in Fig. 5-19.

The distance between two adjacent drill sites is about 50 m, and 12 blasting holes were drilled in every site using mine ZDY4200LS caterpillar-hydraulic drilling machine. The distribution of blasting holes in drill site is illustrated in Fig. 5-20, and the parameters of these blasting holes are listed in Table 10.

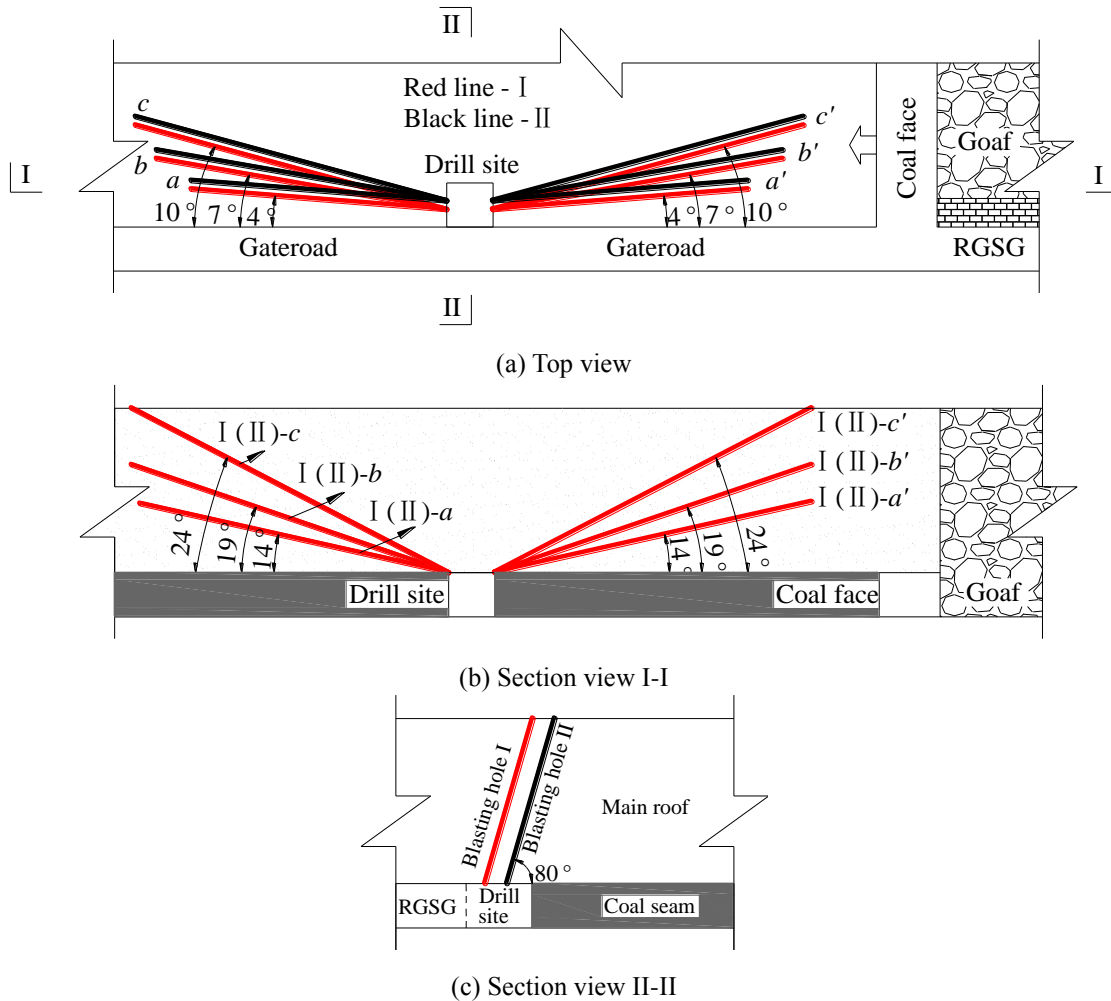


Fig. 5-20 Distribution of the blasting holes in RGSG roof

Three blasting holes a, b and c (red lines) were drilled backward coal face with vertical inclined angle of 14°, 19° and 24° and horizontal rotational range of 4°, 7° and

10°, respectively. Another three blasting holes a', b' and c' (red lines) with same parameters were drilled toward coal face. In order to crack the hard sandstone thoroughly and to ensure the effectiveness of stress relief, additional one set of blasting holes (black lines) with same parameters were also drilled in one drill site. The beginning position of charge was located more than 3 m vertically and 5 m horizontally away from the blasting hole opening to eliminate the adverse influence of blasting on the roadway stability. The blasting charge was professional mine water-gel explosive.

Table 10 Parameters of the blasting settings

Blasting Hole No.	Hole depth /m	Hole diameter /mm	Charge diameter /mm	Charge length /m	Stemming length /m
I (II)-a (a')	28	75	63	20	8
I (II)-b (b')	29	75	63	21	8
I (II)-c (c')	30	75	63	22	8

The constructing material of packfillings in the field is consist of gravel 45%, cement 23%, sand 23%, fly ash 8%, and 1% chemical additives by weight, and the ratio of water to cement is 0.5. The testing uniaxial compressive strength of this constructing material is 9.8 MPa (1 day), 15.6 MPa (3 day), 24.5 MPa (7 day), 32 MPa (17 day), 35 MPa (25 day) and 37.0 MPa (28 day), respectively.

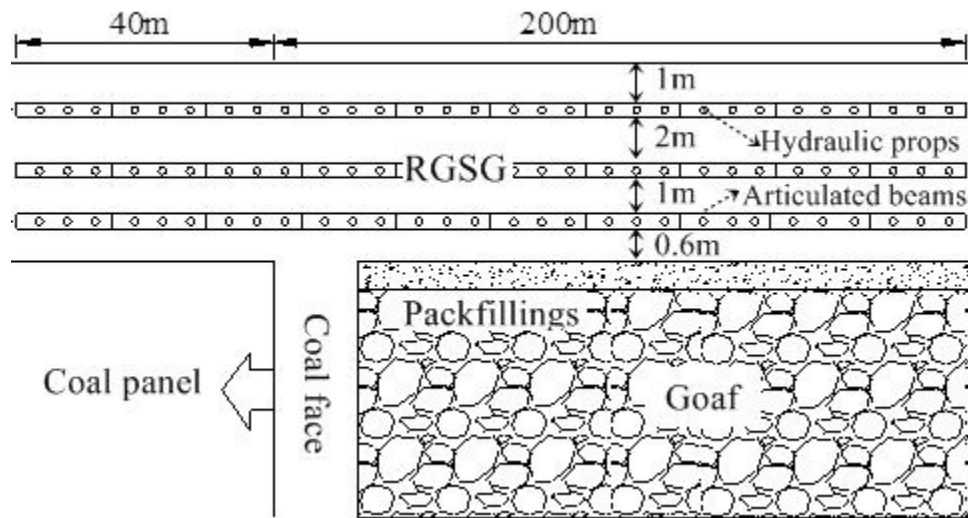


Fig. 5-21 Parameters of the supplemental supporting system behind coal face

Although the vertical stress on packfillings is reduced significantly, the residual compressive stress is still larger than the bearing strength of the packfillings during the

early stage after the packfillings are built. Because of this, a supplemental supporting system comprised of hydraulic props and articulated roof beams installed before coal face were retained until 200 m behind the coal face, to help roadway surrounding rock to bearing the heavy pressure, as shown in Fig. 5-21.

5.3.3 Field Measurement

After application of the above technologies, the RGSG convergence of packfillings was less 145 mm and the roof sag was no more than 131 mm, and the roadway residual section area was larger than 10 m², and it can be reused when the adjacent coal panel mining. The final profiles of the roadway before and after roof pre-split are shown in Fig. 5-22.

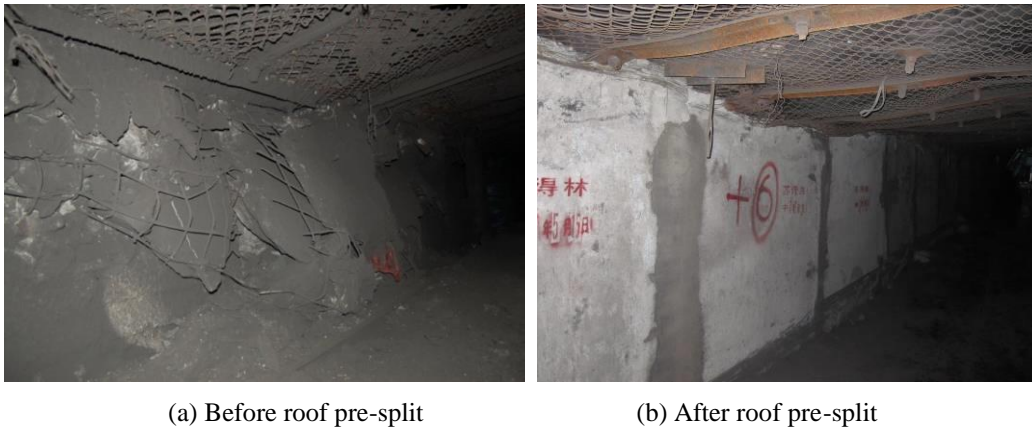


Fig. 5-22 Profile of the RGSG under hard roof before and after roof pre-split application

5.4 Summary

In this chapter, the applications of the staged roadway supporting technology, grout bolting roadway supporting technology and hard roof pre-split roadway maintainance technology proposed in above chapter 4 in three typical deep underground coal mines are introduced and the corresponding effectiveness are discussed based on the field measurements. The detailed conclusions are as follows:

(1) Staged supporting designed in terms of the stress distribution in the surrounding rock is verified as an effective solution. For the RGSG in Zhuji underground coal mine with depth of 980 m, deformations of sidewalls are as much as 1,315 mm in which right sidewall accounts for 73%, and the deformations of roof and floor are 2,200 mm in which floor heave makes up 77%.

Roadway section shrinkage of the RGSG during first coal panel mining is so large that this RGSG has to be enlarged before the second coal panel retreating. After evaluate the stability of the roadway roof structure and supporting function of shallow part of right sidewall to roof, roadway section enlarging processes including floor dinting and sidewall widening are conducted. Finally, roadway section is 4,500 mm \times 2,500 mm (width \times height) that satisfies the requirements of the adjacent panel excavation.

(2) Grout bolting technology can improve the flexibility of the RGSG in deep mining environment. Deformations of roof and coal sidewall of the RGSG in Pan Yidong coal mine are found up to be 1,100 mm and 760 mm, respectively, after experiencing several stress disturbances, when it is supported with conventional method. After installation of the grouting cable bolt, integrity of the cracked surrounding rock is improved, and the separations in roof strata are controlled effectively. The final profile is found to be 4,000 \times 2,800 mm (width \times height) before next longwall panel extraction, satisfying all the requirements during the first and second longwall panel mining.

(3) Rock pre-split blasting technology reduces the influence of long roof cantilever movements on the RGSG surrounding rock effectively. In Pingdingshan underground coal mine of 18 m hard main roof, two sets of blasting holes are drilled in every drill site to ensure thorough breakage to this thick sandstone stratum. When the first coal panel mining finishes, the residual section area of the RGSG in the Pingdingshan coal mine is larger than 10 m², and it can be reused when the adjacent coal panel mining.

Reference

- Liu YW, Wang Q, et al. (2014) Enhanced coalbed gas drainage based on hydraulic flush from floor tunnels in coal mines. *International Journal of Mining, Reclamation and Environment*, DOI:10.1080/17480930.2014.964040.
- Valliappan S, Zgabg WH (1996) Numerical modeling of gas migration in dry coal seams. *International Journal for Numerical and Analytical Methods in Geomechanics*, 571–593.
- Jia TR, Zhang ZM, et al. (2013) Numerical simulation of stress-relief effects of protective layer extraction. *Arch. Min. Sci.*, 521–540.
- Si GY, Shi JQ, Durucan S, et al. (2015) R.D. Monitoring and modelling of gas dynamics in multi-level longwall top coal caving of ultra-thick coal seams, Part II: Numerical modelling. *International Journal of Coal Geology*, 58–70.

- Leigh RD (1963) Strata pressures and rock mass movements induced by longwall mining, Ph.D. diss., University of Durham, UK.
- Malone D (1965) Displacement-and relative movement of strata above a coal faces, Ph.D. diss., University of Durham, UK.
- Qian MG (1982) A study of the behavior of overlying strata in long wall mining and its application to strata control. *Strata Mechanics*, Elsevier Scientific Publishing Company, 13-17.
- Colin J. Booth (1986) Strata-movement concepts and the hydrogeological impact of underground coal mining. *Groundwater*, 507-515.
- Hou CJ, Ma NJ (1989) Stress in In-Seam Roadway Sides and Limit Equilibrium Zone. *Journal of China Coal Society*, 21-28.
- Malan DF (1999) Time-dependent behaviour of deep level tabular excavations in hard rock, *Rock Mech. Rock Eng*, 32, 123–155.
- Dawson PR, Munson DE (1983) Numerical simulation of creep deformations around a room in a deep potash mine. *Int. J. Rock Mech. Min. Sci*, 20, 33–42.

CHAPTER 6

CONCLUSIONS

6.1 Main Conclusions

In order to maintain the stability of the retained goaf side gateroad (RGSG) that plays crucial role in the Y type gateroad layout that has been widely employed in deep underground longwall mining system recently for the purposes of increasing coal recovery rate and reducing gas accumulation, comprehensive methods including theory calculating, numerical simulation and field tests are employed this paper to analyze the roof structures over goaf and RGSG under different roof condition, reveal corresponding failure characters of the RGSG surrounding rock under in each roof condition, and propose the effective roadway supporting methods finally. Main conclusions, innovation points and research respects are summarized as follows.

Roof structures over goaf and RGSG

After coal seam is mined, overlying immediate roof cracks and caves timely and irregularly, and the main roof, however, follows O-X breakage style orderly when the coal face advances continually. As a result of the O-X style breakage of the main roof over goaf, a triangular shaped rock cantilever forms over the RGSG. Surrounding rock of the RGSG are deteriorated results from the compression from the cantilever rotation. The thicker the main roof is and the thinner the immediate roof is, the more serious the influence is.

Improvement of the roof structure over the RGSG by shortening the rock cantilever is proposed to reduce the influence of hard main roof movement on the RGSG surrounding rock. Theatrically, after the main roof is cut off along the outer edge of the packfillings, mechanical connection between the roof over roadway and other part over goaf is cut off, and the rotation of the roof over the RGSG can be decreased considerably, and the roadway surrounding rock suffer little additional abutment pressure and corresponding deterioration.

Distribution of the stress and deformation in RGSG surrounding rock

RGSG suffers the stress disturbances from roadway excavation and coal panel mining, and as a result, roadway surrounding rock perform different deformations in different period. During roadway excavation, the confining stress normal to surface of roadway surrounding rock decreases considerably and the bearing strength of shallow part of surrounding rock reduces reasonably. Consequently, the shallow part of surrounding rock breaks and deforms towards roadway space. During coal panel mining, the influence of abutment stress induced by coal face moving can be divided into three stages: no influence farther than 40 m; severe influence from 40 m ahead of coal face to 40 m back the coal face; slight influence from 40 m back the coalface to 100 m away the coal face. After experiencing these stress disturbances, roadway surrounding rock performs large deformations and the boltability of cable bolts and rock bolts in the shallow part of surrounding rock becomes low considerably because fissures and cracks have appeared in the shallow part of surrounding rock.

As the thickness of the main roof increases and the thickness of the immediate roof decreases, deformations of RGSG surrounding rock decrease during roadway excavation, and during coal panel mining, however, deformations of roadway surrounding rock increase considerably. The deformations of RGSG surrounding rock reach maximum value when the coal seam is beneath the hard main roof of 12 m thickness directly.

Four roadway supporting technologies for the large deformed RGSG

(1) Basically staged supporting strategy. In the first supporting stage, a prestressed bolting system aiming at providing high lateral confining stress is proposed to maintain the stability of the RGSG during roadway excavation. In the second supporting stage, cable bolt system with larger length is suggested within the range influenced by coal face abutment pressure, considering the loose and broken range of the surrounding rock widening. In the third supporting stage, packfillings with gradually increasing strength and reinforcement to the roof over packfillings should be put into mind because of the continually increasing abutment stress behind the coal face.

(2) Roof pre-split technology. Roadway section shrinkage rate is up to 82.5% when the RGSG suffers the influence of long roof cantilever of hard main roof with thickness of 12 m. Pre-split technology is proposed to reducing this influence by shortening the length of roof cantilever. The deformations of the RGSG surrounding rock are reduced

considerable, as expected after roof is pre-split. The RGSG floor heave decreases most obviously by 57% with 767 mm decrement, followed by the roof sag reduced by 55% with 469 mm decrement. The third significant improvement is the left sidewall deformation, with 235 mm decrements accounting for 25% of the previous value. Lastly, the coal sidewall convergence decreases by 24% with 257 mm decrement, ranking forth.

(3) Improved grout bolting technology. The final deformations of the RGSG sidewalls are still very large (more than 700 mm) although some improves have been achieved through roof pre-split. To control the large deformed sidewalls with developed cracks, a modified grout bolting technology is proposed. This modified technology not only can provide higher confining stress at the stage of installation, but also controls the cracks more effectively and has larger bearing capacity during the followed grouting stage. These advantages promote the stability of the RGSG sidewalls effectively. After application of this technology to the RGSG sidewalls, the deformations of left and right coal sidewall can be reduced to 356 mm, and 456 mm from 729 and 792 mm, respectively.

(4) Floor grouting reinforcement. After applications of pre-split to roof and grout bolting technology to coal sidewalls, the deformation of RGSG floor that is not supported, plays the leading role in roadway section shrinkage again. Grouting reinforcement is proposed to reduce the floor heaves by considering the weak rock mechanics of the mudstone, and only 1 m within the floor is grouted because the heaving within 1 m of the floor strata accounts for 72% of whole floor heaving. When the residual cohesion is increased to 30%, 50% and 70% of the original one and residual friction angle is increased to 24.5° , 25° and 25.5° , respectively by grouting, floor heaves are reduced considerably to 273 mm, 202 mm and 194 mm from 516 mm. After grouting, the plastic zone is effectively reduced and the rock failure mechanisms become to shear failure partly.

Effectiveness verification of above proposed roadway supporting method in field

(1) Staged supporting technology is applied in the Zhuji underground coal mine with depth of 980 m. After application of this technology, deformations of the RGSG are controlled effectively. However, right sidewall convergence and floor heave are still large

so that this roadway has to be enlarged before the second coal panel retreating. After evaluating the stability of the roadway roof structure and supporting function of shallow part of right sidewall to roof, roadway section enlarging processes including floor dinting and sidewall widening are conducted.

(2) Grout bolting technology is applied in Pan Yidong coal mine with depth of 850 mm. In order to reduce the deformations of RGSG surrounding rock in deep mining environment during first coal panel mining and to avoid roadway section enlarging to the RGSG before the second coal panel mining, grout bolting technology is applied in Pan Yidong coal mine. After installation of the grouting cable bolt, integrity of the cracked surrounding rock is improved, and the separations in roof strata are controlled effectively. The final profile is found to be large enough for the second longwall panel mining.

(3) Rock pre-split blasting technology is applied in Pingdingshan underground coal mine with depth of 1,100 mm. To reduce the influence of long roof cantilever movements on the RGSG surrounding rock, the hard roof with thickness 12 m over the RGSG is cut off by pre-split blasting technology at the outer edge of packfillings. When the first coal panel mining finishes, the residual section area of the RGSG in the Pingdingshan coal mine is larger than 10 m², and it can be reused when the adjacent coal panel mining.

6.2 Research Prospects

(1) Stress distribution around the goaf in underground longwall mining system is determined by several factors. In this research, the influence of different roof conditions on the stress and deformation distribution in the surrounding rock of a goaf is studied on the assumption that other geological and engineering factors are certain, like mining depth, mining height, retreating speed of coal face, backfilling level of excavations and so on. The influence of these factors on the stress distribution and corresponding disturbance on the RGSG will be studied in the future.

(2) Real stress distribution will be measured in the field. In this study, numerical simulation is the main research method to analyze the stress and deformation distribution in the RGSG surrounding rock. The validity of numerical simulating results, however, is verified only by comparing with real RGSG deformation data measured in field. The stress distribution in the field also will be measured in the future to verify the feasibility

of numerical research in the study of stress distribution in underground coal mine induced by coal seam mining.

(3) Detailed conditions for the application of the RGSG supporting technologies proposed in this research will be studied in detail. In this detestation, the general geological and engineering conditions for the application of different methods for the stability control of RGSG are studied. In the field, several roadway supporting methods are employed together actually. The detailed conditions for the application of different RGSG supporting methods will be researched in the future to simplify the RGSG supporting process and reduce the mining cost.